

# Using small scale morphological features on estuarine tidal flats as indicators for large scale morphological shape and development

A.H. Verheijen





# Using small scale morphological features on estuarine tidal flats as indicators for large scale morphological shape and development

by

A.H. Verheijen

to obtain the degree of Master of Science  
at the Delft University of Technology & National University of Singapore

Thanks to Rijkswaterstaat, who provided aerial photographs and elevation measurements.  
Thanks to KNMI, who provided hourly wind measurements.

Student number: 4234960

Thesis committee: Dr. ir. van Prooijen, B.C.,  
ir. de Vet, P.L.M.  
ir. Zitman, T.J.  
Prof. dr. Herman, P.M.J.  
Dr. ir. Yuan, J.,  
Prof. dr. ir. Reniers, A.J.H.M.

Delft University of Technology  
Delft University of Technology  
Delft University of Technology  
Delft University of Technology  
National University of Singapore  
Delft University of Technology



# Abstract

Intertidal flats and salt marshes can protect hinterland against wave energy and flooding by tides or storm surges. Thus, the development of tidal flats is important to foresee. The presence of specific small scale features could indicate a certain development and large scale morphological shape. The shape is a predictor for development and it is expected to influence small scale feature formation. Tidal flat management could benefit from technological process, e.g. in drones, if these indicators can be used. Hence, the aim of this research is to find indicators and gather sufficient knowledge to make them applicable.

The main research question is: "Can small scale morphological features on estuarine tidal flats be used as indicators for large scale morphological shape and development?". The main question contains two aspects. The first facet is whether the small scale morphological features are indicators for large scale morphological shape and development. It focuses on detecting indicators. The second part is about gathering knowledge to properly use the indicators. It is investigated which mechanisms explain the found indicator roles of the small scale morphological features. The focus is on the identification of the mechanisms. Two sub-questions can be extracted from the above:

1. Are the small scale morphological features on estuarine tidal flats indicators for large scale morphological shape and development?
2. Which mechanisms explain the found indicator roles of small scale morphological features?

Indicators are detected with the analysis of aerial photographs and elevation measurements at transects in the Eastern and Western Scheldt. New and already in literature known features are identified and classified in this process. The mechanism that form and erase the small scale morphological features and their dependence on large scale morphological shape are investigated to explain the found indicators. The mechanisms are determined in various ways: Two 1D models are created, a field campaign is conducted, (subsequent) aerial photographs are looked into, elevation measurements are analyzed in detail and literature research is done.

Small scale morphological features on estuarine tidal flats can be used as indicators in the Western Scheldt. This research detects and explains features that indicate large scale morphological shape, development, hydrodynamic conditions and ecological activity of an area. However, the applicability of the indicators in other systems should be proven by extending this research to other situations. A specific sequence of small scale morphological feature categories between salt marsh and waterfront, a build-up, has been identified as indicator for convex large scale morphological shape and indirectly for accreting behavior. All the features in the build-up are indicators on their own. Megaripples, seen withing build-up, indicate (future) convex profiles. Furthermore, all of the features indicate a certain relative height and slope when they are seen within the build-up. These individual indicator roles are clarified by elaborating on the hydrodynamic conditions that form and erase the features. Therefore, the prevailing conditions can also be determined with the indicators.



# Contents

<b>Abstract</b>	<b>iii</b>
<b>1 Introduction</b>	<b>1</b>
1.1 Background . . . . .	1
1.2 Relevance . . . . .	2
1.3 Research questions . . . . .	3
1.4 Approach and report outline . . . . .	4
<b>2 Detect the indicators</b>	<b>5</b>
2.1 Introduction . . . . .	5
2.2 Methodology . . . . .	6
2.2.1 Large scale morphological shape and development . . . . .	7
2.2.2 Small scale morphological features . . . . .	7
2.3 Results . . . . .	9
2.3.1 Large scale morphological shape and development . . . . .	9
2.3.2 Small scale morphological features . . . . .	11
2.4 Discussion . . . . .	22
2.4.1 Large scale morphological shape and development . . . . .	22
2.4.2 Small scale morphological features . . . . .	23
2.5 Conclusion . . . . .	24
2.5.1 Large scale morphological shape and development . . . . .	24
2.5.2 Small scale morphological features . . . . .	24
2.5.3 Answer to sub-question . . . . .	26
<b>3 Mechanisms explaining the indicators</b>	<b>27</b>
3.1 Introduction . . . . .	27
3.2 Erasing mechanism . . . . .	31
3.2.1 Methodology. . . . .	31
3.2.2 Results . . . . .	34
3.2.3 Discussion . . . . .	41
3.2.4 Conclusion. . . . .	42
3.3 Pool forming mechanism . . . . .	43
3.3.1 Methodology. . . . .	43
3.3.2 Results . . . . .	46
3.3.3 Discussion . . . . .	53
3.3.4 Conclusion. . . . .	55
3.4 Gully forming mechanism . . . . .	57
3.4.1 Methodology. . . . .	57
3.4.2 Results . . . . .	57
3.4.3 Discussion . . . . .	58
3.4.4 Conclusion. . . . .	58
3.5 (Nearly) smooth area forming mechanism . . . . .	59
3.5.1 Methodology. . . . .	59
3.5.2 Results . . . . .	59
3.5.3 Discussion . . . . .	60
3.5.4 Conclusion. . . . .	60
3.6 Ship keel trace forming mechanism. . . . .	61
3.6.1 Methodology. . . . .	61
3.6.2 Results . . . . .	61
3.6.3 Discussion . . . . .	64

3.6.4	Conclusion. . . . .	65
3.7	Megaripple forming mechanism . . . . .	66
3.7.1	Methodology. . . . .	66
3.7.2	Results . . . . .	66
3.7.3	Discussion . . . . .	67
3.7.4	Conclusion. . . . .	67
3.8	Conclusion: Answer to sub-question . . . . .	68
3.8.1	Summary . . . . .	68
3.8.2	Explain build-up as indicator . . . . .	69
<b>4</b>	<b>Discussion</b>	<b>71</b>
<b>5</b>	<b>Conclusion</b>	<b>73</b>
5.1	Indicator detection and explanation . . . . .	73
5.2	Answer to the main question . . . . .	74
5.3	Contribution to literature . . . . .	74
<b>6</b>	<b>Recommendations</b>	<b>75</b>
<b>A</b>	<b>Elevation measurements</b>	<b>77</b>
<b>B</b>	<b>Categorized aerial photographs</b>	<b>85</b>
<b>C</b>	<b>1D SWAN model</b>	<b>97</b>
<b>D</b>	<b>Influence tidal range SWAN run</b>	<b>103</b>
<b>E</b>	<b>Wet density measurements pool shaped features</b>	<b>107</b>
	<b>Bibliography</b>	<b>111</b>



# Introduction

The research topic is introduced in this chapter in four steps. First of all, background information is given about estuaries, intertidal flats, salt marshes and bedforms on intertidal flats. Secondly, the relevance of this research is outlined. This is followed by the research questions. Last of all, it is briefly explained how these questions are answered and the report outline is given.

## 1.1. Background

According to Potter et al. [2010] an estuary is: "A partially enclosed coastal body of water that is either permanently or periodically open to the sea and which receives at least periodic discharge from (a) river(s)". These landforms respond primarily to tidal energy inputs. An estuary achieves an overall form in which tidal energy, significant for a time interval, is reduced to a level at or below the strength of the material in its bed and banks in the intertidal zone. These banks contain mudflats with mostly adjacent vegetated salt marshes or mangroves [Pethick, 1996]. Estuarine tidal flats are soft sediment habitats that submerge and inundate due to the tide [Dyer et al., 2000].

Intertidal flats and salt marshes fulfill a range of environmental and societal functions. They can protect against wave energy and flooding by tides or storm surges [Cooper, 2005]. Furthermore, tidal flats and salt marshes are areas of intense biological activity [Herman et al., 2001] and provide opportunity for recreation [Ribas et al., 2015].

Intertidal flat shape is linked to the development of the flat and depends on wave and tidal energy. Hypsometry is the distribution of horizontal surface area with respect to elevation. Therefore, it is more or less equal to tidal flat shape in a cross section for tidal flats with adjacent salt marshes. Concave hypsometry, see figure 1.1, correlates to small tidal ranges, long-term erosion and/or high wave activity. Convex hypsometry is related to large tidal ranges, long-term accretion and/or low wave activity [Friedrichs and Aubrey, 1996][Kirby and Kirby, 2008][Bearman et al., 2010]. Hence, the shape of a tidal flat has been identified as a predictor for tidal flat development. The forcing conditions appear with a certain probability and it takes time for the profile to adjust to changes in the conditions. The intertidal flats adapt slower than sandy beaches. On a shorter time scale the tidal flat may deviate from the equilibrium, depending on the prevailing short term forcing conditions [Pethick, 1996].

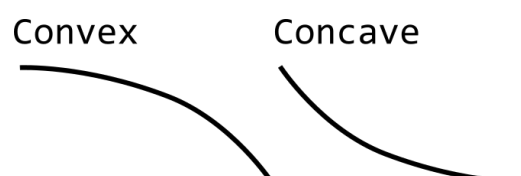


Figure 1.1: Schematic representation of convex and concave large scale morphological shapes.

The salt marsh development is influenced by the tidal flat evolution. E.g., Bouma et al. [2016] show that the tidal flat development influences the salt marsh cliff erosion or progradation.

Bedforms are usually present on intertidal flats. They occur in various sizes. A summary of the bedforms that occur on tidal flats is given by Whitehouse et al. [2000]. A brief description of these bedforms and their forming mechanism is given below.

1. **Channels, creeks and gullies**

A dendritic structure of channels of varying sizes is referred to as channels, creeks or gullies. The channels fulfill a drainage function. They are formed and enhanced by the drainage currents.

2. **Ridge-runnel systems**

The ridge-runnel systems consist of extensive areas of elongated parallel channels that do not continue all the way towards the channel. Their width is in the order of 0.5 to 1 meter and their height is in the order of tens of centimeters. Ridges can be spaced further apart without a trough in between. The channels are mostly oriented shore-normal, have an elongated shape and appear to be caused by wave-induced erosion. The troughs can be filled seasonally with softer muds. The sediment strength is found to be almost twice as high on the ridges as in the runnels. Ridge-runnel systems can be combined with channels, creeks or gullies.

3. **Ripples and microtopography**

Ripples are small scale features that are wave-like shaped in a regular pattern. The typical dimensions are 2 centimeters height and 30 centimeters wavelength. They are formed by waves or currents in predominantly non-cohesive sediment.

4. **Cliffs**

Vertical cliff features are controlled by underlying soil composition or vegetation. They can occur at various heights on the mudflat. Erosion of layers with different sediment properties can form a cliff.

## 1.2. Relevance

The aim of this research is to find small scale morphological features that are indicators for large scale morphological shape and development and gather sufficient knowledge to make them applicable. At this moment little knowledge is available about (the use of) such indicators. However, it is known that large scale morphological shape and development are coupled, see paragraph 1.1. Also the link between some small scale morphological features and hydrodynamic conditions is addressed.

Knowledge about the development of intertidal flats and salt marshes is crucial for a good coastal zone management, since they fulfill a broad range of functions, see paragraph 1.1. This management could benefit from current technological progress if small scale morphological features can be used as indicators for large scale morphological shape and development.

Drones, high resolution aerial photographs and potentially future satellite images increase the possibilities to visually inspect tidal flats in great detail. Hence, information about a remote area could be gathered with increasing ease if the indicators can be used. A drone could be used for example to gather aerial footage, which allows determination of large scale morphological shape and development. The alternative would be to physically go to the site and measure. Figure 1.2 shows an example of aerial footage that could be obtained. The shown tidal flat is not smooth; All sorts of small scale morphological features are present, e.g. pools and gullies can be observed. The small scale is defined in this research as significantly smaller than the cross shore dimension of the tidal flat.

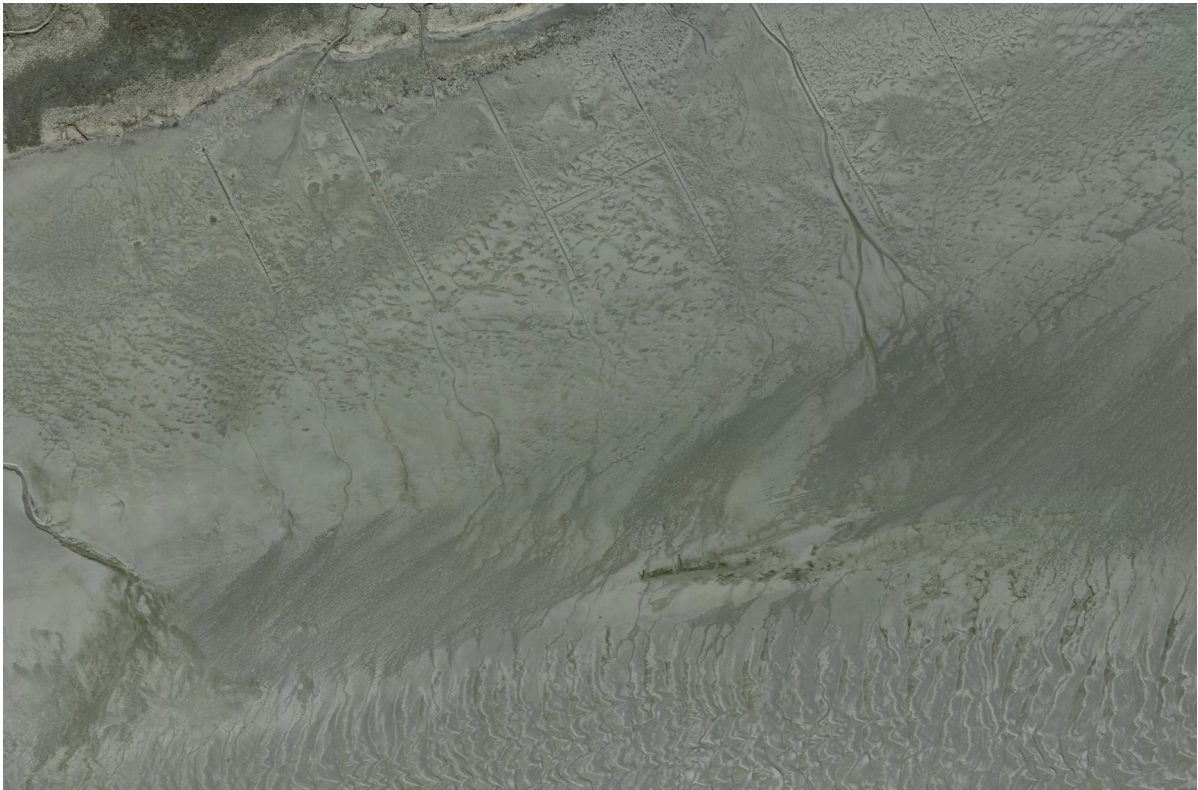


Figure 1.2: Example of an aerial photograph from Zuidgors. The photograph is acquired by Rijkswaterstaat [2017b] in 2009

The presence of specific small scale features on a tidal flat potentially indicates certain large scale morphological shape and development of the flat. The argumentation why this is foreseen consists of two parts. First, tidal flat shape has been identified as a predictor for development, see paragraph 1.1. Secondly, the tidal flat shape is expected to influence the formation of small scale morphological features. Hydrodynamic conditions influence the formation of small scale morphological features, see for example the formation of ridge-runnel systems in paragraph 1.1. These conditions are determined by, among others, water depth and its evolution in cross shore direction. For instance, wave height increases for decreasing water depth, up to a breaking point [Holthuijsen, 2009]. Water depth and its evolution in cross shore direction are coupled to large scale morphological shape. Hence, large scale morphological shape of a tidal flat is potentially linked to small scale morphological features.

### 1.3. Research questions

The main research question is: "Can small scale morphological features on estuarine tidal flats be used as indicators for large scale morphological shape and development?". The main question can be split in two sections. First, whether the small scale morphological features are indicators for large scale morphological shape and development. The second part is about gathering knowledge to explain the indicators. Which mechanisms explain the found indicator roles of the small scale morphology is investigated in the second part. Identification of and knowledge about of these mechanisms are crucial for proper usage of the indicators. The focus in this research is on the identification of the mechanisms and not on gathering knowledge about their temporal behavior. The two sub-questions with related underlying questions are:

1. Are the small scale morphological features on estuarine tidal flats indicators for large scale morphological shape and development?
  - (a) Which large scale morphological shapes and developments are found on estuarine tidal flats?
  - (b) What are the different types of small scale morphological features seen on estuarine tidal flats and where do they occur with respect to large scale morphological shape and development?

2. Which mechanisms explain the found indicator roles of small scale morphological features?
  - (i) Which mechanisms are responsible for **erasing** the small scale morphological features that can be used as indicators and how are they influenced by the large scale morphological shape?
  - (ii) Which mechanisms are responsible for **forming** the small scale morphological features that can be used as indicators and how are they influenced by the large scale morphological shape?

#### 1.4. Approach and report outline

Whether small scale morphological features on estuarine tidal flats are indicators for large scale morphological shape and development is answered in the first part of this research, chapter 2. This concerns sub-question 1. The evaluation is done by analyzing aerial photographs and GPS measurements of bottom elevation along transects in the Eastern and Western Scheldt, both acquired by Rijkswaterstaat [Rijkswaterstaat, 2017b][Rijkswaterstaat, 2017a]. The photographs and elevation measurements are investigated individually and coupled to each other to answer sub-questions (a) and (b).

The found indicator roles of the small scale morphological features are explained in the second part of this research, i.e. sub-question 2 is answered in chapter 3. Mechanisms that form and erase the small scale morphological features are identified to explain the found indicators, answering sub-questions (i) and (ii). The related hypotheses are based on the first part's outcome and given in the chapter's introduction. The hypothetically important mechanisms are looked into in various ways: Two 1D models are created, observations and measurements are done in a field campaign, (subsequent) aerial photographs are looked into, elevation measurements are analyzed in detail and literature research is conducted.

General discussion points are given after the sub-questions are evaluated individually. An overall conclusion follows next. Recommendations are given in the end.

# 2

## Detect the indicators

### 2.1. Introduction

This chapter provides an answer to the first sub-question: "Are the small scale morphological features on estuarine tidal flats indicators for large scale morphological shape and development?". Two related underlying questions are:

- (a) Which large scale morphological shapes and developments are found on estuarine tidal flats?
- (b) What are the different types of small scale morphological features seen on estuarine tidal flats and where do they occur with respect to large scale morphological shape and development?

Three large scale morphological profile shapes are expected to be found on the estuarine tidal flats: convex, linear and concave profiles, see figure 2.1. Convex profiles should show accreting behavior and linear and concave profiles to show eroding behavior. This hypothesis concerns sub-question (a) and is based on literature. Convex hypsometries, and thus profiles, are related to long term accretion of cross shore flow dominated tidal flats, according to literature [Friedrichs and Aubrey, 1996][Kirby and Kirby, 2008][Bearman et al., 2010][van Prooijen et al., 2017]. The literature links concave hypsometries to long term erosion of the tidal flats.

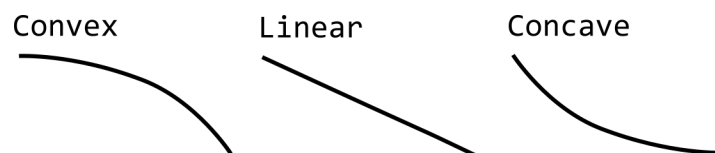


Figure 2.1: Schematic representation of convex, linear and concave large scale profile shape.

Pool shaped small scale features are observed in a few aerial photographs on the upper, milder sloped, part of convex profiles. They are observed to have gully like features on the channelward side of them, on the steeper/lower part. Therefore, the hypothesis is that pool shaped small scale features with adjacent gullies should indicate convex shape and indirectly indicate accreting tidal flats. This hypothesis relates to sub-question (b) and indirectly answers the central sub-question in this chapter.

The large scale morphological shapes and developments of the investigated tidal flats are determined by analyzing elevation measurements along transects, surveyed regularly by Rijkswaterstaat [2017a]. Aerial photographs, acquired by Rijkswaterstaat [2017b], are investigated to look at the different types of small scale features. The location of these features with respect to large scale shape and development is determined by coupling the elevation measurements and photographs. The exact methodology is explained in individual sections for the underlying questions (a) and (b). This is done in the first part of this research. Afterwards, the results are given. They are followed by discussion points. Finally, conclusions are drawn for sub-question 1 and underlying questions (a) and (b).

## 2.2. Methodology

The methodology consists of two elements and is explained in this section. The first part explains the determination method of the tidal flats' large scale morphological shape and development. The second part elaborates on how the different small scale morphological features and their location with respect to the large scale morphological shape and development are determined.

The explained investigations are done for six tidal flats in the Western Scheldt and three in the Eastern Scheldt, see figure 2.2. The tidal flats in the Western Scheldt are Baalhoek, Bath, Knuitershoek, Land van Saefthinghe, Waarde, and Zuidgors. Anna Jacobapolder, Kats and Zandkreek are looked into for the Eastern Scheldt. For every tidal flat, except Waarde, one transect is investigated. The transect most central on the tidal flat is chosen if multiple transects are present. At Waarde two headlands are constructed between 2000 and 2003. These headlands separate three transects that show a different behavior. All three are investigated. The names Rijkswaterstaat [2017a] has given the investigated transects are given in table 2.1.



Figure 2.2: This figure shows the location of investigated tidal flats in Western and Eastern Scheldt.

Tidal flat name	Transect name given by Rijkswaterstaat [2017a]
Anna Jacobapolder	Annajacobapolder_Profiel_ssl_5860_1
Baalhoek	Baalhoek_Profiel_hop_2530_2
Bath	Bath_Profiel_ssl_2810_1
Kats	Kats_Profiel_ssl_5280_1
Knuitershoek	Knuitershoek_Profiel_ssl_2390_1
Land van Saefthinghe	LandvanSaefthinghe_Profiel_hop_2700_62
Waarde's 1 <sup>st</sup> transect	Waarde_Profiel_hop_2610_1
Waarde's 2 <sup>nd</sup> transect	Waarde_Profiel_hop_2625_2
Waarde's 3 <sup>rd</sup> transect	Waarde_Profiel_hop_2650_3
Zandkreek	Zandkreek_Profiel_ssl_5310_1
Zuidgors	Zuidgors_Profiel_ssl_2230_2a

Table 2.1: Names of the transects that are analyzed in this research. These names correspondent to the names Rijkswaterstaat [2017a] uses, who surveys the bottom elevation on these transects with GPS.

### 2.2.1. Large scale morphological shape and development

How the tidal flats' large scale shape and development is determined is explained in this section. It is hypothesized that roughly three large scale profile shapes are seen on the tidal flats: convex, linear and concave profiles, see figure 2.1. The convex profiles are expected to accrete and the linear and concave profiles to erode. GPS measurements of bottom elevation along transects on the tidal flats are used to investigate these hypotheses. Rijkswaterstaat [2017a] is surveying these transects since 1991, 1993 or 1994, depending on the tidal flat. Measurements up to 2016 were available.

The tidal flats are categorized on their large scale shape in a table. Their development is indicated in the same table. Three shape options are considered: convex, linear and concave, see figure 2.1. The options form the columns of the categorized table. The tidal flats are put in the right column. The large scale developments are indicated in this table as well. Five development types are considered, given in figure 2.3. Combinations of these types are possible, e.g. accreting and retreating. Any deviations from the given options for large scale morphological shape or development will be mentioned in the table.

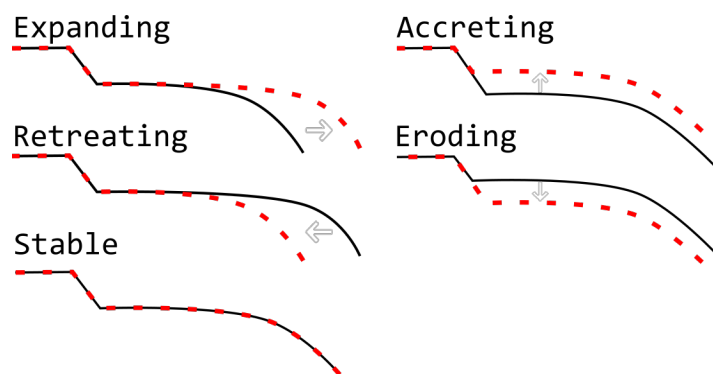


Figure 2.3: Schematic representation of large scale morphological developments that are considered in this research.

### 2.2.2. Small scale morphological features

This section explains first how the different small scale morphological feature types are found. Secondly, it is explained how the features are located and linked to large scale morphological shape and development. The majority is done based on aerial color photographs, Red Green Blue (RGB) photographs. They are acquired by Rijkswaterstaat [2017b]. Photographs from 2000 up to 2016 are available in a resolution of 0.5 meter or finer. The exact resolution is given in table 2.2. Going back further in time than 2000 a resolution of one meter is seen. That resolution is considered inadequate for the purpose of recognizing small scale morphology. From 2012 up to and including 2016 two photographs are available per year, a high (0.1m) and low (0.25m) resolution. The high resolution is mostly acquired in the period February up to and including April. The low one is mostly obtained in the period May up to and including July. Color-infrared photographs are used to determine whether fauna is seen on the tidal flats, if they are available. The availability differs per tidal flat. These photographs capture near-infrared and visible wavelengths. Healthy, growing vegetation reflects a high level of near-infrared wavelengths. This appears red on color-infrared photographs [Geomart.com].

Year	2000	2003	2005	2006	2007	2008-2011	2012-2016
Resolution [m]	0.5	0.5	0.4	0.5	0.4	0.25	0.25 & 0.1

Table 2.2: Resolution of the aerial photographs that are used in this research. From 2012 up to and including 2016 two photographs are available per year, a high (0.1m) and low (0.25m) resolution. The high resolution is mostly acquired in the period February up to and including April and the low one mostly in the period May up to and including July.

## Different small scale morphological feature types

All the aerial RGB photographs are manually looked into to adhere the different types of small scale morphological features and to define categories of small scale features. Two different types of features are mentioned in the hypothesis: pool shaped features and gullies. The defined categories are used further in this research to classify all the aerial photographs. The location of the different small scale morphological features are determined with these classified aerial photographs. The characteristics of the categories are defined accurately to prevent overlay and facilitate objective detection. The amount of categories is kept minimal, while keeping in mind that enough categories have to be defined to cover most features on the tidal flats. Too many categories would make the analysis impossible to oversee. Too few would mean a very large leftover category or large scatter in properties, possibly resulting in scattered outcome.

## Location of small scale morphological features

The location of small scale morphological features are determined from aerial photographs. This is linked to the large scale morphological shape with elevation measurements. The location is determined with Qgis, an open source geographical information system. The coupling with large scale morphological shape is done with Python, a programming language. It is hypothesized that pool shaped small scale features with adjacent gullies are seen on convex profiles. The location determination and coupling with large scale shape involves several steps, given below.

1. The aerial photographs are filtered on suitability, as first step. Every photograph where too high water is seen is neglected, because most of the tidal flat is covered with water. The photo showing small scale morphology clearest is chosen if two low tide photographs are available for one year. This could occur for the years 2012 and later. This mostly results in predominant use of either high or low resolution per tidal flat.
2. The second step is to map out the transect of interest in Qgis and indicate a rectangle around. This rectangle covers 25 meters around the transect, on both sides, and is oriented parallel to it. The area bordered by it is analyzed in the next steps.
3. As third, the suited aerial photographs are classified one by one in Qgis with use of the categories, defined previously. Polygons are created around areas of the same category. Which area of the transect belongs to which category is now indicated for every analyzed aerial photograph. The indications are stored in Qgis files.
4. The fourth step is to read step 3's outcome in Python. This is used to create images with color coded categories and image borders equal to the rectangle explained in step 2. The categories are also labeled. These images are rotated to line them out horizontally, with the channel side on the right. The photographs' measurement moments are displayed on top of the images.
5. The fifth step is to load the elevation measurements in Python, for the transect of interest. The temporally closest elevation measurements are displayed on top of the figures obtained in step 4. Missing day and month values are set to the first of June to find the temporally nearest elevation measurements. The exact measuring date is not known for the years 2000 and 2006. Bed elevations between -3 m NAP and 3 m NAP are displayed.
6. The last step is to vertically stack the images obtained in step 5. Ordered descending on date. A legend of the color coded categories is created and added in this step as well.

The link between small scale feature categories and large scale morphological shape should follow from figures obtained by the steps above. This relation is analyzed per aerial photograph. Large scale development is only observed over multiple years. The link between development and small scale features is therefore analyzed globally. It should be clear at this point whether the small scale morphological features are indicators for large scale morphological shape and development.

Average relative height and linear slope are determined for the small scale features that can be used as indicators. Relative height is obtained by scaling by half of the tidal range. This is done to make different tidal flats comparable. The absolute height is less generic than the relative height and the tidal ranges on the considered flats are not the same. These two parameters are obtained by matching coordinates of the elevation measurements and categories in Python. It has to be noted that not every elevation measurement series covers the whole tidal flat. A category's occurrence is ignored in case of no coverage.



## 2.3. Results

The results are split in two parts. The first section gives the tidal flats categorized based on their large scale morphological shapes. Tidal flat development is shown in this part as well. Secondly, the different types of small scale morphology and their location with respect to the large scale morphological shape are given.

### 2.3.1. Large scale morphological shape and development

The tidal flats' large scale morphological shape and development are given in table 2.3. They are categorized by shape in the three columns. Development and shape are determined from the elevation measurements, see paragraph 2.2.1. The elevation measurements are visualized in appendix A. If multiple large scale shapes are observed, then multiple occurrences of the tidal flat are seen in the table.

Almost all linear and all concave profiles are (slightly) eroding and most convex profiles are accreting, see table 2.3. Waarde's 1<sup>st</sup> transect is the only linear profile that shows no erosion. This is seen during a period of two years. Baalhoek and Waarde's 1<sup>st</sup> and 3<sup>rd</sup> transects are the only convex profiles that show no accreting behavior. Baalhoek is approximately stable at the upper part until 2005. It starts eroding at the channel side and accreting at the landward side in 2005. Therefore, a convex profile with a less wide upper part starts to develop after 2005. The intermediate states show a crooked convex profile. These profiles have a sharp transition between the lower and upper part. A similar crooked convex profile is seen at Knuitershoek in 2000 and onwards. At Waarde's 1<sup>st</sup> transect the accreting behavior stabilizes in 2013. Waarde's 3<sup>rd</sup> transect shows erosion in the whole analyzed period.

The linear profiles show a stable behavior in cross shore direction, see table 2.3. The concave and convex profiles show a mixed development. The linear profiles are mostly stable in cross shore direction, except Waarde's 1<sup>st</sup> transect after 2000. The concave profiles show no trend in cross shore direction development. One concave transect is approximately stable and one is retreating. The convex profiles show both retreating and expanding behavior.


Convex 	Linear 	Concave 
<p><b>Baalhoek</b> Profile deforms to a convex profile with less wide upper part, intermediate it looks crooked. Stable upper part, until 2005. Retreating lower part, until 2005. Accreting upper part, starting 2005. Eroding lower part, starting 2005. Expanding far channelward side, starting 2010.</p>	<p><b>Kats</b> Eroding, except for 1 spot. Approx. stable in cross shore</p>	<p><b>Annajacobapolder</b> Eroding Retreating until 2005. Stable in cross shore starting 2005.</p>
<p><b>Bath</b> Slightly accreting upper part. Slightly retreating lower part.</p>	<p><b>Waarde, 1<sup>st</sup> transect</b> Until approx. 2002. Slightly eroding upper part, until 2000. Approx. stable in cross shore, until 2000. Approx. stable upper part, starting 2000. Expanding starting 2000.</p>	<p><b>Waarde, 2<sup>nd</sup> transect</b> Until approx. 2003. Eroding Approx. stable in cross shore</p>
<p><b>Knuitershoek</b> Profile has a sharp transition between upper and lower part, starting approx. 2000. Accreting on landward side. Eroding on channelward side. Retreating up to 2015 Expanding from 2015</p>	<p><b>Zandkreek</b> Slightly eroding Stable in cross shore</p>	
<p><b>Land van Saeftinghe</b> Accreting upper part. Retreating</p>	<p><b>Zuidgors</b> Until 2001. Eroding Approx. stable in cross shore</p>	
<p><b>Waarde, 1<sup>st</sup> transect</b> Starting approx. 2005. Accreting until 2013, after 2013 only most landward part Expanding until 2012 Stable upper part after 2013, only most channelward part Retreating after 2012</p>		
<p><b>Waarde, 2<sup>nd</sup> transect</b> Starting approx. 2009 accreting expanding</p>		
<p><b>Waarde, 3<sup>rd</sup> transect</b> Eroding upper part. Retreating Connection with sand bank in front mostly gone after 2006.</p>		
<p><b>Zuidgors</b> Starting approx. 2005. Accreting Expanding after 2011 retreat is seen in some years</p>		

Table 2.3: Tidal flats categorized by large scale morphological shape. The tidal flat development is given in blue.

### 2.3.2. Small scale morphological features

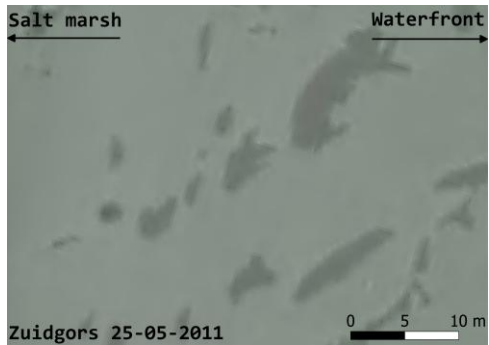
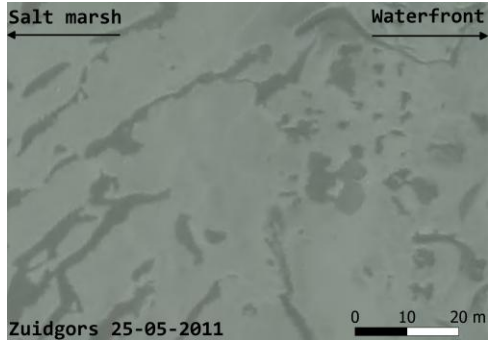
This section displays the different types of small scale morphological features that are seen on the estuarine tidal flats and where they occur with respect to the large scale morphological shape and development. First the different types are given, organized in categories. Their location on the tidal flat is linked to the large scale morphological shape afterwards.

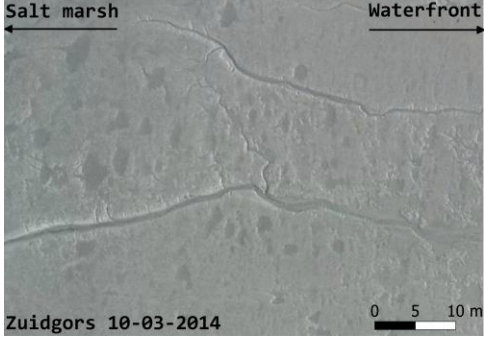
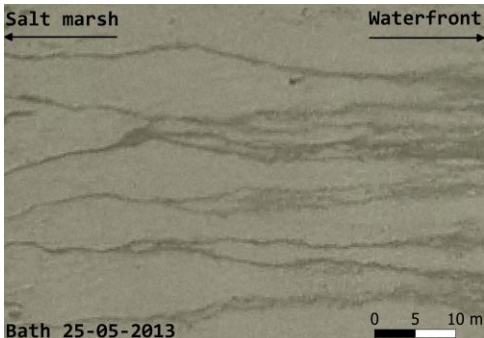
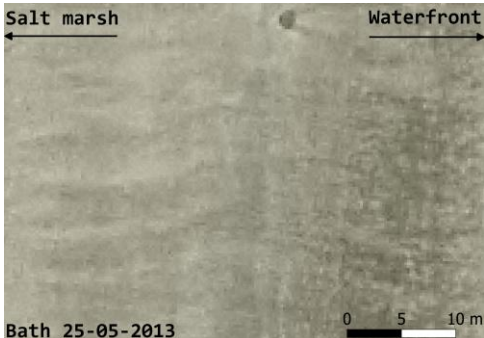
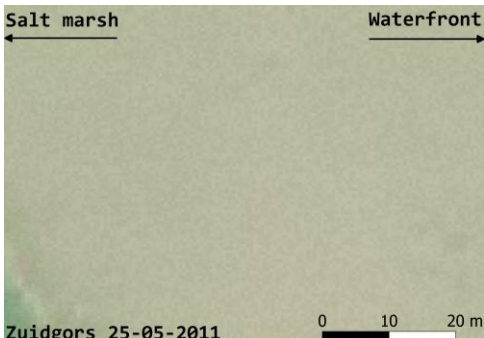
#### Different small scale morphological feature types

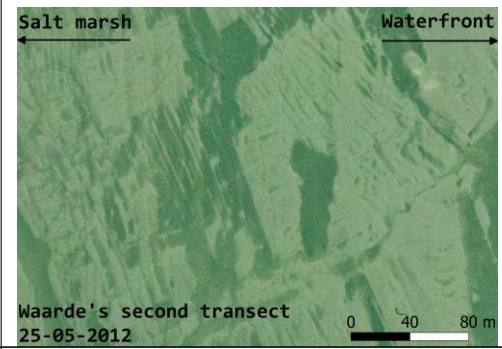
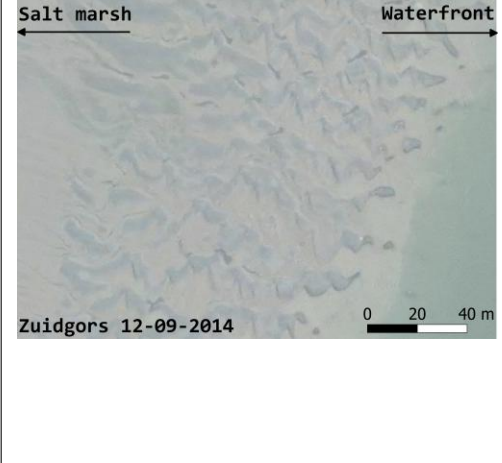
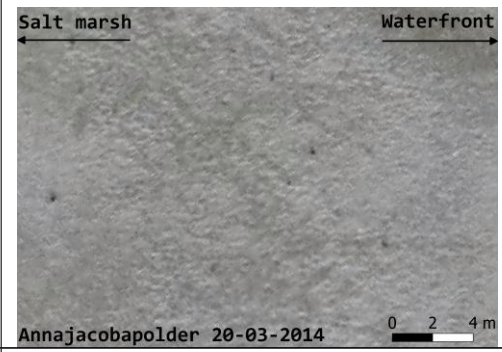
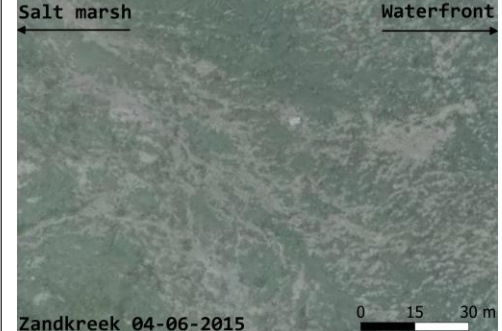
Several categories of small scale morphological features on estuarine tidal flats are defined in this section, see categories (a) to (j) in table 2.4. They cover most of the small scale features seen in this research. Several other categories are given, (01) to (04). These categories cover bigger features and phenomena that are not on the tidal flat or non-morphological. A leftover category is created as well. This category is for all the features that do not match all the other category descriptions.

Distinguishing vague gullies (e) and clearer gullies (d) is not completely objective. At some tidal flats a clear transition is seen where gullies fade to vague gullies or a (nearly) smooth area. The separation between vague and clearer gullies needs to be made to be able to investigate this transition, despite the subjectivity it brings.

Note that the category (j), algae mats, is not really a morphological feature. However, algae mats influence the small scale morphology to such an extent that they are seen in this research as small scale morphological features. Algae mats are known to stabilize the bed [Knaapen et al., 2003], which can cause additional sedimentation [Paarlberg et al., 2005]. Note that they can also cover almost the whole tidal flat, making the small scale doubtful.

Category	Description	Example
a) Pool shaped features	More than approximately 5 percent of the area is covered with pool shaped features. These features can be up to several meters in width, up to tens of meters in length and several centimeters in depth. Width length ratio is in the range 1:1 up to 1:10 (the largest width : total length). The features are characterized by (semi) rounded edges.	
b) Pools and gully formation	(Elongated) pools are seen and some are interconnected. If pools are connected the area belongs to this category and not to category (a). The interconnections and elongated pool shapes make that also width length ratios lower than 1:10 are seen (the largest width of pool:total length). More than approximately 5 percent of the area is filled with (elongated/interconnected) pools.	

<p>c) Pools and gullies</p>	<p>Pools and developed, worn out, gullies are observed mainly separately. The gullies exist mainly independent, with occasionally a pool connected to them. This is in contrast with category (b), where the gully formation is made up from connected pools. Spacing between the pool features succeeding in gully direction is not more than approximately ten times the size of the features. If there is more space in between the pools, then the area is regarded as category (d). Gully length is starting at multiple times the dimensions of the larger pool features seen and is much larger than the gully width. The spacing between gullies is up to tens of meters.</p>	
<p>d) Gullies</p>	<p>Developed, worn out, gullies are observed. The gullies are easily seen by the clear color contrast between them and their surroundings. The length of the gullies is much larger than the width. The spacing between gullies is up to dozens of meters.</p>	
<p>e) Vague gullies</p>	<p>Vague gullies are observed. A vague color contrast between the gullies and their surroundings could be a reason they are not clearly observed. Another possibility is that they don't have the developed, worn out, gully shape. This generally means they are wider, but still identifiable as stretched drainage features. The length of the vague gullies is larger than the width. However, the width:length ratio is generally larger than seen in category (d). The spacing between gullies is up to tens of meters.</p>	
<p>f) (Nearly) smooth</p>	<p>(Nearly) no features can be distinguished. More than 95 percent of the area shows no distinguishable features or more than 40 percent of the area shows no clear texture (see category (i)).</p>	

<p>g) Ship keel traces</p>	<p>These features look like they are traces of ship keels, left after boats have run aground. The shapes are angular, elongated and are often intersecting each other. The angular look and intersections help to separate the ship keel traces from gullies and/or pools.</p>	
<p>h) Megaripples</p>	<p>The megaripples are mostly oriented in approximately the same direction. The ripple orientation aligns more or less with the direction that along shore currents occur in. The width of the crests and troughs are mostly in the same order of magnitude. This is in contrast with the gullies, where low-lying parts are mostly less wide. Also a zigzagging pattern is often seen in the megaripples. This is another contrast with gullies, they are mostly more straight (depending on depth contours). Sometimes large holes are seen in between the megaripples. They look like (nearly) circular pits in the ground.</p>	
<p>i) Texture</p>	<p>Surface texture is seen without forming a clear feature, e.g. a gully or pool. The texture is formed by clearly contrasting colors alternating over a short distance, tens of centimeters up to some meters. This results in a noisy pattern, the color deviates a lot. More than 60 percent of the area is filled with this texture.</p>	
<p>j) Algae mats</p>	<p>Darker and/or green patches are observed. They match with red spots in color-infrared photographs, if available. These photographs indicate healthy, growing vegetation with a red color [Geomart.com]. The patches seem to be algae, or other small fauna without stem or woody component; No shadows are observed in the photographs. More than 5 percent of the area is covered with these patches.</p>	

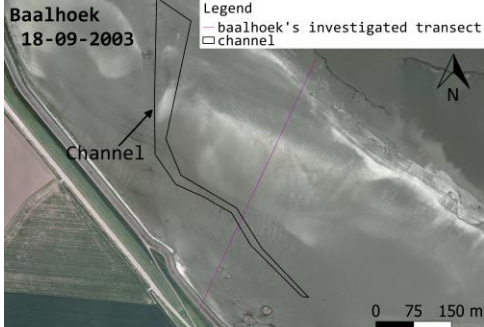


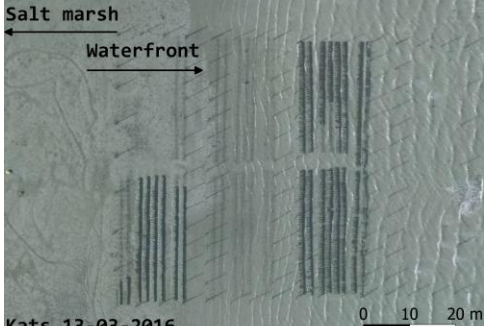
01) Channel, tidal flat size	A channel is seen that covers a large part of the tidal flat.	
02) Water	In most aerial photographs water is also observed, due to the tide. This can be distinguished mostly by the presence of waves or a slight color deviation with the neighboring sand.	
03) Salt marsh vegetation	Brown/green vegetation is observed that belongs to the salt marsh. At some tidal flats patches of salt marsh vegetation are seen in front of the continuous salt march. If they cover more than 5 percent of the area it is still seen as salt march vegetation. Note that this can give some discrepancy with the measured heights.	
04) Other (e.g. mussels)	This category is a leftover category. Features that do not match the descriptions of the other categories are placed in this one. These features can be large or small. In the example picture mussels can be seen.	

Table 2.4: Categories of (small scale morphological) features observed on estuarine tidal flats are given in this table. They have a name and category letter/number. A description and example are given in this table as well. The date and location of the examples is displayed at the upper left corner of the figures.

Five percent coverage is often mentioned in the descriptions in table 2.4. An example of approximately 9 percent coverage is given in figure 2.4 to provide a better feeling of how such a small amount of coverage looks like.

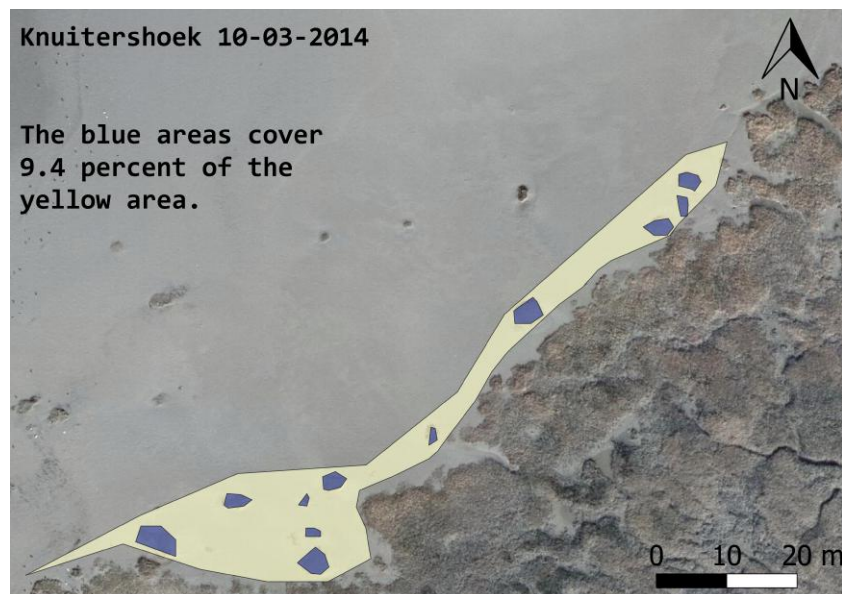


Figure 2.4: The figure displays part of an aerial photograph of Knuitershoek, which is taken on 10 March 2014. A yellow and several blue areas are defined in this figure. The sum of the blue areas covers 9.4 percent of the yellow area. The blue areas represent patches of vegetation in this example. Therefore, the yellow area can be classified as salt marsh vegetation.

Figure 2.4 makes clear that it is possible that an area is classified as salt marsh vegetation, but is rather a tidal flat with some vegetated patches than a salt marsh. The five percent requirement is chosen to prevent that some areas fall in between the categories (nearly) smooth and salt marsh. It is not important for this research where the transition between salt marsh and tidal flat exactly lies. Hence, this definition can be maintained.

### Location of small scale morphological features

This section shows the location of the small scale morphological features with respect to the large scale morphological shape. This is done by analyzing categorized aerial photographs of the investigated tidal flats in combination with the large scale morphological shape. Categorized aerial photographs are obtained by applying the previously defined categories. The method is explained in paragraph 2.2.2. Examples of categorized aerial photographs are given in figure 2.5 and 2.6 for tidal flats Bath and Kats respectively. See figure 2.2 for the location of these tidal flats. All categorized aerial photographs are given in appendix B.

A major part of the categories seen at Bath are in alphabetical order from salt marsh to channelward end, see figure 2.5. This figure shows a very similar pattern in most categorized aerial photographs. Most of the categories are indicated with a color in the gray scaled range. The darkness of these colors is increasing in direction of the channel, in general. This is in line with the alphabetical order. For example, the categorized aerial photograph from 2012 starts with the leftover category at the landward side, left. Salt marsh is seen right of this leftover category. After the salt marsh a (nearly) smooth area is observed. This is followed by an alphabetical order in categories: pool shaped features (a), pools with gully formation (b), pools and gullies (c), gullies (d), vague gullies (e) and then ship keel traces (g). The categories at Bath are in an organized fashion; They have a certain build-up in them.

The categorized aerial photographs from Kats look less organized than seen at Bath, compare figure 2.5 and 2.6. The categories are less often in alphabetical order or increasing in darkness for the gray scaled category colors. The categorized aerial photograph from 2012 shows for instance the leftover category at the most landward side, left, and is then followed by categories: (b), (i), (f), (j), (e), (01), (a), (f), (02), (04) and (02). This order is not organized.

### Bath

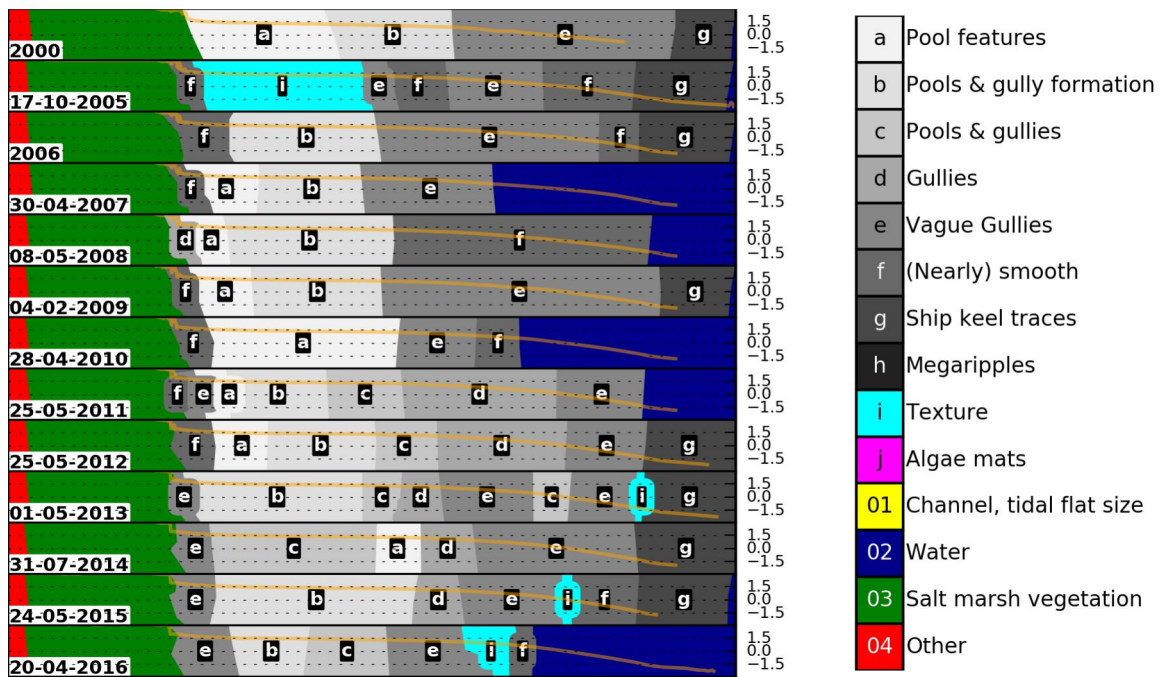


Figure 2.5: This figure displays the aerial photographs of several years sorted in categories for an area around the transect at Bath. This area is a rectangle around the transect that covers 25 meters on both sides of it and is oriented parallel to it. The temporally closest elevation measurement series is displayed in each photograph. On the right side of each photograph is the measured height displayed in m NAP. The date the photos are taken is displayed on at the lower left of each categorized photograph.

### Kats

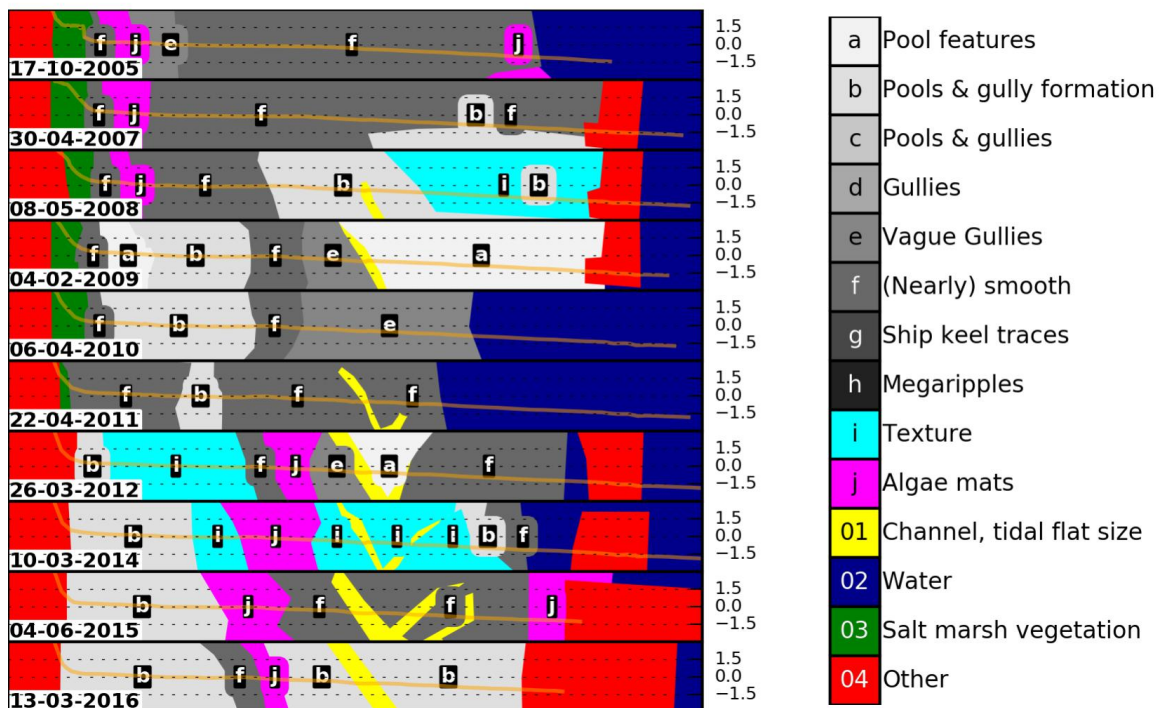


Figure 2.6: This figure displays the aerial photographs of several years sorted in categories for an area around the transect at Kats. This area is a rectangle around the transect that covers 25 meters on both sides of it and is oriented parallel to it. The temporally closest elevation measurement series is displayed in each photograph. On the right side of each photograph is the measured height displayed in m NAP. The date the photos are taken is displayed on at the lower left of each categorized photograph.



**Build-up**

At some of the tidal flats a build-up in categories between salt marsh and waterfront is often observed in the categorized aerial photographs, similar to Bath. This build-up in categories could be an indicator for large scale morphological shape, since it is seen more often on certain tidal flats. A definition of build-up is created, with several iterations, to quantify the number of times it is seen. The iterations are done to capture most of the ordered patterns on convex tidal flats. Build-up in categories meets the following criteria:

1. It starts at the landward side of the tidal flat with pool shaped features (category (a)) or pools with gully formation (category (b)).
2. At least two of the following categories are seen channelwards of this start:
  - (b) Pools with gully formation
  - (c) Pools and gullies
  - (d) Gullies
  - (e) Vague gullies
  - (f) (Nearly) smooth
  - (g) Ship keel traces
  - (h) Megaripples
3. The consecutive categories are in the order mentioned. Some exceptions are made:
  - (a) The following categories may once be reversed: vague gullies with (nearly) smooth areas and ship keel traces with megaripples
  - (b) Sometimes one or two arbitrary categories are seen between the build-up and salt marsh/dyke. This is neglected in the required order, as long as their coverage is small. These categories are mostly (vague) gullies or (nearly) smooth areas.
  - (c) Areas with texture (category (i)) or tidal flat sized channels (category (01)) sometimes disturb the build-up. This is neglected as well.

The build-up, as defined above, is observed in 47 aerial photographs from the 85 analyzed photographs of convex profiles, three times out of 25 at linear profiles and never in the eight photos of concave profiles. It is summarized in table 2.5 how often the build-up is seen at all the analyzed tidal flats. It is often seen at Bath, see figure 2.5, only not in 2005, 2013 and 2014. At Kats it is only seen twice, in 2009 and 2010, see figure 2.6. Note that for convex profiles at Waarde's 1<sup>st</sup>, 2<sup>nd</sup> and 3<sup>rd</sup> transect and Zuidgors deviant behavior around a tidal flat sized channels (category (01)) is seen and ignored in counting the times build-up is seen. This behavior deviates in the sense that the alphabetical descending order in channelward direction is disturbed. This deviating behavior, due to tidal flat sized channel disturbance, is also neglected once at linear tidal flat Kats. At Waarde's 1<sup>st</sup> transect the tidal flat sized channel is always seen, sometimes just outside the investigated area.




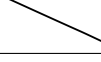
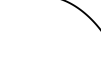

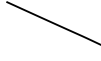




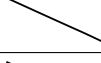
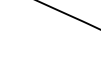

Tidal flat	Build-up observed	Tidal flat shape	Tidal flat development
Anna Jacobapolder	0 out of 7 times		<b>Eroding</b> <b>Retreating</b> until 2005. <b>Stable in cross shore</b> starting 2005.
Baalhoek	3 out of 10 times		<b>Stable</b> upper part, until 2005. <b>Retreating</b> lower part, until 2005. <b>Accreting</b> upper part, starting 2005. <b>Eroding</b> lower part, starting 2005. <b>Expanding</b> far channelward side, starting in 2010.
Bath	10 out of 13 times		Slightly <b>accreting</b> upper part. Slightly <b>retreating</b> lower part.
Kats	2 out of 10 times		<b>Eroding</b> , except for 1 spot. Approx. <b>stable in cross shore</b>
Knuitershoeck	4 out of 12 times		<b>Accreting</b> on landward side. <b>Eroding</b> on channelward side. <b>Retreating</b>
Land van Saeftinghe	8 out of 13 times		<b>Accreting</b> upper part. <b>Retreating</b>
Waarde's 1 <sup>st</sup> transect Until approx. 2002	1 out of 1 times		Slightly <b>eroding</b> upper part, until 2000. Approx. <b>stable in cross shore</b> , until 2000. Approx. <b>stable</b> upper part, starting 2000. <b>Expanding</b> starting 2000.
Waarde's 1 <sup>st</sup> transect Starting approx. 2005	2 out of 9 times		<b>Accreting</b> <b>Expanding</b>
Waarde's 2 <sup>nd</sup> transect Until approx. 2003	0 out of 1 times		<b>Eroding</b> Approx. <b>stable in cross shore</b>
Waarde's 2 <sup>nd</sup> transect Starting approx. 2009	4 out of 7 times		<b>accreting</b> <b>expanding</b>
Waarde's 3 <sup>rd</sup> transect	7 out of 10 times		<b>Eroding</b> upper part. <b>Retreating</b>
Zandkreek	0 out of 13 times		Slightly <b>eroding</b> <b>Stable in cross shore</b>
Zuidgors Until 2001	0 out of 1 times		Until 2001. <b>Eroding</b> Approx. <b>stable in cross shore</b>
Zuidgors Starting approx. 2005	9 out of 11 times		<b>Accreting</b> <b>Expanding</b>

Table 2.5: Summary of how often build-up is observed at the analyzed transects. This is done per large scale morphological shape at the transects. A transect gets two rows if it has two different large scale shapes. Also the shape is visually given and the development is mentioned.

### Megaripples

The megaripples are only observed on convex profiles or profiles that start to evolve to a convex profile. This becomes clear from appendix B and paragraph 2.3.1. How many times the megaripples are observed at the tidal flats is summarized in table 2.6. The flats are categorized on their large scale morphological shape. They are seen seventeen times in aerial photographs of convex profiles and three times on profiles that develop to a convex shape. Build-up is not observed every time the megaripples are found.


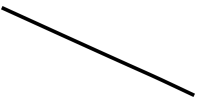

<b>Convex</b> 	<b>Linear</b> 	<b>Concave</b> 
<b>Baalhoek</b> Megaripples seen 0 times	<b>Kats</b> Megaripples seen 0 times	<b>Annajacobapolder</b> Megaripples seen 0 times
<b>Bath</b> Megaripples seen 0 times	<b>Waarde, 1<sup>st</sup> transect</b> Until approx. 2002. Megaripples seen 0 times	<b>Waarde, 2<sup>nd</sup> transect</b> Until approx. 2003. Megaripples seen 1 times Megaripples also seen once in 2005
<b>Knuitershoek</b> Megaripples seen 3 times	<b>Zandkreek</b> Megaripples seen 0 times	
<b>Land van Saeftinghe</b> Megaripples seen 0 times	<b>Zuidgors</b> Until 2001. Megaripples seen 1 times Megaripples also seen once in 2003	
<b>Waarde, 1<sup>st</sup> transect</b> Starting approx. 2005. Megaripples seen 4 times		
<b>Waarde, 2<sup>nd</sup> transect</b> Starting approx. 2009 Megaripples seen 1 times		
<b>Waarde, 3<sup>rd</sup> transect</b> Megaripples seen 2 times		
<b>Zuidgors</b> Starting approx. 2005 Megaripples seen 7 times		

Table 2.6: This table shows how many times the megaripples are observed. This is done for all tidal flats that are analyzed. The flats are categorized based on their large scale shape. A flat has two entries if it has two different shapes in the analyzed period.

### Relative height and linear slope

In the remaining part of this section the 90 percent bootstrap confidence interval is determined and discussed for the average relative height and linear slope of the categories in the build-up. The confidence intervals are used in the second part of this research, in chapter 3. It is for instance used to explain how strong wave induced bottom shear stress is at the location of certain small scale features. The confidence interval determination is also done to show that the categories in the build-up are seen on certain heights and slopes. This is expected if the categories are in alphabetical order on convex profiles. The confidence intervals are determined with the bootstrap method with 10,000 samples. They are determined for all categories in the build-up, if build-up is observed. Thus, build-up on both linear and convex profiles is taken into account. The arbitrary categories between build-up and salt marsh are not considered. The occurrence of a category in the build-up is taken into account when it is covered by elevation measurements and build-up is observed in the aerial photograph of interest. A tidal flat has thus more influence on the determined parameters if more often build-up is seen. This method is chosen instead of assigning each transect the same weight to prevent that linear transects have the same influence as convex profiles, despite build-up being seen more often on the convex ones. Note that the heights are scaled by half of the tidal range to obtain the relative height to make the different tidal flats comparable. The linear slope is determined with the actual heights in m NAP instead of relative height.

The average relative height of the categories in build-up descends with alphabetical order, see figure 2.7, except for category (h), which shows a relatively large vertical spread. The figure's left panel shows the 90 percent bootstrap confidence interval of the average relative height for the categories in the build-up. On the right side is displayed how often a category has occurred in the build-up and at the same time been covered by elevation measurements. The confidence interval's shape is convex-like, if category (h) is neglected. It can also be seen that the confidence intervals show some overlap, a certain average relative height is not only found for one category.

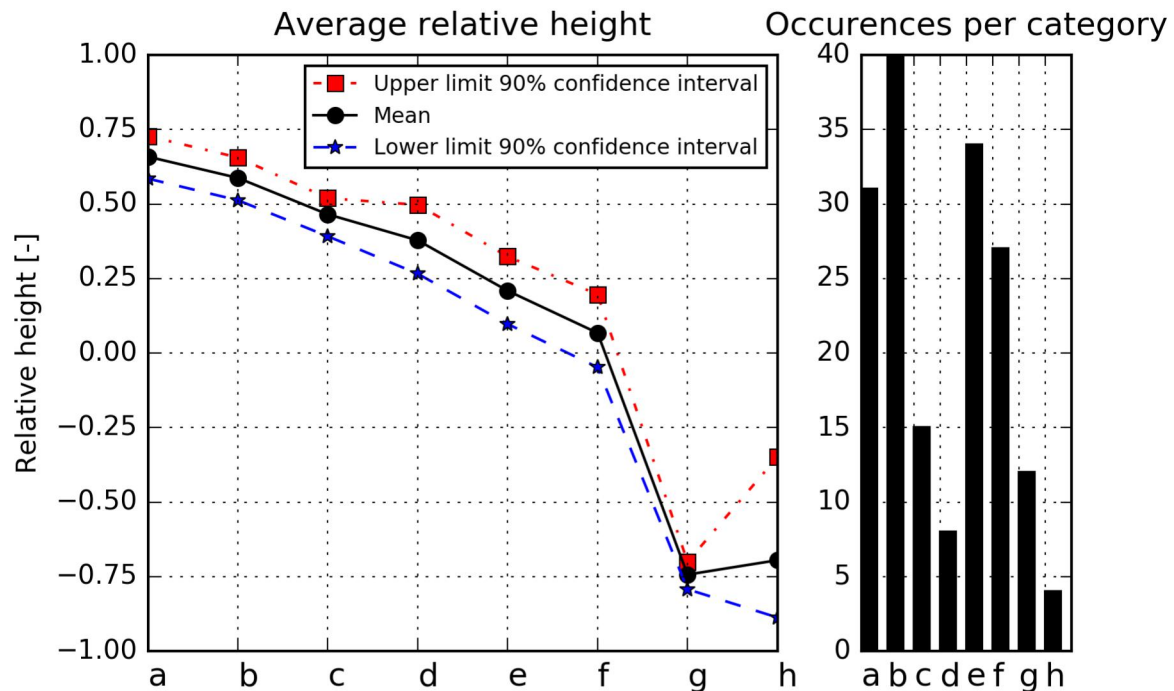


Figure 2.7: The 90 percent bootstrap confidence interval of the average relative height is shown in this figure for all the categories in the build-up. The red line indicates the upper limit, the blue line the lower limit and the black line the mean value of the average relative height. On the right is indicated how often a category has occurred in the build-up and at the same time been covered by elevation measurements.

An area's average relative height lies on average nine out of ten times between approximately -0.7 and -0.8 when build-up is observed and the area is categorized as ship keel traces (g). Relative heights can be read out for other categories in a similar way. The interval width is approximately 0.15 relative height for category (a), (b) and (c), 0.25 for (d), (e) and (f), 0.1 is seen for (g) and 0.5 for category (h).

The linear slope of the categories becomes steeper with alphabetical order, see figure 2.8, except for category (b) and (h). The figure's left panel shows the 90 percent bootstrap confidence interval of the linear slope for all the categories in the build-up. On the right it is indicated how often a category has occurred in the build-up and at the same time been covered by elevation measurements. The width of the interval decreases with alphabetical order up to (e), except for category (b). The confidence interval is approximately the same for category (e) and (f), in width and value. Category (g) has a slightly larger interval width than (e) and (f). This increases further with category (h). The confidence intervals of (a) and (b) are also similar. Overlay is seen for the linear slope of the categories; A certain slope can be found for multiple categories.

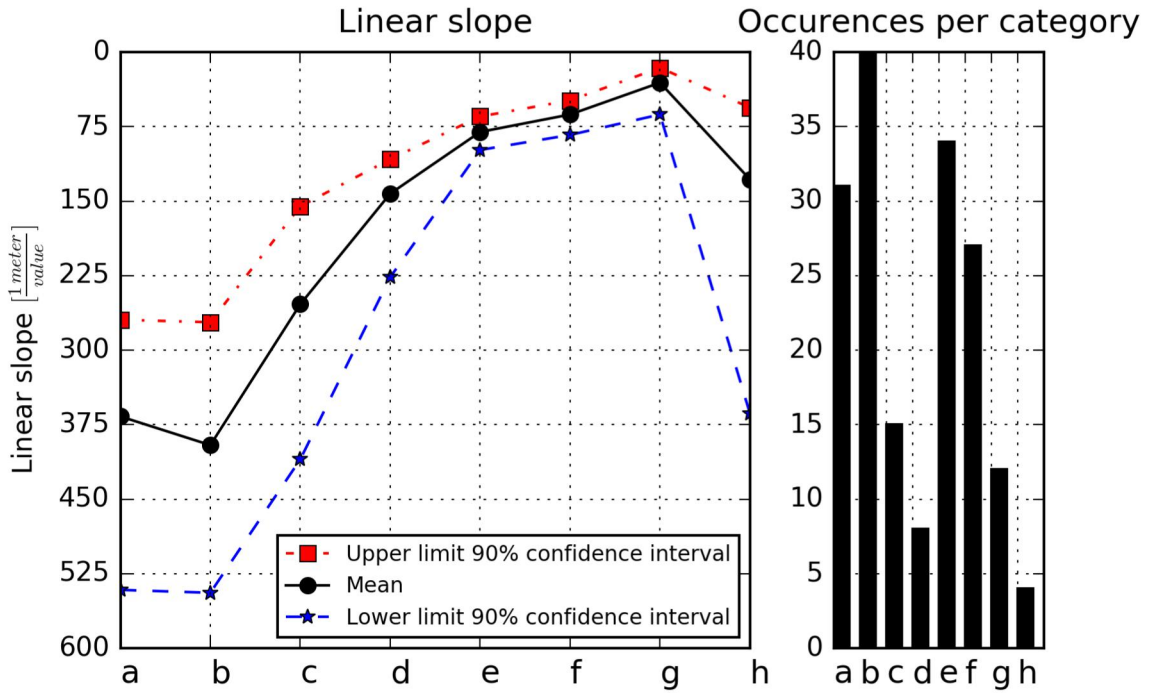


Figure 2.8: The 90 percent bootstrap confidence interval of the linear slope is shown in this figure for all the categories in the build-up. The red line indicates the upper limit, the blue line the lower limit and the black line the mean linear slope. On the right is indicated how often a category has occurred in the build-up and at the same time been covered by elevation measurements.

In most cases it is likely justified to fit a sloped line through the height measurements that are used to determine the linear slopes. Figure 2.9 shows box plots of the probabilities that actually no slope is present in the measurements. A high probability indicates that a series of elevation measurements is likely to represent a flat, not inclined, area. Note that this probability does not say anything about the precision of the determined slope. Mostly outliers are seen in figure 2.9 and no complete box plots. This indicates that in most cases it is probably justified to fit a sloped line through the data. For category (a), (b), (g) and (h) are several larger probabilities seen. Thus, several areas covered by these categories are more probable to be flat than inclined.

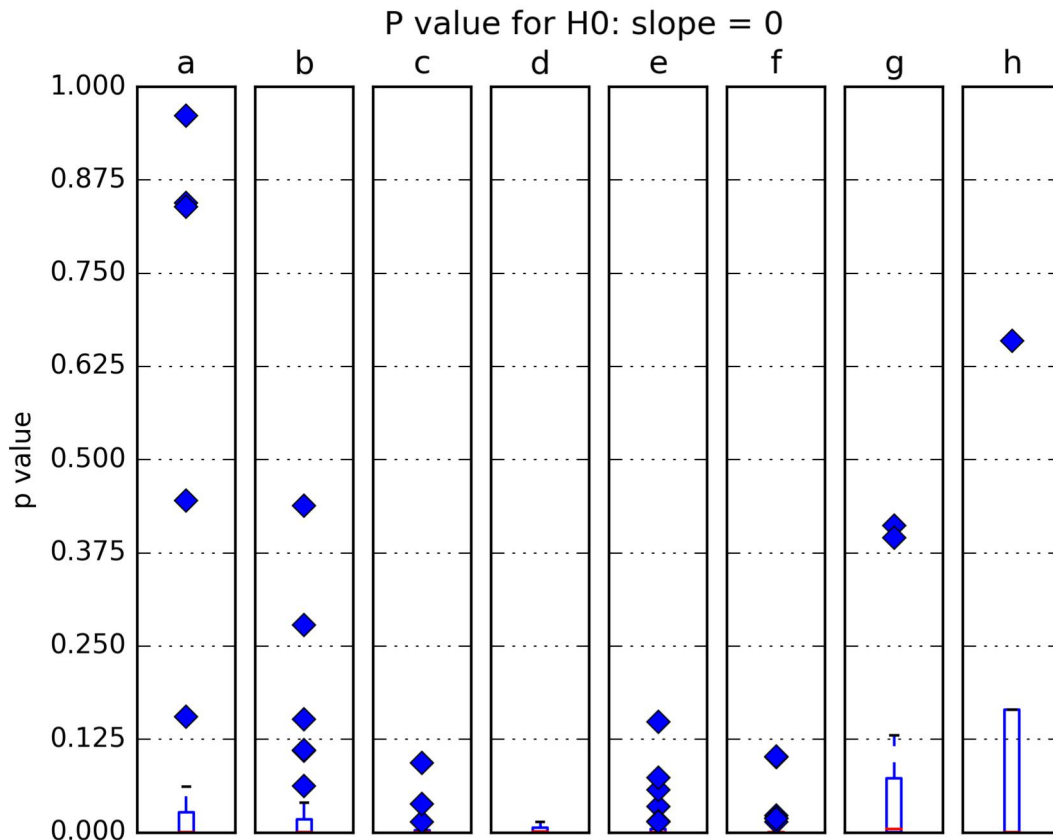


Figure 2.9: This figure shows box plots of the probabilities that actually no slope is present in the height measurements that are used to determine the linear slopes. Thus, high probabilities indicate that a linear slope is fitted wrongly.

## 2.4. Discussion

The results seen in paragraph 2.3 are further discussed in this paragraph. This is done in two sections. Remarks on the large scale morphological shape and development are given first. Secondly, the types of small scale morphological features and their location with respect to the large scale morphology are discussed.

### 2.4.1. Large scale morphological shape and development

Except for Baalhoek, Waarde's 1<sup>st</sup> transect (for two years) and Waarde's 3<sup>rd</sup> transect all convex profiles are accreting, see table 2.3. At Baalhoek the shipping channel and/or human induced measures to protect this channel could be the reason for this deviating behavior. The stabilization of the accreting behavior at Waarde's 1<sup>st</sup> transect is only seen for two years. This doesn't necessarily mean this transect will be non-accreting in the future. Therefore, it could be argued that only two convex profiles show non-accreting behavior. The reason for the deviating behavior of Waarde's 3<sup>rd</sup> transect could be the large tidal flat in front of this transect or the headlands that are present.

Not always a complete profile is measured with GPS, see appendix A. This could have to do with the water elevation during the measurement moments. During a lower stage of the tide a more complete profile can be measured, because a larger part of the tidal flat is emerged. The years mentioned in table 2.3 could be inaccurate, due to this missing information. A transition in large scale shape or development could have been present in a year with an incomplete measured transect.

Almost all linear profiles are classified as stable in the cross shore direction, see table 2.3. This is not always clearly distinguishable for two reasons. The first reason is that not all measurements have an equal extent. This makes the coverage at the waterfront not perfect and concluding a cross shore evolution hard. The second reason is that the linear profiles are long. This makes small deviations in cross shore direction hard to observe.

### **2.4.2. Small scale morphological features**

Points of discussion are mentioned for the small scale morphological feature investigations in this section. First the different types of features are treated and afterwards the location of them with respect to large scale morphological shape.

#### **Different small scale morphological feature types**

Resolution and contrast in the aerial photographs could be important in category determination. Two photographs of the same area at the same moment could be judged differently if the resolution and/or contrast differ(s). An area could be classified as (nearly) smooth for instance in low resolution, while texture is seen in a high resolution photograph. The same mistake between texture and pools can be made. Lack in contrast also could result in wrongful classification as nearly smooth.

It could be argued that the categories defined in paragraph 2.3.2 have some overlay in their definitions and that their interpretation is not completely objective, despite the effort done in this research. This means that a redo of the research could give slightly different results. Thus, some exceptions on the conclusions are likely to occur, because of the classification. It also means that the definitions can not be used in a fool proof way.

#### **Location of small scale morphological features**

Build-up in categories between salt marsh and waterfront is seen regularly at five of the eight convex transects, see table 2.5. Build-up is observed regularly if it is seen in more than half of the categorized aerial photographs. In total it is seen 47 times out of the 85 photographs that are analyzed for convex shapes. Temporal variation of the important mechanisms for build-up formation and too high water while acquiring the photo could explain that it is not always seen at the five convex transects where build-up is observed regularly. Photos are observed where build-up is not seen according to the definition, but it seems to be present at the upper part. Lower categories of the build-up appear to be covered in these photographs by water. Baalhoek, Knuitershoek and Waarde's 1<sup>st</sup> transect are the three convex profiles that do not show the build-up regularly. At Baalhoek build-up is seen thrice, in 2000, 2003 and 2006. After 2005 the profile shape starts to deform to a crooked convex profile, see paragraph 2.3.1. That the build-up isn't seen after 2006 could be caused by this. Knuitershoek shows the build-up four times. A large channel is located in between the two parts of salt marsh. This could be the reason for the absence in categorical build-up. Another reason could be the sharp transition between the lower and upper part of the profile, see paragraph 2.3.1. Waarde's 1<sup>st</sup> transect is the last tidal flat where the build-up in categories is not seen regularly. This transect only shows it twice. An explanation could be that a tidal flat sized channel that is always located next to the transect or goes through it, see paragraph 2.3.2. Also at other tidal flats is seen that tidal flat sized channels disturb the presence of the build-up in categories.

The concave and most linear transects in this research don't show a build-up in categories, see table 2.5. Kats shows the build-up twice in ten aerial photographs and Waarde's 1<sup>st</sup> transect shows it once in one photo, both tidal flats have a linear shape. Temporal variations in the mechanisms important for the formation of this build-up could explain that it is sometimes seen on some linear transects, instead of never. Linear profiles can be seen as profile shape in between convex and concave. This makes it logical that build-up is sometimes seen on linear profiles when it is often seen on convex and never on concave profiles.

The megaripples are seen in less than a quarter of the analyzed aerial photographs from convex profiles, 17 out of 85 times. That these features are seen at the far channelward side could be an explanation for why they are not observed often. They could be covered by water in aerial photographs that are not acquired during low water.

Ship keel traces, category (h), are not often observed in the build-up and covered by elevation measurements, only four times. This could explain the deviant behavior and large confidence interval widths seen in paragraph 2.3.2. A convex like shape is shown for the confidence interval of the relative heights that are coupled to the build-up's categories. The ship keel traces are the only exception. The slope of the categories in the build-up is shown to become steeper with alphabetical order, an exception is again seen for the ship keel traces. The confidence interval of the relative heights and slope is wider for the ship keel traces than for all other categories, another deviation.

Large confidence interval widths are observed for linear slope of the pools (a) and pools with gully formation (b), see paragraph 2.3.2. These areas have a very mild declination. This could explain the large band width. The linear fitted slope is more influenced by small deviations in the data when an area has a milder slope. For some occurrences it is also more likely that no slope is seen, see figure 2.9. This fact also adds to the interval width. These mild slopes can also explain why the average slope decreases instead of increases between category (a) and (b). The slope increases in general with alphabetical order. That build-up indicates convex profiles is in agreement with the found slope increase. Therefore, this behavior is also expected for the pools and pools with gully formation.

## 2.5. Conclusion

The central sub-question in this chapter and its two underlying questions are repeated first. Their hypotheses are recapitulated and evaluated in individual sections.

"Are the small scale morphological features on estuarine tidal flats indicators for large scale morphological shape and development?" is the central sub-question in this chapter. The two related questions are:

- (a) Which large scale morphological shapes and developments are found on estuarine tidal flats?
- (b) What are the different types of small scale morphological features seen on estuarine tidal flats and where do they occur with respect to large scale morphological shape and development?

### 2.5.1. Large scale morphological shape and development

The question treated in this section is: "Which large scale morphological shapes and developments are found on estuarine tidal flats?". The hypothesis is: "Convex profiles that show accreting behavior and linear and concave profiles that show eroding behavior will be found."

All three profile types mentioned in the hypothesis are indeed found; Convex, linear and concave profiles are found in this research, see paragraph 2.3.1. However, convex profiles are only found in the Western Scheldt. Linear and concave profiles are found in both the Western and Eastern Scheldt.

The other part of the hypothesis links large morphological scale shape and development. This part is also true, with some exceptions. All, except one, linear profiles and all concave profiles are eroding. All, except two, convex profiles are accreting, see paragraph 2.4.1.

It can be concluded, in addition to the hypothesis, that the linear profiles show a stable behavior in cross shore direction and the concave and convex profiles show a mixed development, see paragraph 2.3.1. The linear profiles show mostly a stable behavior in the cross shore direction. Concave profiles are found to be retreating and stable. Both retreating and expanding behavior is seen for convex profiles.

### 2.5.2. Small scale morphological features

The question treated in this section is: "What are the different types of small scale morphological features seen on estuarine tidal flats and where do they occur with respect to large scale morphological shape and development?". The hypothesis is that pool shaped small scale features with adjacent gullies should indicate convex shape and indirectly indicate accreting tidal flats.



Besides pool shaped and gully features also (nearly) smooth areas, ship keel traces, megaripples, texture and algae mats are seen on the tidal flats. This part of the hypothesis is thus incomplete, more features than pools and gullies are seen. In paragraph 2.3.2 ten categories of small scale morphological features are distinguished. Five of these are (combinations of) pools and/or gullies. Thus, five small scale feature types are seen that are not mentioned in the hypothesis: (nearly) smooth areas, ship keel traces, megaripples, texture and algae mats. Algae mats are not directly morphological features, but they do influence the small scale morphology to a large extent, see paragraph 2.2.2. The (nearly) smooth areas are not a morphological feature as well. However, they are characteristic and therefore considered important.

The hypothesized link between accreting convex profiles and pool shaped features with adjacent gullies is not confirmed in this research. Convex profiles turn out to be indicated by megaripples and/or a build-up in the categories, introduced in paragraph 2.3.2. However, the absence of the indicators does not mean that the large morphological shape is not convex. Most of the convex profiles are accreting. It is also found that all features in the build-up are indicators on their own. They indicate certain relative height and slope, when they are seen in the build-up.

47 of the 85 analyzed aerial photographs of convex profiles show the build-up. For linear profiles this is three out of 25 and for concave profiles none out of eight, see also paragraph 2.3.2. Five out of eight convex profiles show the build-up regularly, meaning that it is seen in at least half of the processed aerial photographs. Sharp transitions in the convex profile and build-up disturbance by tidal flat sized channels could be the reason that the other three don't show the build-up regularly, see paragraph 2.4.2. Note that this disturbance by large scale channels is neglected where possible. High water and temporal variations in important mechanisms could explain that build-up is not always seen on the five transects where build-up is observed regularly. The few times it is seen on linear profiles could also be due to temporal variations in mechanisms important for the build-up formation, see paragraph 2.4.2.

The convex profiles that are indicated by the build-up in categories are not exclusively accreting. Four out of five convex transects that show the build-up regularly are accreting, one is eroding. The build-up is also seen on both retreating and expanding profiles.

The megaripples indicate a convex profile or a profile that develops to a convex profile, see paragraph 2.3.2. Thus, they indicate a large scale shape or a development. The megaripples are observed in less than a quarter of the analyzed aerial photographs from convex profiles, seventeen out of 85 analyzed aerial photographs from convex profiles. This is less than the build-up occurs. However, they are an accurate indicator for large scale shape or development; They are not observed on a linear or concave profile that does not develop to a convex profile. Therefore, this indicator is valuable.

All the feature categories in the build-up are indicators on their own. They indicate a certain relative height and slope when they are seen within the build-up, see paragraph 2.3.2. This is not a large scale morphological shape or development. However, together they indicate a convex profile. For all categories in the build-up significant confidence intervals of relative height and slope are found for the areas where they occur in the build-up. The found developments are in line with the indicated profile: convex. The confidence intervals are also used in chapter 3, where the indicator role of the build-up is explained. Only the occurrences are counted when build-up is observed and the category's area is covered by elevation measurements. The relative heights of categories in build-up are descending with alphabetical order in convex like fashion, see paragraph 2.4.2. The slope of the areas the categories occur increases in steepness with alphabetical order of the categories.

In addition to the hypothesis, it is found that large scale channels are dominant over small scale morphological features. The presence of large scale channels often disturbs the build-up in small scale morphological features. It is mentioned in paragraph 2.4.2 that at Waarde's 1<sup>st</sup> transect almost no build-up is seen. The tidal flat sized channel next to the transect is given as a possible reason. In paragraph 2.3.2 is mentioned that at several tidal flats also deviant behavior is seen around large scale channels. Therefore, it is concluded that large scale channels are dominant over small scale morphological features.

### **2.5.3. Answer to sub-question**

The central sub-question in this chapter is: "Are the small scale morphological features on estuarine tidal flats indicators for large scale morphological shape and development?". The answer is: Yes, they are. The presence of a build-up in small scale morphological feature categories is an indicator for convex large scale morphological shape and indirectly for accreting development. It is also found that all the feature categories in the build-up are indicators on their own. The megaripples indicate (future) convex profiles. Additionally, all of them indicate a certain relative height and slope, when they are seen within the build-up. Together this indicates a convex profile.

# 3

## Mechanisms explaining the indicators

### 3.1. Introduction

The indicators that are found in chapter 2 are explained in this chapter. The presence of a build-up in small scale morphological feature categories is found to be an indicator for convex large scale morphological shape and indirectly for accreting development. Descriptive text and examples of the categories are given in paragraph 2.3.2. The build-up definition is:

1. It starts at the landward side of the tidal flat with pool shaped features or pools with gully formation.
2. At least two of the following categories are seen channelwards of this start: pools with gully formation, pools and gullies, gullies, vague gullies, (nearly) smooth, ship keel traces and megaripples.
3. The consecutive categories are in the order mentioned. Some exceptions are made:
  - (a) The following categories may once be reversed: vague gullies with (nearly) smooth areas and ship keel traces with megaripples
  - (b) Sometimes one or two arbitrary categories are seen between the build-up and salt marsh/dyke. This is neglected in the required order, as long as their coverage is small. These categories are mostly (vague) gullies or (nearly) smooth areas.
  - (c) Areas with texture (contrast is seen but no distinguishable features) or tidal flat sized channels sometimes disturb the build-up, this is neglected.

It is also found that all the feature categories in the build-up are indicators on their own. The megaripples indicate (future) convex profiles. Additionally, all of them indicate a certain relative height and slope when they are seen within the build-up. Together they indicate a convex profile. Five different small scale morphological feature types are important for this indicator: pool shaped features, gullies, (nearly) smooth areas, ship keel traces and megaripples.

"Which mechanisms explain the found indicator roles of small scale morphological features?" is the sub-question answered in this chapter. Build-up of feature types is the main indicator that is found. All other indicators are seen within the build-up. Therefore, the sub-question can be rephrased to: "Why is the build-up in small scale morphological feature categories coupled to the convex large scale morphological shape?". This covers indirectly the other indicators as well. Pool shaped features are the most important feature type for the build-up; Without pool shaped features the definition can never be met, because of demand 1 in the build-up definition. Therefore, the focus is on pool shaped features in this chapter's research.

Forming and erasing mechanisms of the feature types are probably important for the indicators and their link to (convex) profile shape. Two facts indicate that forming and erasing mechanisms could be important. First of all, the build-up and megaripples are not always found at the convex shaped tidal flats, see paragraph 2.3.2. Secondly, the small scale morphological features in the build-up are mostly not found at the same location in subsequent aerial photographs, observed during part 1's analysis. The following two questions can be extracted from the above:

- (i) Which mechanisms are responsible for **erasing** the small scale morphological features that are seen in the build-up and how are they influenced by the large scale morphological shape?
- (ii) Which mechanisms are responsible for **forming** the small scale morphological features that are seen in the build-up and how are they influenced by the large scale morphological shape?

Large wave induced bottom shear stresses are foreseen to erase the small scale morphological features. Furthermore, it is expected that these stresses are less on the upper part of convex profiles than seen on top of linear and concave profiles. These hypotheses concern question (i). Erosion is observed during storms [Xie et al., 2017] and during a storm the bottom shear stresses due to waves are dominant [Lawson et al., 2007][Fagherazzi and Wiberg, 2009]. Hence, it is hypothesized that large bottom shear stresses, due to waves, are the erasing mechanism for the small scale morphological features in the indicator. This holds for all feature types involved in the build-up.

The forming mechanisms of the small scale morphological features in the indicator are assumed to differ per feature type. This concerns question (ii). The five feature types are treated separately. The focus is on the pool shaped features; They are most important for the build-up definition. All the hypotheses are stated below.

### 1. Pool shaped features

A mechanism with positive feedback or event based forming mechanism is expected to create the pool shaped features. The features are sometimes seen on the same location in subsequent aerial photographs. This is observed by the author while doing the first part's analysis and is proven in this research. The constant location indicates that the pools are formed by events or that the forming mechanism has a positive feedback on itself. A period without the event based forming mechanism would explain why the location remains constant. A mechanism with positive feedback keeps enforcing the pool shaped features by deepening them after they are initiated. This makes the pools more persistent and allows them to remain at the same location between two photographs. Some evolution of the pools is seen when pool shaped features are not erased in the period between two aerial photographs. They expand/shrink, get more connected and move. The evolution favors the forming mechanism with positive feedback. The evolution makes more sense for something that is ongoing than for a mechanism that happens once in a while. The forming mechanism with positive feedback is treated first and more extensively, because it is the favored theory. Note that the positive feedback should be counteracted by a negative feedback at some point or frequent influence of the erasing mechanism. Otherwise, the positive feedback continues deepening the pools and deep pools would be seen, deeper than several centimeters. These are not observed, which is proven in this research.

#### 1.1. Forming mechanism with positive feedback

The forming mechanism with positive feedback can be split in four components: initialization, positive feedback, evolution of the pools and negative feedback starting to become important at some point. Each component is elaborated on below. The mechanisms important for initialization and negative feedback are not investigated in this research. However, the existence of the negative feedback is evaluated, by looking at the existence of deep pools.

##### 1.1.1. Initialization

Heterogeneity in soil composition and forces during a storm and/or influence of organisms living in/on the soil can cause local indents on the top of convex tidal flats. This is the assumed initializing mechanism. Water will remain in these indents if the area has a mild slope, due to drainage incapacity. This mild slope links the initiation to profile shape. The positive feedback can start once water remains in the indents.

### 1.1.2. Positive feedback

Unequal distribution of soil strength and erosion are expected to cause the positive feedback. A lower critical bed shear stress, soil strength, is expected at the inside of the pools. This makes them more sensitive to erosion. Moderate eroding forces, compared to the soil strengths, can cause differences in development in- and outside pool features, due to unequal strengths. A combination of processes during emergence and submergence is foreseen to be important. Therefore, a certain ratio between submergence and emergence time is required. This makes the relative height and tide important for the positive feedback, linking the positive feedback to the profile shape. The mechanisms that cause the unequal critical bed shear stresses and erosion are elaborated on below.

#### \* Uneven critical bed shear stresses

Diverging critical bed shear stresses could be formed by wind waves in the pool shaped features and unequal drying. Both processes occur during emergence. The slightly higher located parts will dry easier than the indents that store a small layer of water. This unequal drying will cause higher critical shear stresses at the upper parts, the soil compacts better. Wind blowing over the small water layers forms wind waves in the pools. Waves can bring soil in movement if they are big enough. Hence, they could prevent the soil in the pools from settling, or at least decrease the settling effect. This decrease of settling means less compaction and consequently less strength. The unequal drying is not looked into in this research.

#### \* Uneven erosion

Erosion takes place during submergence of the flat due to wind waves from the estuary. The waves are generated in this case over a longer fetch than seen during emergence. The erosion is uneven when the eroding forces are in the order of the critical bed shear stresses. Approximately equal erosion will be seen for large eroding forces; In- and outside the pools the critical bed shear stress will be exceeded. No erosion will be seen for small eroding forces, because the threshold for erosion is not reached.

### 1.1.3. Evolution of pools

Locally generated wind waves and drainage are expected to cause the evolution of the pool shaped features. Drainage induced currents are foreseen to erode the edged of the pool shaped features and form connections. The edge of a pool is eroded when water is flowing to a lower pool. A transition to gullies can be thought of when evolution happens fast or during a long time. Wind waves generated in the pools can cause expansion of the pool in direction opposite to the wind direction.

### 1.1.4. Negative feedback

Deeper pools attract more sediment, hypothetically. This is the negative feedback on pool shaped morphology. Water with sediment propagates over the tidal flat during rising and falling tide. The deposition/erosion rate of this sediment depends on bottom shear stress and on settling velocity. The stresses are induced by currents and waves. The settling velocity is coupled to sediment size. A stagnant water body is reached when rising/falling water reaches a pool. The flow slows down and the wave heights are expected to decrease, due to bigger water depth. Both cause the bottom shear stresses to drop and sedimentation is triggered. Furthermore, for the same wave height a decrease in bottom shear stress will be seen, because of the larger water depth. This also causes more sedimentation. The explained mechanisms are more prevailing for deeper pools. The existence of the negative feedback is evaluated. This is done by looking at the existence of deep pools.

## 1.2. Event based forming mechanism

Drainage after a high water event, without severe wave impact, is hypothesized to be the event based forming mechanism of pool shaped features. Water is piled up in the Western Scheldt during strong and persistent northwestern winds. Wave impact is small on most tidal flats for this wind direction, because of their orientation. Drainage after this high water event could cause strong cross shore currents on the upper part of the tidal flat. These currents could form the pool shaped features. They are caused by drainage of a large water volume from the salt marsh. Therefore, the mechanism is linked to the large scale morphological shape.

## 2. Gullies

Drainage forms the gullies, see paragraph 1.1. At a certain point on the tidal flats drainage induced currents are expected to be big enough to cause gully formation. In other words, a certain minimum requirement should be met to form gullies. This depends on the large scale morphological shape.

## 3. (Nearly) smooth area

The erasing mechanism is, hypothetically, stronger than each of the forming mechanisms of small scale features at the (nearly) smooth areas in the build-up. Most forming mechanisms and the erasing mechanism are linked to large scale morphological shape. Their ratio is therefore linked to the shape as well.

## 4. Ship keel traces

The ship keel traces could be formed by ships running aground. It is seen in paragraph 2.3.2 that these features are strongly linked to a relative height close to the channel. It is expected that the features are not linked to large scale morphological shape, only to relative height; Profile shape does probably not determine whether a ship runs aground.

## 5. Megaripples

Strong along shore current form the megaripples, hypothetically. These features are found as indicator for (future) convex profiles.

The hypotheses for the small scale feature forming and erasing mechanisms are evaluated in various ways: Two 1D models are created, a field campaign is conducted, (subsequent) aerial photographs are looked into, elevation measurements are analyzed in detail and literature research is conducted. Most aerial photographs and all elevation measurements are the same as mentioned in the first part, in paragraph 2.2. They are obtained by Rijkswaterstaat [Rijkswaterstaat, 2017b][Rijkswaterstaat, 2017a]. All locations mentioned in this chapter are indicated in figure 3.1.

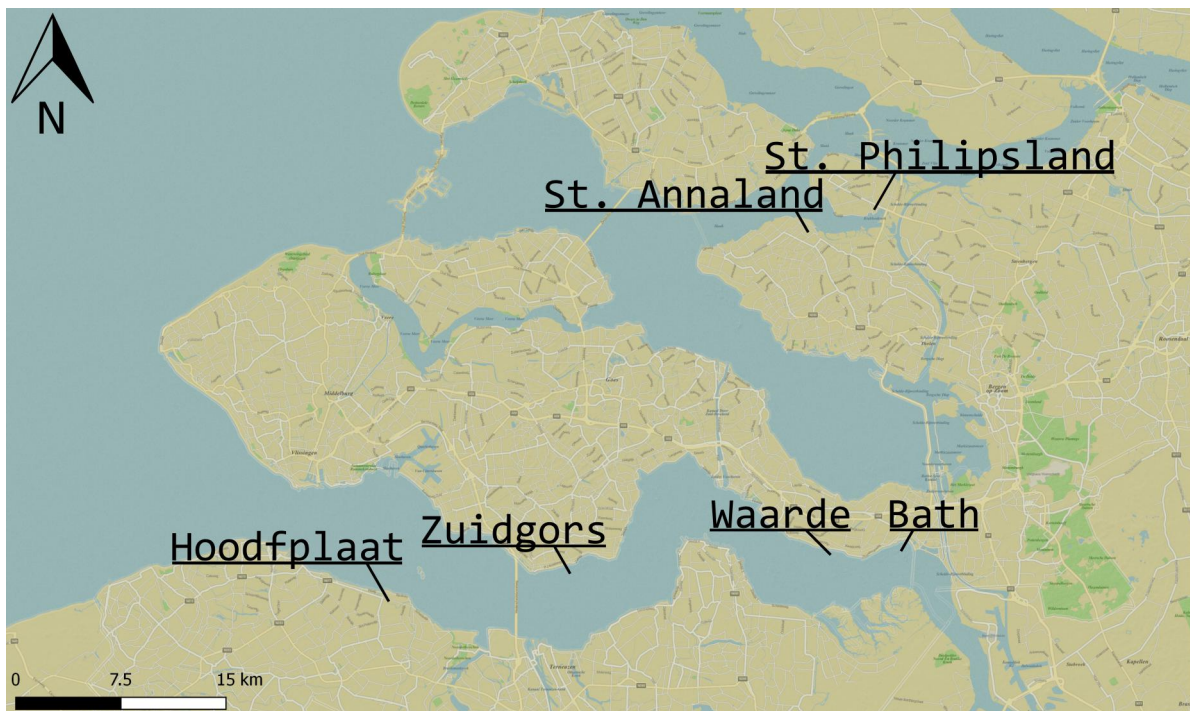


Figure 3.1: This figure shows the location of all places mentioned in this chapter.

Separate sections are used in the remaining part of this chapter to discuss the methodology, results, discussion and conclusion of investigating the erasing mechanism and each feature type's forming mechanism. The erasing mechanism is treated first, because obtained insights are important for explaining some features' forming mechanisms. Answer is given in the end of this chapter to the treated sub-question, which is: "Why is the build-up in small scale morphological feature categories coupled to the convex large scale morphological shape?"

## 3.2. Erasing mechanism

The question treated in this section is: "Which mechanisms are responsible for erasing the small scale morphological features that are seen in the build-up and how are they influenced by the large scale morphological shape?". The hypothesis is: "Large wave induced bottom shear stresses erase the small scale morphological features. These stresses are less on the upper part of convex profiles than seen on top of linear and concave profiles."

This erasing mechanism is determined by looking at aerial photographs and a 1D model that makes use of SWAN to calculate the wave propagation. The exact methodology is given first. Secondly, the results are given. The flaws of this determination are given next, in the discussion. Finally, the hypothesis is evaluated and a conclusion is given on the erasing mechanism and its dependence on large scale morphological shape.

### 3.2.1. Methodology

In this section is given how aerial photographs and a 1D model are used to determine the mechanism that erases small scale morphological features. First the aerial photographs are discussed and secondly the model. The "Sinterklaasstorm" is mentioned in both approaches. This storm event took place on 5 and 6 December 2013 in Northern Europe. It is chosen for two reasons. First of all, the storm is completely covered with wind measurements from the KNMI [2017] at the required locations. Secondly, the storm was severe and coincided with spring tide.

#### Aerial photographs

Two approaches with aerial photographs are used to evaluate the hypothesis that large wave induced bottom shear stresses are the mechanism that erases the small scale morphological features. The approaches are:

1. Investigate aerial photographs from the tidal flat opposite St. Philipsland and next to St. Annaland, see figure 3.1 for these locations. It is unlikely that currents and waves play an important role at this tidal flat. The presence of small scale morphological features in these photos indicates whether the hypothesis could be true. It is possible that waves and/or currents are an erasing mechanism if the features are observed at this tidal flat. Another mechanism could be important in erasing the features when they are not present. That the small scale features are not formed at this location is another possibility when the features are not seen. Note that the aerial photographs of this tidal flat are the only photographs that are not used in the first part of this research, which is shown in chapter 2.
2. Visually determine the impact of the "Sinterklaasstorm" at Zuidgors and Waarde's second transect from aerial photographs taken before and after the storm, see figure 3.1 for these locations. Aerial photographs and the categorized images are used for this purpose.

#### SWAN model

A 1D model is used to investigate how bottom shear stresses due to waves and currents depend on large scale morphological shape. It is also used to look at the difference in storm impact at Zuidgors and Waarde's second transect. The "Sinterklaasstorm" in 2013 is simulated for this purpose. In the remaining part of the research this model is also referred to as SWAN model, because another 1D model is used as well. "SWAN is a third-generation wave model, developed at Delft University of Technology, that computes random, short-crested wind-generated waves in coastal regions and inland waters", according to The SWAN Team [2017]. It is used to calculate wave propagation under influence of currents. Bottom shear stresses are estimated with help of this propagation. Higher bed shear stresses are more important for sediment entrainment, which is important for an erasing mechanism. Therefore, a high percentile of the bottom shear stresses due to waves and currents during a tidal cycle is calculated from the SWAN output. The 90<sup>th</sup> percentile is chosen. This means that the calculated bottom shear stresses are exceeded ten percent of the submerged time of a tidal cycle. A tidal cycle is defined in this research from high tide until the next high tide. The required model input is summarized below. See appendix C for a more detailed description of the model set-up, including the used formulas.

### 1. Bottom levels

An equally spaced computational grid is obtained by interpolating bottom levels, measured with GPS. The location and year of these measurements depend on the location of interest.

### 2. Wind speed, wind direction and fetch length

The waves are estimated by a JONSWAP spectrum at the offshore boundary of the computational grid. The spectrum represents young sea states, which can be expected in estuaries, and follows from the Joint North Sea Wave Project (JONSWAP) [Hasselmann, 1973]. Wind speed, wind direction and fetch length are required to calculate the spectrum. The fetch length is the distance to upwind coastlines [Holthuijsen, 2009], i.e. the distance over which wind can generate waves. Wind measurements from the KNMI [2017] are used when realistic wind characteristics are required.

### 3. Water level measurements

Volume balances in cross and along shore direction are used to determine current velocities in both directions. These balances use measured water levels from Rijkswaterstaat [2017c]. All these measurements have a temporal resolution of ten minutes. The cross shore current velocities are determined with a volume balance in cross shore direction that assumes a horizontal water level and uniform current speed over the depth. The measured water levels at the nearest station are used for this purpose. They are also used to represent the tide at the investigated tidal flat. The along shore current velocities are determined with a volume balance that involves all measurement stations up stream of the investigated tidal flat. The balance gives the net volume change upstream of the transect of interest. An average current velocity, uniform over depth, is determined by dividing the net volume change by the average water depth of the concerned cross section. The average current velocity is scaled with the square root of the water depth in the cross shore direction.

For every water level measurement a new run with the SWAN model is done. This means that the wave propagation is calculated with a new imposed water level every ten minutes.

Three important assumptions are done in this model. First of all, the minimum water depth is set at five centimeters. Every positive water depth smaller than this is set to five centimeters. Secondly is the wind and wave induced setup is neglected in this model. The third assumption is that the JONSWAP spectrum is fully developed for every run (every ten minutes); The spectrum is fetch limited and not time limited.

Details of the analyses with SWAN are given below. First the influence of large scale morphological shapes is discussed. Secondly, the "Sinterklaasstorm" impact at Zuidgors and Waarde's second transect is treated. The results of both analyses are visualized in plots showing the bottom shear stress due to currents, waves and both combined. The bottom profile and tidal range are also given in these plots.

### Large scale morphological shape

Bottom shear stresses at convex, linear and concave profiles under different forcing conditions are analyzed with the SWAN model to investigate the influence of large scale morphological shape. The model input is summarized below. In total, three different wind speed with three different tidal ranges are inspected for three different tidal flat shapes, resulting in 27 simulated tidal cycles.

#### 1. Bottom levels

Realistic profiles are obtained for the convex, linear and concave profiles by using measured profile shapes at the tidal flat Waarde. These three profile shapes are seen over the years at Waarde. The separation of the three transects at Waarde by headland construction is probably the reason for this. The convex and concave profile are measured with GPS at Waarde's second transect, in 2013 and 1993 respectively. The linear profile is measured at Waarde's first transect in 2001. The computational grids for the model are acquired by linear interpolation of these elevation measurements on a grid with a one meter interval. The measurements are extrapolated to depths significantly beneath low water, if necessary. This extrapolation could result in an unrealistic profile end. However, a sufficient water depth makes sure that instabilities due to boundary conditions have damped before they reach the area of interest. The part of the tidal flat that emerges during low water is of interest. The stress behavior at the area with potential unrealistic extrapolation is less important than at the area of interest. Therefore, the used approach is justified.



## 2. Wind speed, wind direction and fetch length

Three different wind speeds are analyzed to invest mild and stormy conditions: 5, 10 and 15 meter per second. The wind speed is kept constant during a simulated tidal cycle. Increasing/decreasing the fetch length gives qualitatively the same effect as increasing/decreasing the wind speed; The wave spectrum gets more/less peaked, with a higher/lower peak energy and lower/higher peak frequency. Hence, only the wind speed is varied. The fetch length is set at 5000 meters. The modeled wind direction is perpendicular to the tidal flat.

## 3. Water level measurements

The local tide is simulated with water levels measured at Baalhoek and along shore currents are calculated with measurements from all stations upstream of Baalhoek. The measurements are done by Rijkswaterstaat [2017c]. An arbitrary tidal cycle is chosen. Resulting in the period between 17 April 2013 07:20:00 and 17 April 2013 19:20:00. The water levels representing the tide are also used to calculate the cross shore currents. The water levels are multiplied by factors 0.8, 1.0 and 1.2 to evaluate different tidal ranges.

### "Sinterklaasstorm"

The "Sinterklaasstorm" is simulated for Zuidgors and Waarde's second transect with the SWAN model by simulating two tidal cycles. These cycles cover the storm duration. The model input is summarized below

#### 1. Bottom levels

The computational grids for the model are obtained by linearly interpolating 2013's elevation measurements at Zuidgors and at Waarde's second transect on a one meter spaced grid. The measurements are extrapolated to depths significantly beneath low water, if necessary. This extrapolation could result in unrealistic profile ends. However, a sufficient water depth makes sure that instabilities due to boundary conditions have damped before they reach the area of interest. The approach is justifiable, because the stress behavior at the area with potential unrealistic profile is not important.

#### 2. Wind speed, wind direction and fetch length

Wind speeds and wind directions are taken from measurements done by KNMI [2017] at Hoofdplaat and Hansweert, for respectively Zuidgors and Waarde. Wind directions deviating less than 90 degrees from the transect direction are taken into account. The fetch lengths, distances to upwind coastlines, are determined with help of Qgis and Python. A polygon is drawn in Qgis that represents the hard boundaries of the Western Scheldt. This is based on satellite images. The polygon is assumed to coincide with the coastlines. The fetch length, distance between transect and polygon, is determined for all angles of interest in Python. This is visualized in figure 3.2 for Zuidgors.

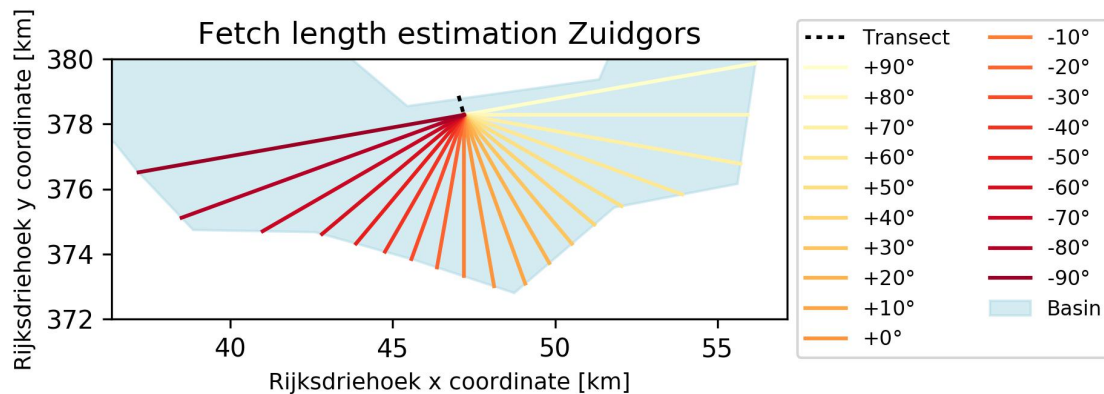


Figure 3.2: Visualization of fetch length determination at Zuidgors. Fetch length is the distance to upwind coastlines and is determined for all angles that deviate less than 90 degrees from the transect.

#### 3. Water level measurements

The tide at the flats is simulated with water level measurements at Terneuzen and Baalhoek, respectively for Zuidgors and Waarde. The along shore currents are calculated with measurements upstream of these stations. Two tidal cycles cover the storm duration. These cycles are defined to be from high tide to high tide. For Zuidgors this is between 5 December 2013 03:50:00 and 6 December 2013 04:20:00. These tidal cycles are between 5 December 2013 04:40:00 and 6 December 2013 05:00:00 for Waarde.

### 3.2.2. Results

This results section can be split in two parts. Both elements reflect on the hypothesis that large wave induced bottom shear stresses erase the small scale morphological features. Aerial photographs are given first. Secondly, results from a model are shown. They indicate how the wave induced bottom shear stresses depend on the large scale morphological shape and whether they dominate the current induced bottom shear stresses.

#### Aerial photographs

Aerial photographs with two different purposes are given. First, aerial photographs are shown of the tidal flat opposite to St. Philipsland and next to St. Annaland. They show that small scale morphological features are seen on an estuarine tidal flat with small wave and current impact. Secondly, categorized and real aerial photographs of Zuidgors and Waarde's second transect are given for the years 2013 and 2014. They show that the "Sinterklaasstorm" erased the pool shaped features to a large extent on both flats.

#### Tidal flat opposite St. Philipsland: a flat with small waves and currents

Small scale morphological features are found at approximately the same location in subsequent years on a tidal flat with small tidal current and wave impact. Figure 3.3 displays a tidal flat opposite to St. Philipsland and next to St. Annaland, see figure 3.1 for these locations. The channel is blocked on the East side. Currents along the tidal flat are expected to be small for that reason. The wave impact is expected to be small as well; The channel is narrow and the tidal flat is surrounded by other flats. Small scale morphological features can be distinguished in the upper left figure, which displays a part of the flat in detail. Pool shaped features are seen near the salt marsh vegetation and gullies are observed more to the waterfront. Figure 3.4 displays a part of the tidal flat in 2009 and in 2014. The small scale morphological features are seen at approximately the same location. The 2014 photograph is after the "Sinterklaasstorm". This a severe storm in 2013, treated in the next part of this research. Hence, even after a significant storm are the features still seen at the same location.

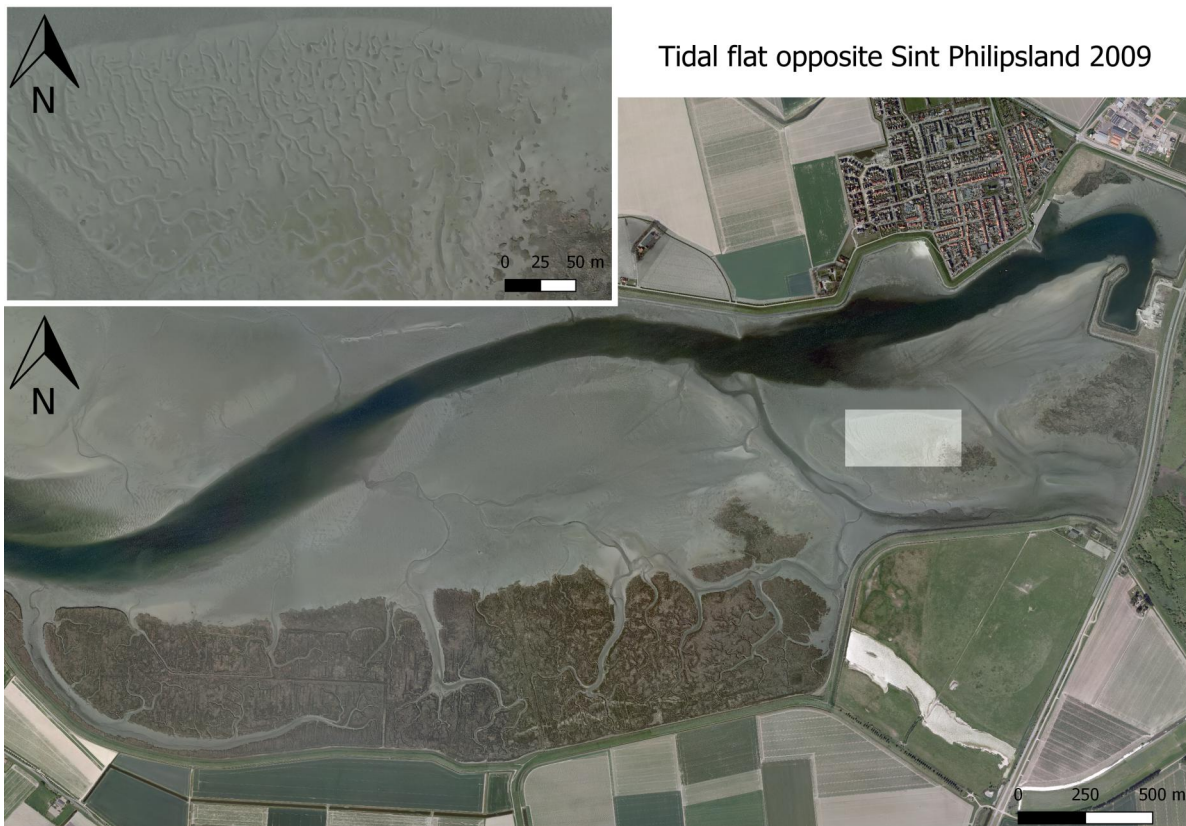


Figure 3.3: Aerial photograph of the tidal flat opposite St. Philipsland and next to St. Annaland in 2009. A part of the tidal flat is given in more detail on the upper left figure. This area is indicated by a bright rectangle in the main figure.

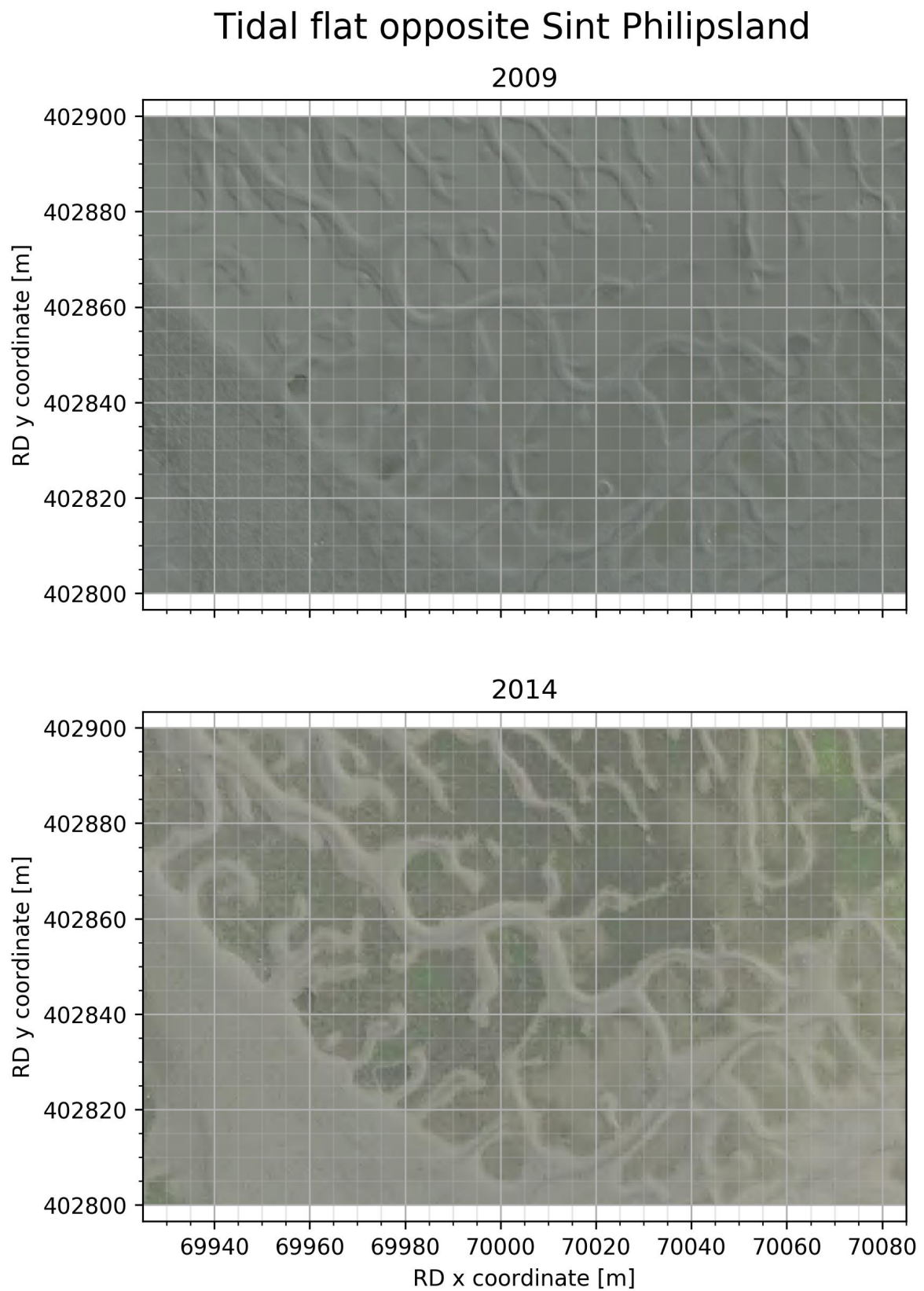


Figure 3.4: A part of aerial photographs of the tidal flat opposite St. Philipsland and next to St. Annaland. The upper one is taken in 2009 and the lower one in 2014.

### ”Sinterklaasstorm” Zuidgors and Waarde

The pool shaped features are erased after the ”Sinterklaasstorm” for Waarde’s second transect and remain at Zuidgors, according to the categorized aerial photographs. Categorized aerial photographs from before and after the storm are displayed in figure 3.5. The pool shaped features are clearly removed after the storm at Waarde; Category (a) and (b) are no longer observed after the storm. Disappearance of the pool shaped features at Zuidgors doesn’t become clear from figure 3.5; Category (a) is still seen after the storm.

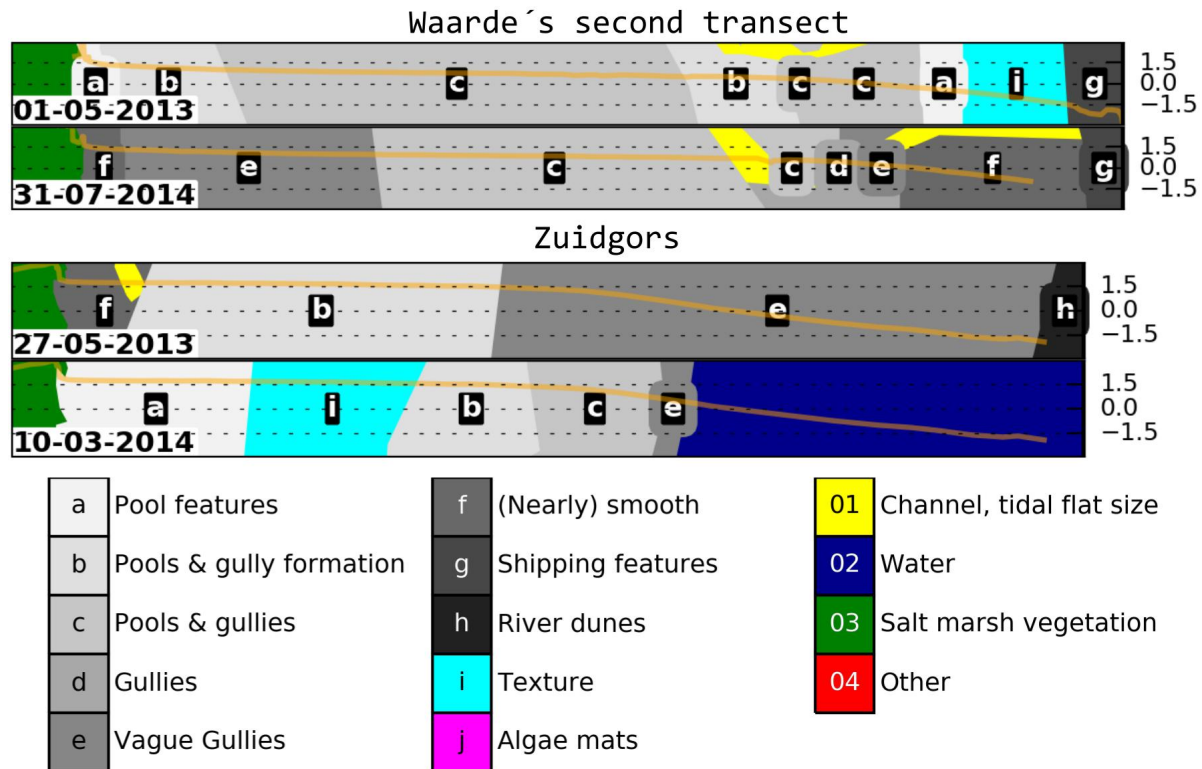


Figure 3.5: Categorized aerial photographs from before and after the ”Sinterklaasstorm” for Waarde’s second transect and Zuidgors. The upper figures are obtained before and the lower ones after the storm.

Partially erased pool shaped features at Zuidgors are seen in the non-categorized aerial photographs in figure 3.6. This figure shows a part of aerial photographs of Zuidgors in 2013 and 2014, zoomed in on the pool shaped features. Some of the pools observed in 2014 can be recognized from 2013. Figure 3.7 displays a part of the non-categorized aerial photographs for Waarde’s second transect in 2013 and 2014. The figure is focused on the pool shaped aerial photographs as well. Complete removal of pool shaped features can be seen in figure 3.7. This is similar to observations from the categorized aerial photographs in figure 3.5.

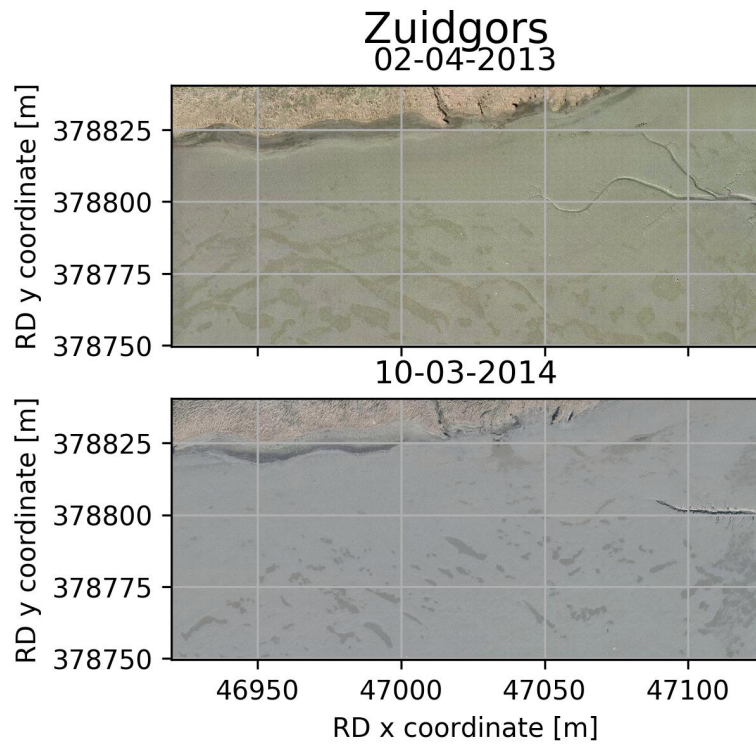


Figure 3.6: Small part of aerial photographs from before and after the "Sinterklaasstorm" for Zuidgors. The pool shaped features are given in detail. Therefore, only a small area is displayed. The upper figure is from before the storm and the lower one after it.

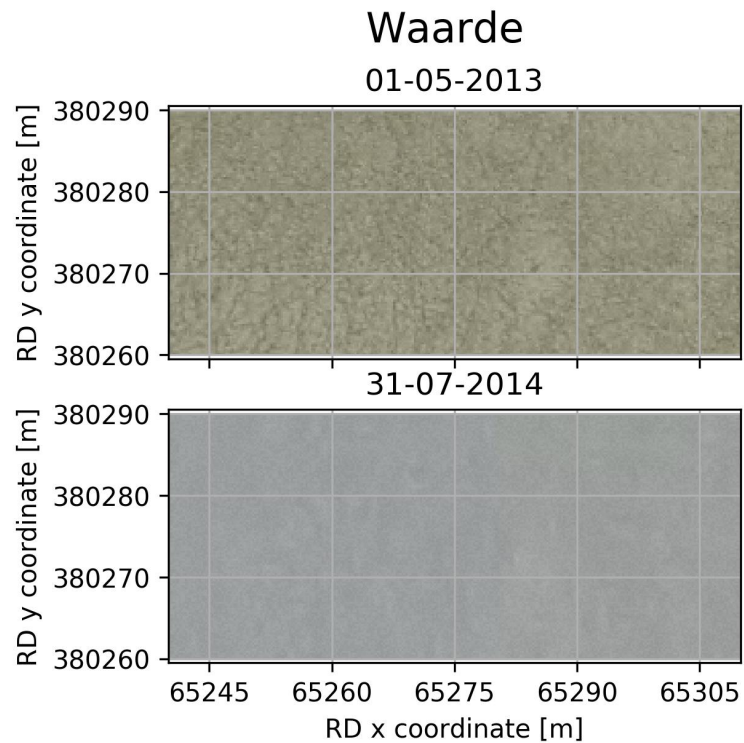


Figure 3.7: Small part of aerial photographs from before and after the "Sinterklaasstorm" for Waarde's second transect. The pool shaped features are given in detail. Therefore, only a small area is displayed. The upper figure is from before the storm and the lower one after it.

## SWAN model

Estimates of wave and current induced bottom shear stresses are given in this section with two different purposes. They are obtained with a 1D model that makes use of SWAN to calculate wave propagation under influence of the currents, for details on the model see paragraph 3.2.1. First, it is shown that estimated bottom shear stress, due to the combined effect of waves and currents, is less on the upper part of convex profiles than seen on top of linear and concave profiles. It is also shown in this first section that bottom shear stresses develop differently in the cross shore direction for the three large scale shapes. Comparable impact of the "Sinterklaasstorm" at Zuidgors and Waarde is displayed in the second part. It becomes clear from both sections that wave induced bottom shear stresses dominate current induced bottom shear stresses during storms.

### Large scale morphological shape

Bottom shear stresses due to the combined effect of waves and currents are less on the upper part of convex profiles than on top of linear and concave profiles. Figure 3.8 gives the estimated 90<sup>th</sup> percentile bottom shear stresses due to waves, currents and a combination of both for one tidal cycle. Different forcing conditions and different large scale morphological shapes are analyzed. The combined stresses are observed to be less on the upper part, right in front of the salt marsh, on the convex profiles than on top of the linear and concave profiles. This phenomenon becomes more clear when wind speed increases. Stresses under  $0.75 \frac{N}{m^2}$  are observed for the convex profile with a wind speed of fifteen meter per second. Stresses around this value are found for the linear profile and above this value for the concave profile. Changing the tidal range has limited influence on the observed behavior of the bottom shear stresses. A larger tidal range imposes slightly higher current velocities, and vice versa. The location where shear stresses are observed is also influenced by the tidal range. The results of different tidal ranges are given in appendix D.

Bottom shear stresses develop differently in cross shore direction for diverging large scale morphological shapes, see figure 3.8. The combined bottom shear stresses decrease in the landward direction for the convex profile, for all wind speeds. These stresses remain approximately constant on the linear profile, after the waves start to feel the bottom. On the concave profiles the stresses increase in landward direction. The observed developments are mainly due to the wave induced bottom shear stresses.

Wave induced bottom shear stresses dominate the current induced stresses for large wind speeds. This becomes clear from figure 3.8. Additionally, high stresses are observed on the salt marsh cliffs.

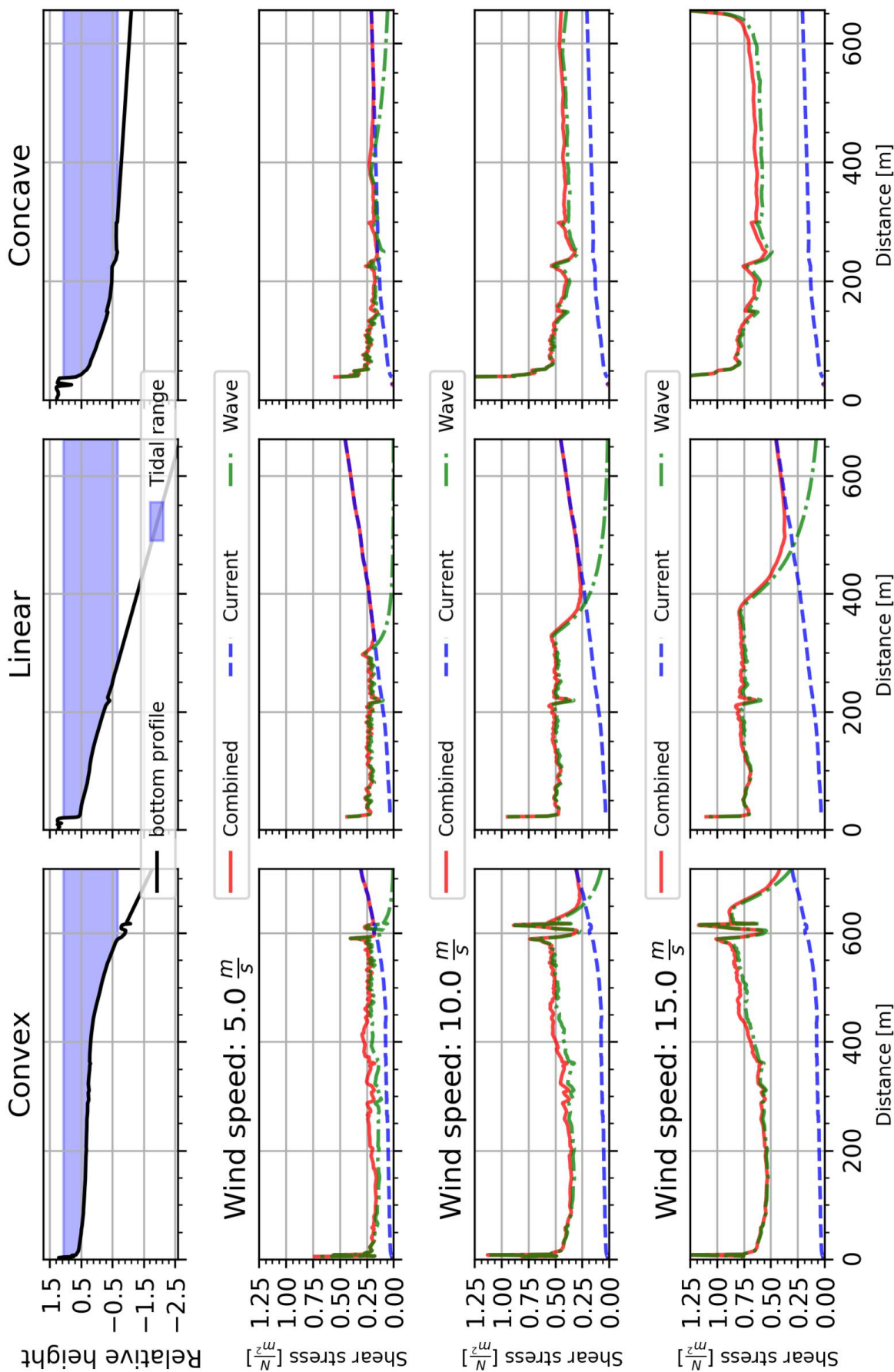


Figure 3.8: This figure shows the estimated 90<sup>th</sup> percentile bottom shear stresses due to waves, currents and a combination of both for one tidal cycle under different forcing conditions and for different large scale morphological shapes. These estimates are done with a 1D model that makes use of SWAN to calculate wave propagation under influence of currents, see paragraph 3.2.1. Every large scale morphological shape has its own column. The left column displays the estimates for three different wind speeds on a convex profile. In the middle and right column this is done for linear and concave profiles respectively. The estimated bottom shear stresses that belong to one wind speed are displayed in the same row. This holds for the bottom three rows. The upper row shows the highest and lowest water level in the analyzed tidal cycle and the bottom profile that is used as model input.

### "Sinterklaasstorm"

The impact of the "Sinterklaasstorm" storm is comparable at the upper part of the profile at Zuidgors and Waarde's second transect. Figure 3.9 displays the estimated bottom shear stresses due to waves, currents and the combined effect at Zuidgors during two tidal cycles. These cycles cover the duration of the "Sinterklaasstorm" and are from high tide to high tide. The 90<sup>th</sup> percentile during each cycle is given for the three stresses. The same is displayed for Waarde's second transect in figure 3.10. Wave induced bottom shear stresses dominate the current induced stresses in both figures. At Zuidgors only one tidal cycle gives significant wave impact. The wind direction deviates too much from the transect's direction during the other cycle, more than 90 degrees. Therefore, the waves are estimated as very small. At the upper part of the tidal flats comparable values for combined bottom shear stresses are observed for the most significant tidal cycle. At Zuidgors the combined bottom shear stress is just under  $0.50 \frac{N}{m^2}$  in front of the salt marsh. At Waarde it is just above this value. High bottom shear stresses are seen on the salt marsh cliff and wiggles are observed at Waarde as well.

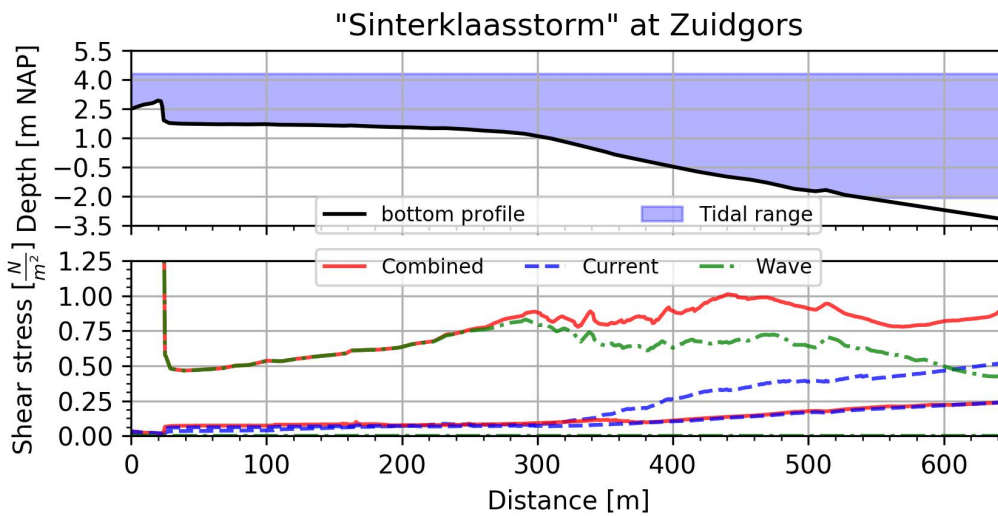


Figure 3.9: The lower figure displays estimated bottom shear stresses due to waves, currents and a combination of both for two tidal cycles at Zuidgors. These cycles cover the duration of the "Sinterklaasstorm". The 90<sup>th</sup> percentiles are displayed for each cycle. The upper image shows the highest and lowest water level in the two tidal cycles and the bottom profile that is used as model input.

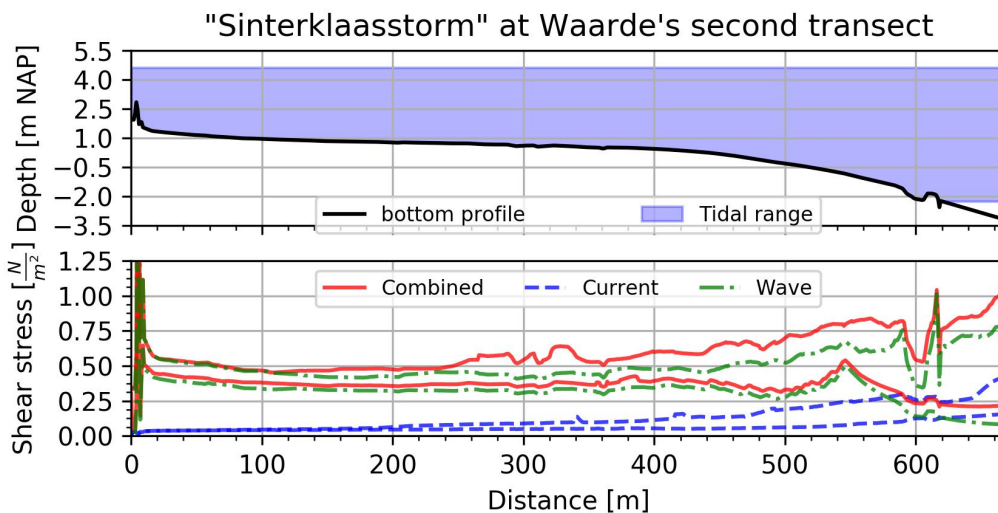


Figure 3.10: The lower figure displays estimated bottom shear stresses due to waves, currents and a combination of both for two tidal cycles at Waarde's second transect. These cycles cover the duration of the "Sinterklaasstorm". The 90<sup>th</sup> percentiles are displayed for each cycle. The upper image shows the highest and lowest water level in the two tidal cycles and the bottom profile that is used as model input.



### 3.2.3. Discussion

The SWAN model simulations are discussed in this section. The simulations are done to investigate whether wave induced bottom shear stresses erase the small scale morphological features. The aerial photographs did not bring up any discussion points.

Current induced bottom shear stresses could also dominate the wave induced stresses, depending on the tidal flat location in estuary. Waves are found to be more important than currents during storm conditions, see paragraph 3.2.2. The way the offshore along shore currents are estimated in this research is not considered accurate. The currents are estimated by volume balances and assume equal distribution over the cross shore and depth, see paragraph C.1.3.2 for more details. A more complex 3D distribution of flow is to be expected, based on the estuary's bathymetry. Therefore, the quantities obtained by the SWAN model should not be used. Along shore currents, instead of waves, could erase the small scale morphological features if a tidal flat is situated in a location where strong along shore currents are found. The approach in this research is considered to be just if the along shore currents at the channelward end of the tidal flat are well known. The along shore currents on the tidal flat can be expected to downscale with the water depth in that case, as is done in this research.

The bottom shear stress development in cross shore direction is different for convex, linear and concave profiles, see paragraph 3.2.2. This partially explains the large scale morphological development seen in paragraph 2.5.1. An decrease in bottom shear stresses is linked to accreting behavior, under the assumption that we can simplify the more correct formulation. Accretion is seen when sediment transport decreases, according to the more correct formulation. This sediment transport is related to bottom shear stresses, making our simplification justifiable [Friedrichs and Aubrey, 1996]. Eroding behavior is linked to increasing bottom shear stresses and stable behavior to constant shear stresses, under the same assumptions. Most convex profiles were found to be accreting. The bottom shear stresses are found to be decreasing in landward direction. The two behaviors correspond. The concave profiles and most linear profiles are eroding. The eroding behavior of the concave profiles can be explained by the found stress increase towards the shore. For the linear profiles an approximately constant bottom shear stress is found in the cross shore direction, after the moment the waves start to feel the bottom. This alone can not explain the found erosion. Lag processes need to be included to explain the erosion. The higher bottom shear stresses are looked into to explain the profile behavior. These occur at the tidal front during raising tide. This is observed by the author, while creating the model mentioned in paragraph 3.2.2. Water propagates from estuary to shore during raising tide. At the start of the profile this water contains probably less sediment than the equilibrium concentration, due to lag processes. The bottom shear stress rises quickly at the point where waves start to acknowledge the bottom, see figure 3.8. The sediment concentration can not keep up with this quick raise due to lag processes [Winterwerp, 2015]. Therefore, the rising tide collects more sediment during propagation over the tidal flat and erosion is seen.

Fetch lengths are overestimated for some wind directions during estimation of the impact of the "Sinterklaasstorm". Large fetch lengths are obtained for wind directions with a large angle with the transects, see figure 3.2. These lengths are unrealistic; Waves have probably refracted to the shore and/or lost energy on shallow areas before they have propagated the distance towards the analyzed transect. Therefore, the large fetch length is not completely effectively available. The comparison of the storm's impact is still justified, despite the overestimation. Both transects have approximately the same orientation, they differ twenty degrees. The impact on both transects is therefore overestimated.

Using another high percentile to compare the bottom shear stresses might give other model results than seen in paragraph 3.2.2. Bottom shear stresses are compared by their 90<sup>th</sup> percentile over a tidal cycle. It is stated in paragraph 3.2.1 that a high percentile must be chosen. However, the 90<sup>th</sup> percentile is arbitrary chosen. The influence of taking another high percentile is not investigated. Other outcomes could be possible. Summation of the bottom shear stresses, higher than a certain threshold, during a tidal cycle might give a more robust comparison. This will enhance the found differences in shear stresses in the cross shore; The upper part of the tidal flats are emerged for a larger part of the time.

High bottom shear stresses are observed on the salt marsh cliffs in paragraph 3.2.2. This can be explained by the model set-up and the steep slope at the cliff. A steep slope forces waves to shoal and break in SWAN, which is used to calculate the wave propagation. The cliff could also cause wave reflection. This induces less shear stresses than shoaling and breaking. Reflection is not included automatically in the SWAN model

according to the author's knowledge, gained from the model documentation [The SWAN Team]. The cliff is not modeled as an obstacle. This is required to get reflection. Therefore, the high shear stresses could be an overestimation. The overestimation is not important, because the focus is on the tidal flat instead of the salt marsh. Slightly higher bottom shear stresses could be observed at the upper part of the tidal flats when reflection at the cliffs are taken into account. Due to reflection higher waves could be observed at the upper part of the tidal flats; The reflected wave's peaks and troughs can align with the inbound wave's peaks and troughs and thereby form bigger waves. Wiggles are observed at the salt marsh cliff at Waarde's second transect in figure 3.10. They are caused by the big transitions in bottom elevation.

### 3.2.4. Conclusion

The question treated in this section is: "Which mechanisms are responsible for erasing the small scale morphological features that are seen in the build-up and how are they influenced by the large scale morphological shape?". The hypothesis is: "Large wave induced bottom shear stresses erase the small scale morphological features. These stresses are less on the upper part of convex profiles than seen on linear and concave profiles."

Large wave induced bottom shear stresses are the mechanism that erases small scale morphological features. The features are observed at approximately the same location in subsequent years on a tidal flat with small influence of waves and currents, see paragraph 3.2.2. Furthermore, pool shaped small scale morphological features are (partially) erased after the "Sinterklaasstorm" at tidal flats with severe wave and current impact during a storm. It is shown that wave induced shear stresses dominate the current induced stresses during storm conditions, see paragraph 3.2.2. Hence, large wave induced stresses erase the small scale morphological features.

Wave induced bottom shear stresses are smaller on the upper part of convex profiles than on top of linear and concave profiles, see paragraph 3.2.2. This proves the hypothesis is true. The mentioned area mostly contains pool shaped features. These smaller shear stresses could indicate that pool shaped features are more often erased on concave and linear profiles than on convex profiles, assuming they are formed on all three large scale shapes. This can explain that pool shaped features are not seen on concave profiles, see appendix B. However, the pool shaped features are seen on linear profiles. Whether they are seen less on linear profiles than on convex profiles is not investigated. This should be the case if the difference in shear stresses causes more often a wipe out on linear profiles.

Deviating development of the bottom shear stresses in cross shore direction is observed for different large scale morphological shapes in paragraph 3.2.2. This is not mentioned in the hypothesis. The combined bottom shear stresses decrease in the landward direction for the convex profile, for all wind speeds. These stresses remain approximately constant on the linear profile, after the waves start feeling the bottom. On the concave profiles the stresses increase in landward direction. This deviating development of bottom shear stresses can explain the accreting convex profiles and eroding concave profiles, see paragraph 3.2.3. Together with lag processes they could also explain the eroding behavior at the linear profiles.

In summary can be concluded that the hypothesis is true. Large wave induced bottom shear stresses are smaller at the top of convex profiles than on linear and concave profiles and it is the mechanism that erases small features. In addition to the hypothesis can be concluded that bottom shear stresses decrease in landward direction for convex profiles, remain approximately constant for linear profiles and increase for concave profiles.

### 3.3. Pool forming mechanism

In this section the following question is answered with respect to pool shaped small scale morphological features: "Which mechanisms are responsible for forming the small scale morphological features that are seen in the build-up and how are they influenced by the large scale morphological shape?". A mechanism with positive feedback or event based mechanism is hypothesized to form pool shaped features. The mechanism with positive feedback is the favored hypothesis. This mechanism has four important components: initialization, positive feedback, evolution and negative feedback. The mechanisms important for initialization and negative feedback are not looked into, see paragraph 3.1 for their hypotheses. However, the existence of the negative feedback is evaluated, by looking at the existence of deep pools. The positive feedback should be due to uneven soil strengths (critical bed shear stresses) and resulting uneven erosion. Diverging critical bed shear stresses can be formed by wind waves in the pool shaped features and unequal drying, processes during emergence. The unequal drying is not looked into. Uneven erosion has to take place during submergence of the flat, due to wind waves from the estuary. These waves should induce bottom shear stresses in the order of the critical bed shear stresses. Wind waves in pools and drainage are expected to cause the evolution of the pools. High current velocities during drainage after a high water event without severe wave impact is foreseen as event based mechanism.

The mechanism with positive feedback is looked into by analyzing aerial photographs, elevation measurements, wind measurements, field observations and field measurements. The drainage after a high water event without severe wave impact is looked into by a 1D model simulation. The exact methodologies are given first. The results are given subsequently. Some discussion points are given next. Finally, the hypotheses are evaluated and a conclusion is given on the pool shaped feature forming mechanism and its dependence on large scale morphological shape.

#### 3.3.1. Methodology

The methodology to investigate pool shaped feature formation is separated in three parts. The first part is the determination whether pools are sometimes observed at approximately the same location in subsequent aerial photographs. This constant location is the foundation for the hypothesized pool forming mechanisms, see paragraph 3.1. Secondly, the investigation of the forming mechanism with positive feedback is explained. This is done with observations on Zuidgors, field measurements and showing elevation measurements. The third and last aspect contains the methodology to determine whether drainage after a high water event can form pool shaped features.

#### Pool shaped features at constant location

Examples of pool shaped features at the same location in subsequent aerial photographs are given for Zuidgors and Bath, see figure 3.1 for these locations.

#### Mechanism with positive feedback

Three components are investigated that are important for the pool forming mechanism with positive feedback. How this is done is explained in this section. These mechanisms are: positive feedback, evolution and negative feedback. They are discussed in this order.

##### Positive feedback

Unequal distribution of soil strength (critical bed shear stress) and erosion are discussed below, in the order mentioned. Both are important for the positive feedback.

##### a Uneven critical bed shear stresses

Field measurements of the wet soil density in and around two pool shaped features are done to get insight in the uneven critical bed shear stresses. Higher soil densities are coupled to higher critical bed shear stresses. Winterwerp [2015] mentions this is generally the case. Soil samples are gathered in and around two pool shaped features. One pool is lower on Zuidgors and the other is higher located, pool A and B respectively. These locations are indicated in figure 3.11. Three measurements are taken inside pool A and three outside it. For pool B two measurements are done inside and two outside the pool. The

volume and weight of these samples are determined to calculate the wet density. The weight of water layers on top of the sediment is subtracted, if present. The height and location where the samples are acquired are measured with Real Time Kinematic (RTK) GPS. The contours of the pools are measured as well with GPS.

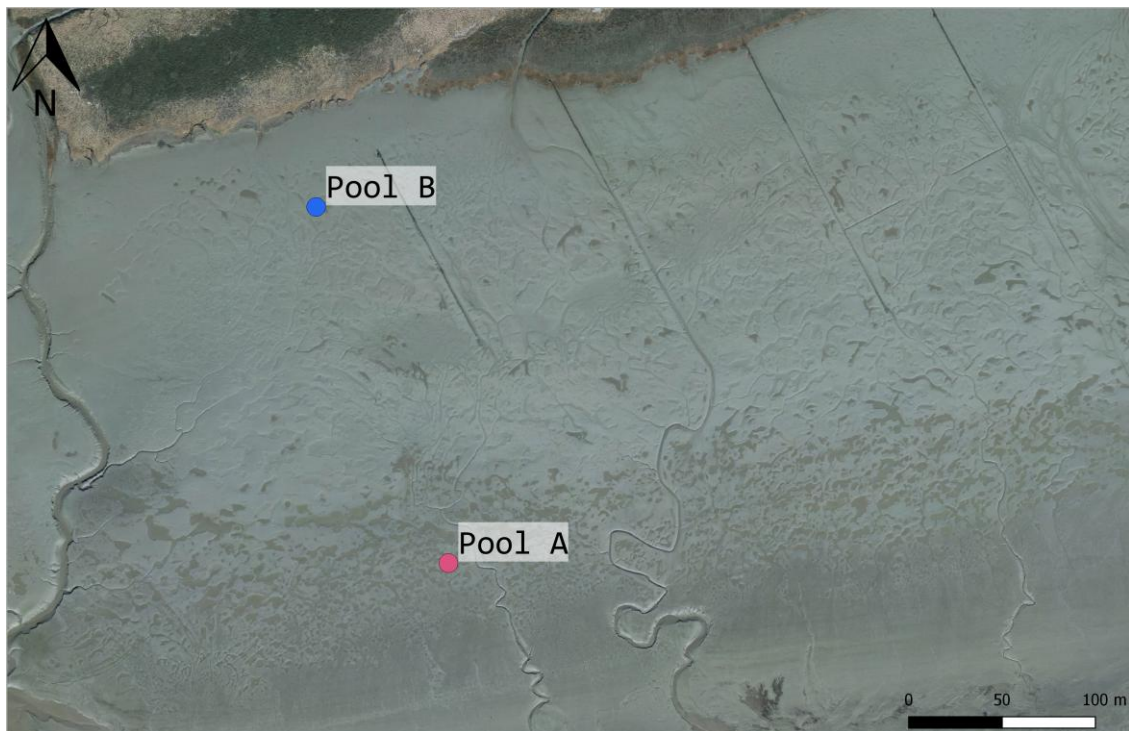


Figure 3.11: Location of the pools where wet density measurements are conducted on Zuidgors. The location is displayed on top of an aerial photograph from 2016.

The height and existence of wind waves in the pools, during emergence, is visually analyzed in a field campaign to Zuidgors on 25 October 2017. The wind waves in a pool near pool B, see figure 3.11, are recorded by a camera. The plausibility of wind waves causing uneven critical bed shear stresses is determined in this way. High wind waves can bring soil into movement. Therefore, they could prevent the soil in the pools from settling, or at least decrease the settling effect. This decrease of settling results in less compaction. Hence, smaller critical bed shear stresses are present in the pools.

#### b Uneven erosion

The eroding force of wind waves is looked at through the model results of the erasing mechanism. The 90<sup>th</sup> percentile of wind wave induced bottom shear stresses during a tidal cycle is obtained with help of a 1D model. Different forcing conditions are inspected. See paragraph 3.2.2 for the results. These stresses indicate the power to erode at the area with pool shaped features. Bed shear stresses in the same order of magnitude as the expected critical bed shear stresses indicate that unequal erosion is likely to occur. The wave induced shear stresses have less impact on the outside in this case, a higher critical bed shear stress is seen there. Severe wave attack is likely to cause erosion at both the in- and outside of the pools. The forces easily exceed the critical shear stresses on both locations during severe wave attack.

In literature critical bed shear stresses between 0.1 and 5  $\frac{N}{m^2}$  are found [Winterwerp, 2015]. The critical values for the area with pool shaped features will be lower in the spectrum, because relatively fine sediment is found on top of the tidal flats [van Eck, 1999].

#### Evolution of pools

It is evaluated whether evolution of the pool shaped features is caused by wind waves generated in the pools and drainage with help of aerial photographs. These photographs should give details about the evolution. The evolution, the prevailing wind conditions and drainage direction are used to evaluate whether locally generated wind waves and drainage cause the evolution. The prevailing wind conditions are obtained from measurements done by KNMI [2017].

### Negative feedback

Elevation measurements are given for the upper part of Zuidgors to investigate whether deep pools exist. Pools are considered deep when the height deviations are more than several centimeters. This investigation evaluates the existence of a negative feedback on the positive feedback mechanism. The positive feedback could continue deepening the pools without a negative feedback or frequently triggered erasing mechanism. This would likely result in pools deeper than several centimeters.

### Drainage after high water event

Drainage induced flow velocities after a high water event are estimated with a 1D model. This model contains mass and momentum balances, formulas 3.1 and 3.2 respectively. The induced bottom shear stresses are determined with formula 3.3. The currents are obtained by solving the mass and momentum equations with a staggered grid approach. This is described in Stelling and Duinmeijer [2003]. The only difference is that flow velocity in the water level points is approximated by a midpoint scheme. Taking the average of two faces gives a more accurate estimate of the flow velocity near the tidal front [Maan et al., 2015].

$$\frac{\partial h}{\partial t} + \frac{\partial uh}{\partial x} = \text{mass balance} \quad (3.1)$$

$$\frac{\partial u}{\partial t} + u * \frac{\partial u}{\partial x} = -g * \frac{\partial \zeta}{\partial x} - \frac{\tau_{bc}}{\rho_w * h} = \text{momentum balance} \quad (3.2)$$

$$\tau_c = \frac{1}{8} * \rho_w * f_c * u^2 = \text{current induced bottom shear stress} \left[ \frac{N}{m^2} \right] [\text{Van Rijn, 1993}] \quad (3.3)$$

with:

$h$  = water depth [m]

$u$  = cross shore current velocity  $\left[ \frac{m}{s} \right]$

$\zeta$  = water level [m]

$g$  = gravitational acceleration =  $9.81 \left[ \frac{m}{s^2} \right]$

$\rho_w$  = water density =  $1000 \left[ \frac{kg}{m^3} \right]$

$\tau_{bc}$  = bed shear stress =  $\rho_w * C_d * u^2 \left[ \frac{N}{m^2} \right]$  [Soulsby, 1997]

$C_d = \frac{g * n^2}{h^{\frac{1}{3}}} [-]$  [Soulsby, 1997]

$n$  = manning coefficient  $\left[ \frac{s}{m^{\frac{1}{3}}} \right]$

$f_c = 0.24 * \left( \log \left( \frac{12 * h}{2.5 * d_{50}} \right) \right)^{-2} [-]$  [Van Rijn, 1993]

$d_{50}$  = median sediment diameter [m]

The model is set up to simulate the high water even on October 22<sup>nd</sup> 2014. This event was large enough to cause closure of the Eastern Scheldt barrier. The most important points of the set-up are:

1. Water levels measured in Terneuzen are used for the analysis. They are interpolated linear on the temporal resolution of the model, one second.
2. The elevation measurements from 2014 on Zuidgors are used to obtain a computational grid. It is interpolated linear on a one meter grid. The measurements do not contain information about the salt marsh behind the flat. However, the salt marsh stores a big amount of water during a high water event. Therefore, a salt marsh with representative dimensions is added to the interpolated values. The obtained profile is smoothed to suppress instabilities.
3. The roughness of the tidal flat and salt marsh are represented by manning coefficients, respectively 0.033 and  $0.05 \frac{s}{m^{\frac{1}{3}}}$ . A gradual transition in roughness between the two areas is constructed to suppress instabilities.
4. A minimum water depth of three centimeters is used in the calculation. Flow velocities are defined zero for smaller water depths.

### **3.3.2. Results**

Examples of pool shaped features and proofs of the two hypothesized forming mechanisms are given in this section. Aerial photographs are given in the first section. These show pool shaped features at approximately the same location in consecutive years. This is done for two tidal flats: Zuidgors and Bath. Secondly, results concerning the pool forming mechanism with positive feedback are given. This explanation contains three parts: positive feedback, evolution and negative feedback. As third and last, the simulated drainage after a high water event is given.

#### **Pool shaped features at constant location**

Figure 3.12 and 3.13 give evidence that pool shaped features are sometimes seen at approximately the same location in subsequent years. This was already stated in paragraph 3.1, where the hypotheses are discussed, and is now backed-up. Pool shaped features are seen at approximately the same location at Zuidgors in 2011, 2012 and 2013, see figure 3.12. They are erased to a large extent in 2014, due to the "Sinterklaasstorm". This storm is treated in paragraph 3.2.2. It also becomes clear that the pools evolve from this figure. This is discussed later in this paragraph, together with more detailed images. The aerial photographs of Bath in 2014 and 2015 show pool shaped features at an approximately constant location, see figure 3.13. The pool shaped features from 2014 can be recognized easily in the photograph from 2015. This doesn't hold for the years 2015 and 2016; The pools are at different locations in 2016.

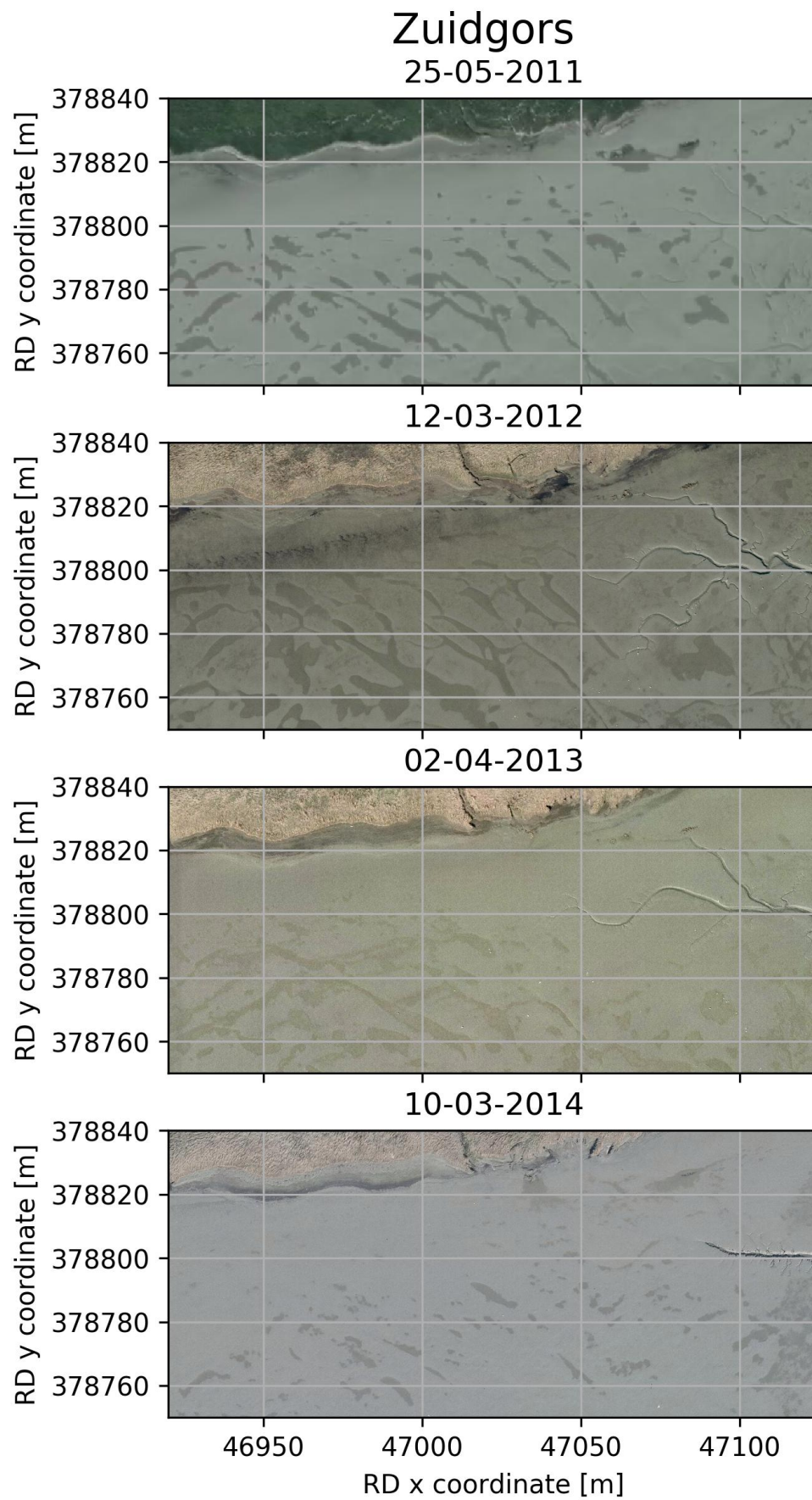


Figure 3.12: Aerial photographs of pool shaped features at Zuidgors in four subsequent years: 2011, 2012, 2013 and 2014.

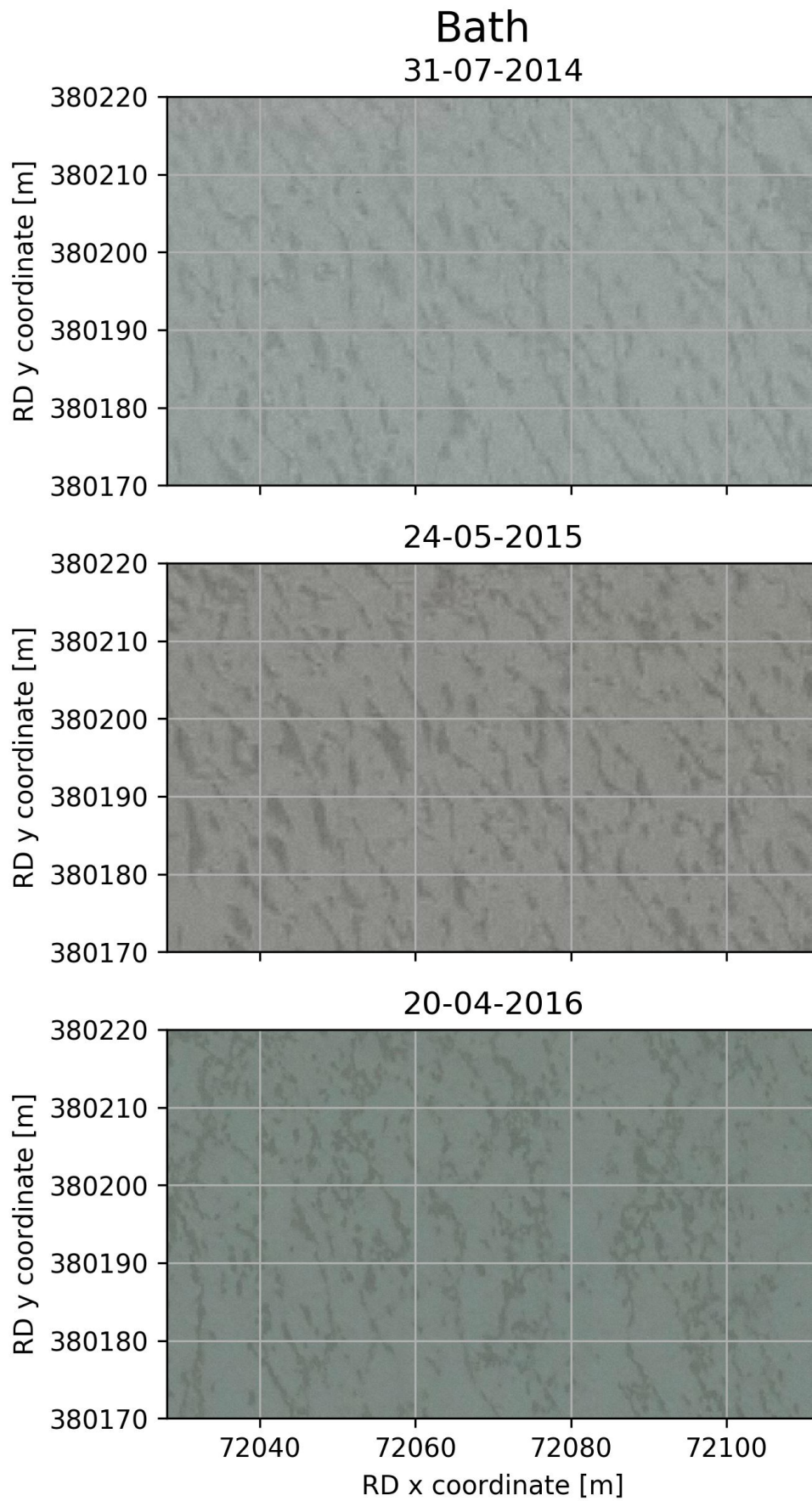


Figure 3.13: Aerial photographs of pool shaped features at Bath in three subsequent years: 2014, 2015 and 2016.



### Mechanism with positive feedback

The pool forming mechanism with positive feedback can be split in four components: initialization, positive feedback, evolution of the pools and negative feedback. These are elaborated on in paragraph 3.1. The positive feedback, evolution and existence of negative feedback are discussed in this section, in that order.

#### Positive feedback

The critical bed shear stresses in a pool shaped feature high on Zuidgors are approximately the same as outside the pool. Lower on the profile the critical bed shear stresses are different. The measured wet densities are averaged and displayed in table 3.1, for both pool A and pool B. Pool A is lower on the profile than pool B. Exact locations are given in figure 3.11. The individual measurements and coordinates of the sample locations and the pool contours are given in appendix E. It can be seen in table 3.1 that the average densities in- and outside pool B are approximately the same. Therefore, the critical bed shear stress is approximately the same in- and outside the pool; Critical bed shear stress is related to the wet density of the soil, see paragraph 3.3.1. However, diverging soil properties were observed in the field. Outside pool B the soil seemed stronger than inside it. The average critical bed shear stresses in- and outside pool A are different, the averaged densities differ. Pool A is deeper than pool B, the height difference in table 3.1 is larger.

It has to be noted that the individual measurements, making up the average, differ to a large extent. The standard deviations of the measurements are given in table 3.1. They are larger than the differences between the averages in- and outside the pools.

Pool name	Average wet density $\frac{kg}{m^3}$		Standard deviation $\frac{kg}{m^3}$		Height difference
	inside	outside	inside	outside	
Pool A	1637	1672	101	65	$\approx 4$ cm
Pool B	1681	1683	12	12	$\approx 2$ cm

Table 3.1: Averaged wet densities measured in- and outside pool A and B and their standard deviation are given. The height difference between in- and outside are mentioned as well. The individual measurements and information about the pools is given in appendix E

Wind waves in the pools are observed to be significant. Figure 3.14 gives an example of observed wind waves in a pool during a field campaign to Zuidgors on 25 October 2017. This pool is located just channelwards of pool B. See figure 3.11 for pool B's location. The average wind velocity was eight meter per second and the strongest wind gusts were around eleven meter per second [KNMI, 2017]. The wind comes from the right side in figure 3.14. The observed waves are in the order of one centimeter, estimated visually. This is significant for the water depth, which is only several centimeters.



Figure 3.14: Observed wind waves during a field campaign on 25 October 2017 in a pool just seaward of pool B. See figure 3.11 for the location of pool B. The wind comes from the right in this figure.

Different material properties in- and outside the pool shaped features are observed during a field campaign to Zuidgors on 25 October 2017, see figure 3.15. These observations also show that wind waves in the pools are likely capable of moving sediment. Peat, darker material, and bottom ripples are observed inside a pool. Peat is a light material, indicating lesser critical bed shear stresses in the pools. The bottom ripples are partially in the wind direction. This shows that the wind waves in the pools can mobilize the sediment. This diverging behavior is less seen lower on the tidal flat, see figure 3.15.

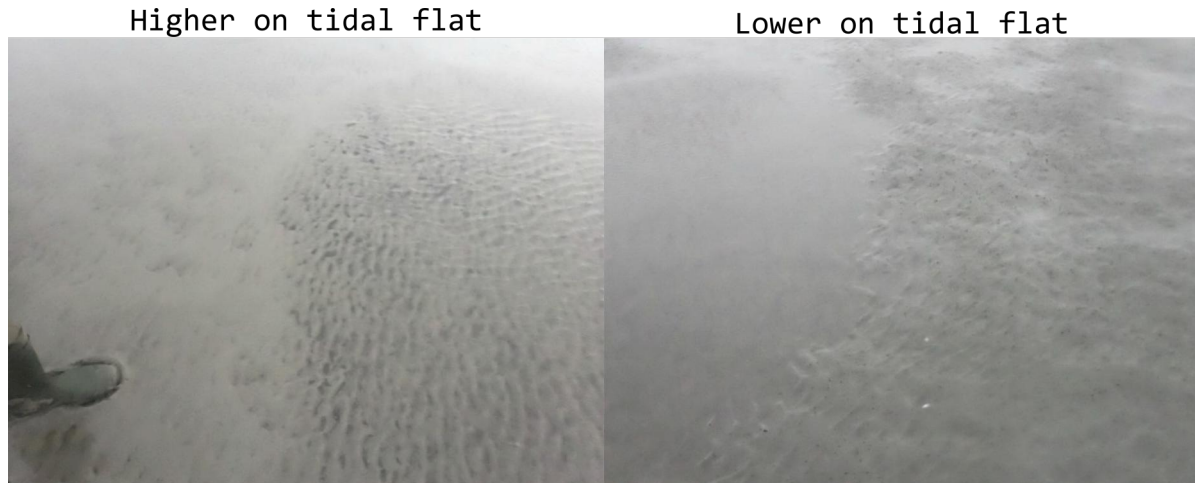


Figure 3.15: Photographs during ebb of areas on the tidal flat Zuidgors where a small water layer remained. The left image shows an area higher on the profile at Zuidgors and the right image an area lower on the profile.

Bottom shear stresses in the order of magnitude of the expected critical bed shear stresses are observed on the upper part of the convex and linear profiles. Stresses between approximately  $0.15$  and  $0.35 \frac{N}{m^2}$  are observed for wind speeds between five and ten meter per second and a convex profile, see figure 3.8. At the upper part of linear profiles this is up to  $0.5 \frac{N}{m^2}$ . Critical bed shear stresses between  $0.1$  and  $5 \frac{N}{m^2}$  are found in literature [Winterwerp, 2015]. The strengths at areas with pool shaped features will be in the lower part of the spectrum, because relatively fine sediment is found on top of the tidal flats [van Eck, 1999]. Therefore, the critical bed shear stresses are in the order of magnitude of the found bottom shear stresses for medium wind speeds.

### Evolution of pools

The pool shaped features at Zuidgors move a little North and East, get connected and grow in size between 2011 and 2012, see figure 3.16. These connections are mostly formed in the South East/South South East direction.

The gradient in bottom elevation at the investigated part of Zuidgors is in South East/South South East direction. The pool connections are mostly formed in this direction as well. This gradient direction is determined from the orientation of the salt marsh and gullies in figure 3.11. The salt marsh cliff is likely to be oriented parallel to the contour lines. The contour lines are perpendicular to the gradient. The gullies' main directions, without the meandering behavior, are approximately parallel to the gradient.

The wind rose in figure 3.17 shows that the dominant wind directions are South West and South South West in the investigated period. This means that the wind is mostly blowing towards the North East or North North East. The direction of the pool movement is also in that direction. These two directions are observed more than 25 percent of the investigated period. The wind speeds are measured at Hoofdplaat. This is the measurement station from the KNMI that is nearest to Zuidgors [KNMI, 2017].

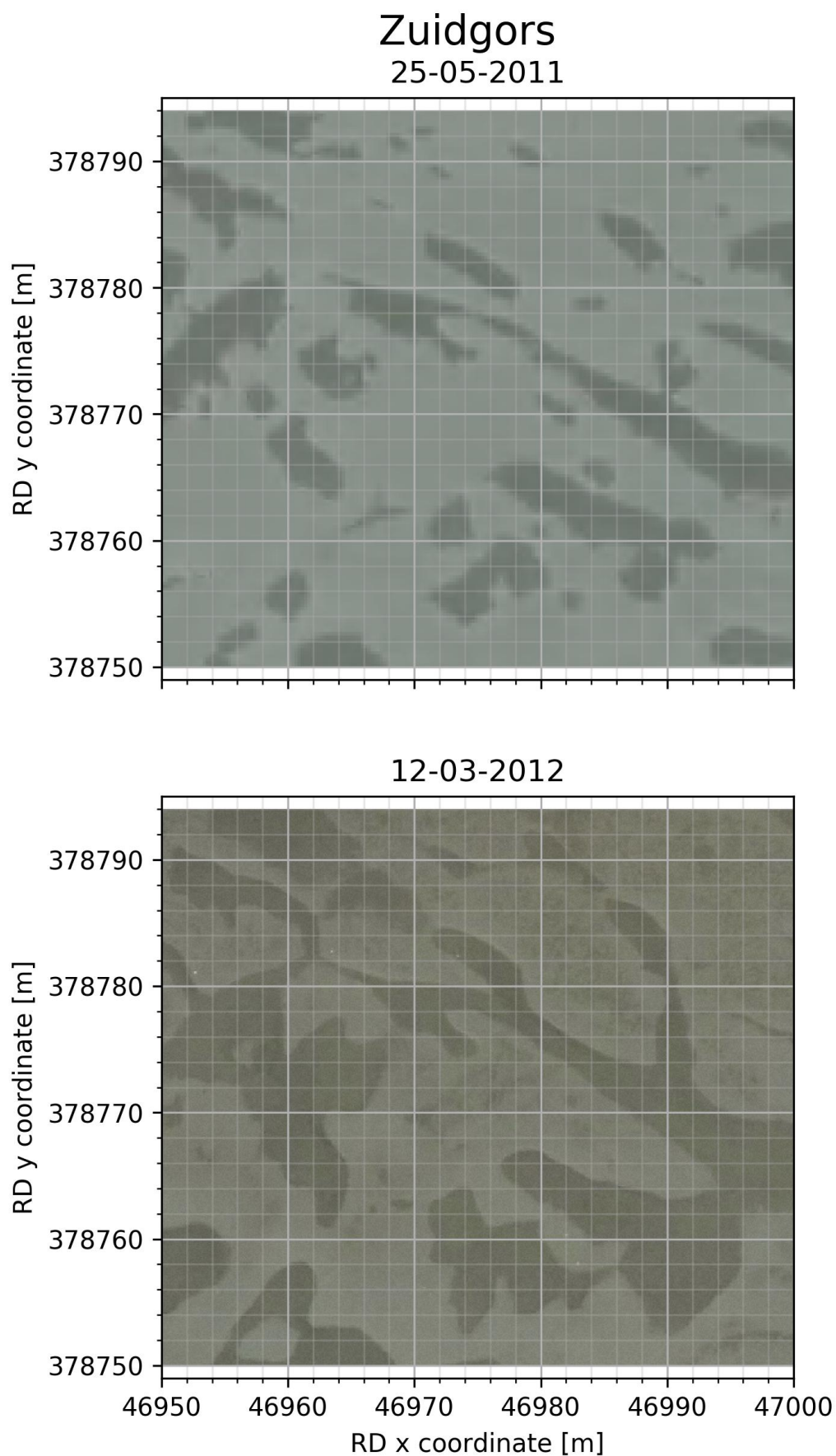


Figure 3.16: Aerial photographs of Zuidgors' pool shaped features on a detailed level. The photos are from 2011 and 2012.

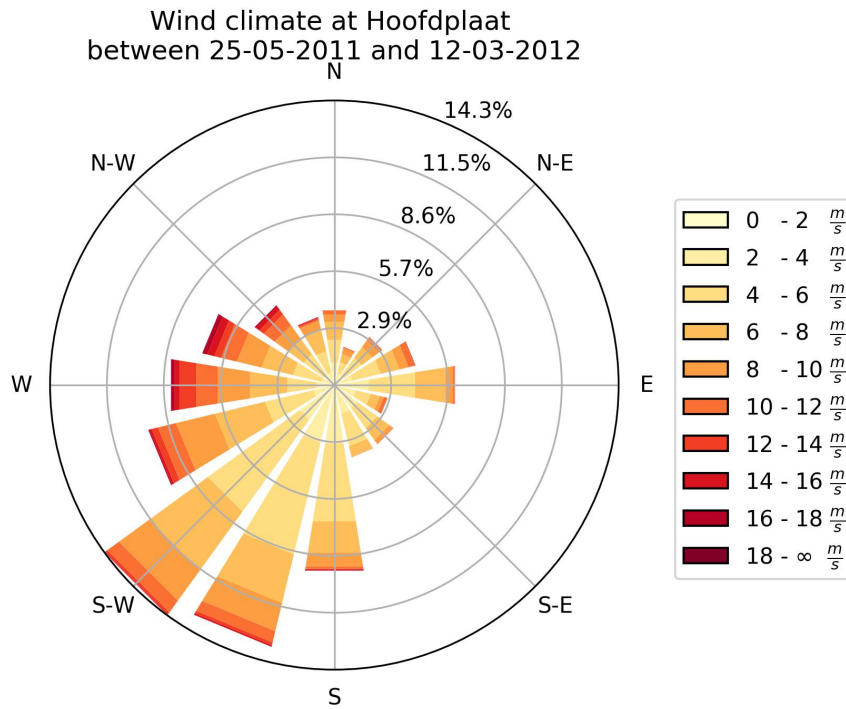


Figure 3.17: Wind rose of the measured wind speeds and directions between 25-05-2011 and 12-03-2012. The aerial photographs in figure 3.16 are taken on these dates. The given percentage represents the amount of time a certain wind speed and direction are seen with respect to the total period. The wind speeds are measured at Hoofdplaat, the measurement station from the KNMI that is nearest to Zuidgors [KNMI, 2017].

**Negative feedback**

Figure 3.18 shows that no pools deeper than several centimeters are observed at Zuidgors between 2007 and 2016. The figure displays elevation measurements at the upper part of Zuidgors. The shown area contains mostly pool shaped features, but not exclusively. The biggest height difference between point measurements is approximately 7.5 centimeter and is seen in 2007 around 100 meter distance along the transect. Also in 2011 similar differences are observed.

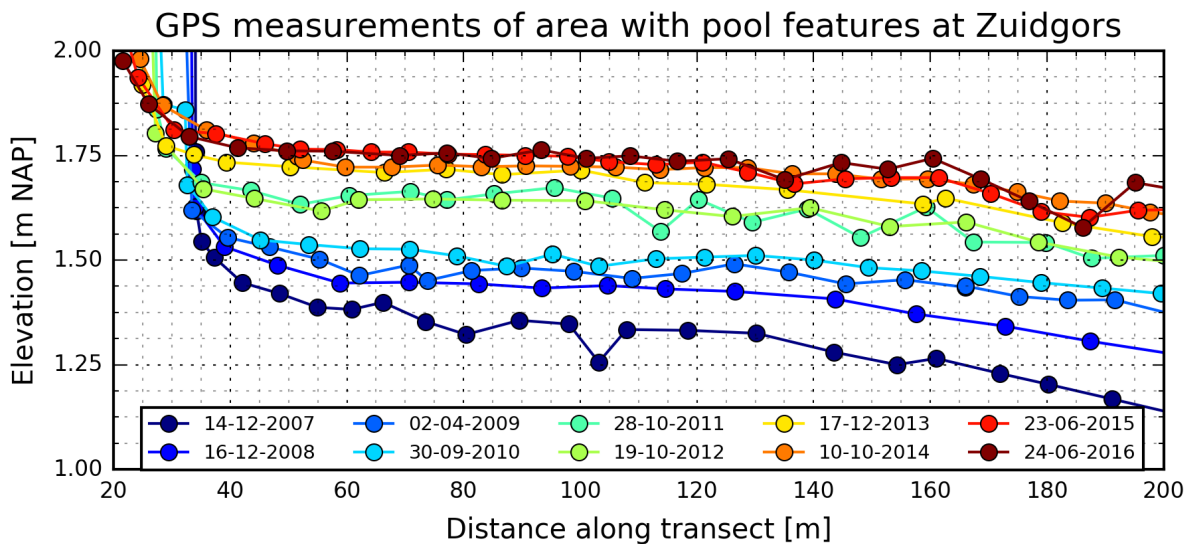


Figure 3.18: Elevation measurements between 2007 and 2016 of upper part of Zuidgors. The visualized area contains mostly pool shaped features, but not exclusively. The measured points are indicated with a dot. The years are color coded, starting dark blue and going towards dark red.

### Drainage after high water event

The estimated bottom shear stresses during drainage of a high water event do not exceed  $0.1 \frac{N}{m^2}$ . Bottom shear stresses after the high water event on 24 October 2014 are estimated with a model simulation for Zuidgors. The model is explained in paragraph 3.3.1. The area of interest is where the pool shaped features occur, since their forming mechanism is investigated. Therefore, the maximum shear stresses that occur at their location are sought for. The moment they occur is displayed in figure 3.19. Some wiggles are observed on the transition between salt marsh and tidal flat. This is probably due to numerical instability. The instability could be caused by the transition in bottom roughness on the salt marsh cliff. Increasing temporal and spatial resolution did not solve the instability. The model result is considered reliable enough to conclude that the maximum estimated bottom shear stress does not exceed  $0.1 \frac{N}{m^2}$ .

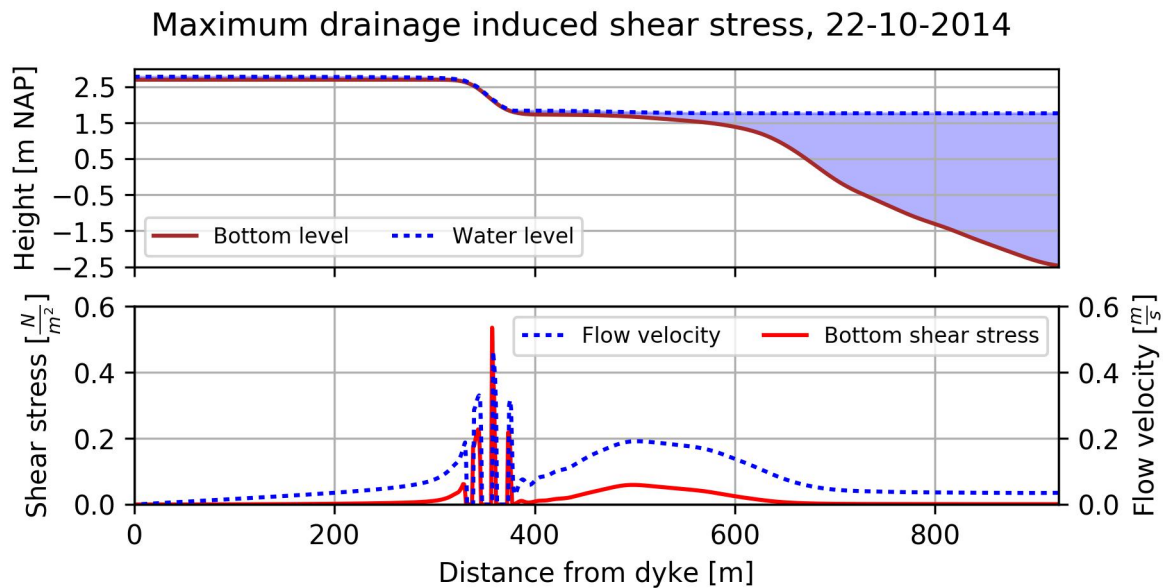


Figure 3.19: Drainage induced bottom shear stresses and flow velocities at one moment during the high water event at 22 October 2014. This is simulated with a 1D model with mass and momentum balance. The moment with maximum bottom shear stress around the area with pool shaped features is given. The simulation is done for the tidal flat Zuidgors.

#### 3.3.3. Discussion

Discussion points of the results and investigations of the two pool forming mechanisms are given in this section. The mechanism with positive feedback is discussed first. Secondly, the event based mechanism is treated.

#### Mechanism with positive feedback

The comparable impact of the "Sinterklaasstorm" on the upper part of the profiles at Zuidgors and Waarde does not explain that the pool shaped features are partially erased on Zuidgors and completely erased on Waarde. A forming mechanism with positive feedback can explain this. On Zuidgors some pool shaped features are still observed after the "Sinterklaasstorm", while at Waarde the pool shaped features are completely erased, see paragraph 3.2.2. However, the impact of the storm on both flats is comparable at the region with pool shaped features. The forming mechanism with positive feedback could explain the deviating behavior under similar forces. Positive feedback could have made the pools at Zuidgors more persistent. At Zuidgors the pools are observed at approximately the same location in subsequent years, see paragraph 3.3.2. This indicates that the positive feedback mechanism has been ongoing for years. Therefore, the pools are expected to be more persistent at Zuidgors than at Waarde's second transect; At Waarde they are not seen in consecutive photographs. The pools at Waarde are also much smaller than at Zuidgors, compare figures 3.6 and 3.7. This indicates that they are less persistent.

Not all aspects that are important for the pool forming mechanism with positive feedback are sufficiently investigated. Not all aspects are investigated and most of the investigated aspects are looked into by doing observations or rough comparisons, instead of reliable measurements. The mechanisms behind initialization and negative feedback are untreated, just as unequal drying of the soil. The measurements of wet density are done in an unreliable way, see section below. The influence of wind waves in pools is observed instead of measured, see paragraph 3.3.2. The bottom shear stress induced by wind waves from the estuary is estimated with a 1D model. This is considered a reliable estimate. However, the critical bed shear stresses they are compared to are determined roughly from values mentioned in literature and a map with sediment diameters, see paragraph 3.3.2. The evolution of the pool shaped features is determined reliably from the aerial photographs. The influence of the wind on this evolution is also determined from measurements. In contrast, the influence of the drainage on evolution is just reasoned from an aerial photograph.

The measurements of wet density, in and around the pool shaped features, are considered unreliable. The standard deviations are larger than the differences between the averages in- and outside the pools, see table 3.1. Therefore, the measurements are considered unreliable. The sample taking method could cause the high spread or the high spread could occur really in the field. The samples were obtained by putting plastic tubes into the ground, erase them with sediment and then seal them off with caps. Water leaking away from some of the samples could for instance explain the big differences. Another possibility is that the sediment has been settling on the way to the lab, where their weight and volume were measured. Taking several samples from the same location should reveal whether the sample taking method is unreliable or that the high spread is realistic. Without this the measurements are unreliable. However, diverging sediment properties were observed while taking the samples; The soil felt more rigid outside the pools than inside them. Another lack of this field measurement is that the sediment compositions are not looked at.

Only global results of pool evolution are obtained by the investigation, due to the large temporal resolution. The pool evolution is now looked at by two photographs that are almost ten months apart. What happens exactly in the meantime is unknown. Therefore, only the prevailing wind climate and direction of movement can be compared in paragraph 3.3.2. With a higher temporal resolution the comparison could have been done more exact. An average wind direction over a period with larger wind speeds could for instance have been compared to the direction of movement in that period. This would also enable decoupling of drainage induced evolution and wind wave induced evolution. Note that a higher photo resolution is probably also required; The evolution is relatively small.

Another lack in the evolution investigation is that the pool depths are not measured. Measurements of the depth (with a high temporal resolution) could give insight in the positive feedback mechanism and the (importance of) negative feedback. It is argued in paragraph 3.1 that negative feedback should be seen or the erasing mechanism has to occur frequently. The argument is that no deep pools are found on the tidal flats, which is proven in paragraph 3.3.2. The evolution of the pool depth will give information about the importance and existence of the negative feedback. E.g., negative feedback is unlikely to exist if pools are getting deeper at the same rate. At this moment, without measurements of pool depth, nothing can be said about the existence of a negative feedback. The erasing mechanism could also occur frequently enough to prevent pools from becoming deeper than several centimeters. The rate at which pools get deeper also tells whether positive feedback is likely or an event based mechanism is more likely to be important.

### **Drainage after high water event**

Contraction of flow during drainage of a high water event is not considered, since the drainage model is 1D. Contraction due to channels in the salt marsh is likely to happen in reality. This would give higher bottom shear stresses. These could be high enough to form the pool shaped features. However, the channels in the salt marsh have a different interval in along shore direction than the pool shaped features. Therefore, the flow contraction is unlikely to be important.

Drainage after a high water event is the only considered event based pool forming mechanism. The author did not come up with other event based mechanisms that could be important. This does not necessarily mean that no other event based mechanisms exist.

### 3.3.4. Conclusion

In this section the following question is answered with respect to pool shaped small scale morphological features: "Which mechanisms are responsible for forming the small scale morphological features that are seen in the build-up and how are they influenced by the large scale morphological shape?". A mechanism with positive feedback or event based mechanism is expected to form pool shaped features. The mechanism with positive feedback is the favored hypothesis and discussed first in this section. It can be split in four components: initialization, positive feedback, evolution of the pools and negative feedback. The drainage after a high water event is discussed after the mechanism with positive feedback. This is the event based forming mechanism. Finally, a summary is given that concludes what the pool shaped forming mechanism is and how it depends on large scale morphological shape.

### Mechanism with positive feedback

The pool forming mechanism with positive feedback can cause pools to be more persistent at one location than at another. This explains the observed differences in storm impact on Zuidgors and Waarde, see paragraph 3.3.3. The observed deviating persistence favors the pool forming mechanism with positive feedback. The four components of the mechanism are elaborated on below.

#### 1. Initialization

Heterogeneity in soil composition and forces during a storm and/or benthos can cause local indents on the top of convex tidal flats. This is the assumed initializing mechanism. Water will remain in these indents if the area has a mild slope, due to drainage incapacity. This mild slope links the initiation to profile shape. The positive feedback can start once water remains in the indents. This hypothesized initialization is not investigated in this research.

#### 2. Positive feedback

Unequal distribution of soil strength and resulting uneven erosion are expected to cause the positive feedback. Diverging critical bed shear stresses should be formed by wind waves in the pool shaped features and unequal drying, both seen during emergence. The unequal drying is not looked into. Erosion takes place during submergence of the flat. This is induced by wind waves from the estuary. A certain ratio between submergence and emergence time is probably required; Processes during emergence and submergence are important. The tide and relative height of the upper part of the convex profile shape determines how long the area is submerged. This links the positive feedback to the large scale morphological shape.

Uneven distribution of soil strength is observed in a field campaign at Zuidgors and is partially measured in an unreliable way. This backs up the expectations. The wet density measurements in paragraph 3.3.2 show equally strong soil in- and outside a pool high on the tidal flat. Stronger soil is found outside a pool lower on the flat, compared to the inside of this pool. The high standard deviations of these measurements make them unreliable, see paragraph 3.3.3. However, diverging soil properties were observed while taking the samples. Furthermore, photos taken during this field campaign show peat in the higher located pools and no peat outside the pools, see paragraph 3.3.2. This shows that lighter, weaker, material is captured in the pools. These two observations indicate that the soil outside the pool shaped features is indeed stronger.

Wind waves, generated in the pools, can cause unequal critical bed shear stresses, as is hypothesized. Significant wind waves were observed in paragraph 3.3.2 for an average wind speed of eight meter per second and wind gusts up to eleven meter per second. Bottom ripples were observed in this paragraph as well. They were seen in the higher located pool shaped features. These ripples are partially in the wind direction, indicating that the wind waves are capable of mobilizing sediment. The settling/compacting effect can be decreased by these significant waves. The movement of sediment decreases the settling/compaction. Outside the pool shaped features this decrease is not seen, since there are no wind waves. Therefore, unequal critical bed shear stresses can be caused by the wind waves generated in the pools.

Uneven erosion patterns can occur during submergence of the tidal flat, due to wind waves generated in the estuary. The wave induced bottom shear stresses are in the order of the critical bed shear stresses at the location of pool shaped features at convex and linear profiles for moderate wind speeds, see paragraph 3.3.2. Therefore, unequal erosion can take place. More erosion is expected in the pools than outside it; The bed shear stresses will be closer to/just above the critical bed shear stresses in the pools and further apart from/under the critical values outside the pools.

### 3. Evolution

The evolution of the pool shaped features should be induced by wind waves generated in the pools and drainage. This evolution is observed when the features are not erased in the period between aerial photographs.

The hypothesis is correct. The pools move, get connected and grow in size when they are not erased in the period between subsequent aerial photographs, see paragraph 3.3.2. The gradient in bottom elevation is in the same direction as the connections are formed in. This gradient probably indicates the drainage direction. The prevailing wind has the same orientation as the pool movement.

### 4. Negative feedback

The negative feedback is expected to control the pool depth and be triggered by the fact that deeper pools attract more sediment, see paragraph 3.1. The mechanisms behind this negative feedback mechanism are not looked into. However, the existence of the mechanism is evaluated, by looking at the existence of deep pools.

It is shown that no pools deeper than several centimeters exist, see paragraph 3.3.2. This indicates that negative feedback on the positive feedback should become important at some point or that the erasing mechanism should occur frequently enough. Deeper pools should be observed if the positive feedback mechanism can continue unhampered. It is stated in paragraph 3.3.3 that the necessity of the existence of this negative feedback is questionable. The reason is that it is not known how the pool depths develop and whether the erasing mechanism occur frequently enough to prevent occurrence of deep pools.

## Drainage after high water event

Drainage after a high water event, without severe wave impact, is foreseen to cause strong cross shore currents that form the pool shaped features. It is proven that this mechanism can not form pools, i.e. the hypothesis is false. Drainage after a high water event induces bottom shear stresses that are less than seen for wind speeds of five meter per second. This follows from a 1D model simulation of the drainage after a high water event. The maximum estimated bottom shear stresses around the area with pool shaped features do not exceed  $0.10 \frac{N}{m^2}$ , see paragraph 3.3.2. This is already exceeded for wind speeds of five meter per second, see paragraph 3.2.2. Therefore, this event based mechanism is unlikely to form pool shaped features. Flow contraction, induced by the channels in the salt marsh, probably increases the cross shore flow velocities. Therefore, bottom shear stresses increase locally. This is not incorporated in the 1D model. However, this cannot explain the pool shape feature formation; The channels have different intervals in the along shore direction than the pools, see paragraph 3.3.3.

## Summary: answer to sub-question

The pool shaped features should be formed by the described mechanism with positive feedback and not by the event based mechanism. They are seen on mild slopes that allow water to remain at the tidal flat and relative heights that allow for submergence and emergence. These criteria are not observed on concave profiles and are on linear and convex profiles. This explains why pool shaped features are not seen on concave profiles in the categorized aerial photographs in appendix B.

Additionally, it should be noted that the pool shaped features show resemblance with the ridge and runnel systems, see paragraph 1.1. Both systems have diverging soil strengths; The lower areas contain weaker sediment than the higher areas. Furthermore, both systems' forming mechanisms are driven by wind waves and they both are observed in combination with gullies. The systems differ in their orientation and shape. Ridge and runnels are oriented shore normal and pools are also observed in other directions. The shape of the pools is less elongated than the ridge and runnel systems.



### 3.4. Gully forming mechanism

In this section the following question is answered with respect to the small scale morphological feature type gullies: "Which mechanisms are responsible for forming the small scale morphological features that are seen in the build-up and how are they influenced by the large scale morphological shape?". Drainage forms the gullies, see paragraph 1.1. At a certain point on the tidal flats drainage induced currents are expected to be big enough to cause gully formation. In other words, a certain minimum requirement should be met to form gullies. This depends on the large scale morphological shape.

The methodology is given first. Consecutively, the results are given. The results are discussed next. In the end, the expectation is evaluated and a conclusion is given on the gully forming mechanism and its dependence on large scale morphological shape.

#### 3.4.1. Methodology

A literature research is conducted to investigate how drainage forms the gullies. The link with the large scale morphological shape is also looked into.

#### 3.4.2. Results

Drainage can form gullies in two different ways, with and without initiation around vegetation, according to the literature. The gully forming mechanism is found to decrease in strength if slope or Shields parameter increases. This holds when gullies are observed. From this is derived that the gully forming mechanism gets weaker in channelward direction on convex profiles and is approximately equal over the cross shore for linear profiles.

Gullies can be formed by converging runoff on bare mudflats. This runoff consists of retained seawater and/or rainfall. The water tends to converge in lateral concentrations, because smooth and mildly sloped mudflats are not very efficient in draining the water. Such concentrations can generate slight channel like depressions by increasing flow velocities that result in uneven erosion. The depressions attract more flow and this gives more erosion in the depressions than outside them. Consequently, these depressions have a positive feedback on channel formation [Whitehouse et al., 2000].

Gullies can also be formed by converging runoff due to the presence of vegetation. Vegetation slows down the flow and enhances sedimentation in the vegetated patches. Flow acceleration is seen around the patches, due to the slow down within them. The acceleration initiates erosion. The gullies formed around the vegetated patches will deepen, because of flow attraction and diverging bottom shear stresses [Schwarz et al., 2014].

The gully forming mechanism gets weaker in channelward direction on convex profiles and is approximately equal in the cross shore for linear profiles, when gullies are observed. Marciano et al. [2005] show that gully width and interval between them decreases when the slope of the bottom profile or the Shields parameter increases. This holds for situations where gullies are observed. The Shields parameter is used as mobility parameter in Marciano et al. [2005]. It represents the load divided by the strength. The load depends on the shear stress and the strength on the particle weight. The Shields parameter indicates whether a particle movement is likely to occur, it is a mobility parameter [Schiereck, 2012]. Decreasing gully width and interval between them results in less strong embedded gullies. Hence, the forming mechanism can be considered weaker if the slope or Shields parameter increases. The slope is increasing in channelward direction on a convex profile shape and is approximately constant on a linear profile. Figure 3.8 shows that bed shear stresses increase in channelward direction on the convex profile. This figure also shows that bed shear stresses are approximately equal in the cross shore direction on linear profiles. Higher bed shear stress gives a higher Shields parameter, assuming the same sediment composition. Therefore, it can be concluded that the gully forming mechanism gets weaker in channelward direction on a convex profile, considering the slope and bottom shear stress increase. On the linear profile both slope and Shields parameter remain approximately constant. This results in a gully forming mechanism that has approximately the same strength over the cross shore for a linear profile.

### 3.4.3. Discussion

The gully forming mechanism gets weaker in channelward direction on convex profiles and is approximately equal over the cross shore for linear profiles, see paragraph 3.4.2. This holds from the moment gullies are observed. The moment gullies are observed depends probably on a minimum required slope and/or drainage volume. Two arguments can be given for this. The first argument is based on the gully forming mechanism's strength development and the location gullies are found in the build-up. Gullies are found lower in the build-up than where their maximum forming mechanism occurs. The found literature indicates indirectly that the gully forming mechanism gets weaker in channelward direction on convex profiles. This means the maximum strength of the forming mechanism is seen on top of the convex tidal flats. Gullies are mostly not observed at this location, but pool shaped features are, see paragraph 2.3.2. This favors the minimum requirement. The second argument is based on the found forming mechanism. Without the minimum requirement water will not flow hard enough to cause erosion, even with convergence. Therefore, no depressions can be formed on the mud flat that can grow to gullies, see paragraph 3.4.2.

The gully formation around vegetated patches can explain the arbitrary categories seen between build-up and salt marsh. The occurrence of these categories is mentioned in the definition of build-up, see paragraph 3.1. Mostly gullies, vague gullies or (nearly) smooth areas are seen between build-up and salt marsh. The (vague) gullies are thus located near the salt marsh. Therefore, their occurrence could be explained by gully formation around vegetation patches. Drainage induced flow contracts around the vegetated patches in this case and forms gullies, see paragraph 3.4.2. Figure 3.8 shows a slight increase in bottom shear stresses right in front of the salt marsh cliff. This could explain that the gullies in front of the cliff are sometimes wiped out as well, creating vague gullies or a (nearly) smooth area.

### 3.4.4. Conclusion

In this section the following question is answered with respect to the small scale morphological feature type gullies: "Which mechanisms are responsible for forming the small scale morphological features that are seen in the build-up and how are they influenced by the large scale morphological shape?". Drainage forms the gullies, see paragraph 1.1. At a certain point on the tidal flats drainage induced currents are expected to be big enough to cause gully formation. In other words, a certain minimum requirement should be met to form gullies. This depends on the large scale morphological shape.

Drainage causes indeed the formation of gullies that are seen in the build-up. Gullies can be formed in two different ways, see paragraph 3.4.2. They can be formed on a bare tidal flat and around vegetation patches. Gullies in the build-up are all on a bare flat. These gullies are initiated by flow convergence due to inefficient drainage of a smooth and mildly sloped tidal flat.

The gully forming mechanism gets weaker in channelward direction on convex profiles and is approximately equal in the cross shore for linear profiles, see paragraph 3.4.2. This holds from the moment that the minimum required slope and/or drainage volume are seen. That a minimum slope or drainage volume is required to form gullies is not found in the literature research. However, it is argued in paragraph 3.4.3. The requirement makes the formation of gullies in the build-up depends on the large scale morphological shape. The strength of the gully forming mechanism depends also on large scale morphological shape, because it develops differently on linear and convex profiles. The second part of the hypothesis is supported by these two facts; The gully formation is influenced by large scale morphological shape.

### 3.5. (Nearly) smooth area forming mechanism

In this section the following question is answered with respect to the small scale morphological feature type (nearly) smooth area: "Which mechanisms are responsible for forming the small scale morphological features that are seen in the build-up and how are they influenced by the large scale morphological shape?". The erasing mechanism is expected to be stronger than each of the small scale feature forming mechanisms at the (nearly) smooth areas in the build-up. The erasing mechanism and most forming mechanisms are linked to large scale morphological shape. Therefore, their ratio should be linked to the shape as well.

The hypothesis is investigated by comparing the erasing strength with the strength of all forming mechanisms at the location of (nearly) smooth areas in the build-up. The exact methodology is given first. Afterwards the results are given. The results are discussed next. Finally, the hypothesis is evaluated and a conclusion is given on the mechanism that forms the (nearly) smooth areas in the build-up and its dependence on large scale morphological shape.

#### 3.5.1. Methodology

Whether the (nearly) smooth areas in the build-up are formed by dominating erasing mechanisms is investigated by combining already found results. It is argued whether the erasing mechanism is stronger than each of the forming mechanisms at the location of (nearly) smooth areas in the build-up. The strength of the erasing mechanism is estimated with a 1D model; The results are given in paragraph 3.2.2. This is linked to the location of (nearly) smooth areas and the vague gullies in the build-up with help of the relative height they occur on, given in paragraph 2.3.2. The gully forming mechanism's strength is looked into for these two areas as well. This is done by combining the relative heights of the areas and the dependence of the gully forming mechanism on large scale morphological shape. It is also reasoned why other forming mechanisms are not important at the location of (nearly) smooth areas in the build-up.

#### 3.5.2. Results

The eroding force is stronger on the (nearly) smooth areas in the build-up than on the vague gullies in the build-up. Figure 3.8 shows that higher bed shear stresses are observed lower on convex profiles. These profiles are indicated by the build-up. The category (nearly) smooth, (f), is in general more channelward located than the category vague gullies, (e), if both are in the build-up. This follows from the build-up definition, see paragraph 3.1, and from figure 2.7. A comparison of the eroding force on both areas is obtained by combining both locations with the bed shear stress development: The eroding force has a stronger influence on the (nearly) smooth areas than on the vague gullies.

The forming mechanism for gullies is weaker on (nearly) smooth areas than on the vague gullies, both in the build-up. The gully forming mechanism gets weaker in channelward direction on convex profiles, see paragraph 3.4.4. The (nearly) smooth areas are observed lower on the convex profiles than the areas with vague gullies. A comparison in gully forming mechanism strength arises from combining the strength development with occurrence locations: The strength of the gully forming mechanism is less on the (nearly) smooth areas than on areas with vague gullies.

The mechanisms forming pool shaped features, ship keel traces and megaripples are not important on (nearly) smooth areas in the build-up. The slope seen at (nearly) smooth areas in the build-up is too steep for the pool shaped feature forming mechanism to be important. It is stated in paragraph 3.3.4 that a mild slope is required. The ship keel traces (category (g)) exist at the same location for years, see paragraph 3.6.4. The relative height where they occur is also very specific, approximately -0.75, see figure 2.7. This figure also shows that this relative height is not observed in the 90 percent confidence interval of the nearly smooth area' relative height, given by category (f). These two facts indicate that the forming mechanism of ship keel traces is not important at the location of the (nearly) smooth areas. The along shore currents are mild at the location of the (nearly) smooth areas in the build-up, compared to the location of the megaripples (category (h)), see figures 2.7 and 3.8. Along shore currents form the megaripples, see paragraph 3.7.4. Hence, the megaripple forming mechanism is not important at the location with (nearly) smooth areas.

### 3.5.3. Discussion

The results given in paragraph 3.5.2 are all based on other parts of the research. The conclusion on the (nearly) smooth area forming mechanism is incorrect in case any of these used outcomes is wrongful. The mechanisms forming pool shaped features, ship keel traces and megaripples are for instance not important on (nearly) smooth areas in the build-up. This argumentation assumes that the hypothesized forming mechanisms are indeed the actual forming mechanisms. These hypotheses are backed-up in this research in paragraphs 3.3.4, 3.6.4 and 3.7.4. However, these forming mechanisms could be important if the hypotheses are wrongly concluded to be true.

The (nearly) smooth areas that are seen outside of the build-up are not considered in this research. Various reasons why (nearly) smooth areas occur can be thought of, besides dominating eroding forces. Large accretion is one of them. This is not a logical formation mechanism of the smooth areas in the build-up. The accretion should also be observed on other areas in the build-up when it is seen at one of the areas. Hence, it should be covering the other objects as well. This is not observed.

### 3.5.4. Conclusion

In this section the following question is answered with respect to the small scale morphological feature type (nearly) smooth area: "Which mechanisms are responsible for forming the small scale morphological features that are seen in the build-up and how are they influenced by the large scale morphological shape?". The erasing mechanism is expected to be stronger than each of the small scale feature forming mechanisms at the (nearly) smooth areas in the build-up. The erasing mechanism and most forming mechanisms are linked to large scale morphological shape. Therefore, their ratio should be linked to the shape as well.

The erasing mechanism is indeed found to be stronger than the forming mechanisms at the (nearly) smooth areas in the build-up. The erasing mechanism is stronger and the gully forming mechanism is weaker at the location in the build-up where (nearly) smooth areas are observed than at areas with vague gullies, see paragraph 3.5.2. Therefore, the erasing mechanism is stronger than the forming mechanisms at the (nearly) smooth areas. The gully forming mechanism is just stronger than the erasing mechanism at an area with vague gullies, since they are only vaguely observed. The erasing mechanism becomes stronger than the gully forming mechanism when this ratio is shifted slightly towards the erasing mechanism. This transition is linked to the convex large scale shape. It also argued in paragraph 3.5.2 that the mechanisms forming pools, ship keel traces and megaripples are not important on (nearly) smooth areas in build-up. This argumentation is mainly based on large scale profile shape. From the above can be concluded that the erasing mechanism is stronger than forming mechanisms on (nearly) smooth areas in the build-up.

The mechanism forming (nearly) smooth areas in the build-up gets stronger in channelward direction on convex profiles and stays approximately equal on linear profiles, when only the gully forming mechanism is considered. The forming mechanism for gullies gets weaker in direction of the channel on convex profiles and is approximately equal in the cross shore for linear profiles, see paragraph 3.4.4. The erasing mechanism is increasing in channelward direction on convex profiles and is approximately constant in the cross shore direction for linear profiles, see paragraph 3.2.4. A development in the cross shore direction of the (nearly) smooth area forming mechanism is obtained when these two developments are combined; The mechanism forming (nearly) smooth areas in the build-up gets stronger in direction of the channel on convex profiles and is approximately constant on linear profiles. This holds when only the gully forming mechanism is considered.

## 3.6. Ship keel trace forming mechanism

In this section the following question is answered with respect to the ship keel traces: "Which mechanisms are responsible for forming the small scale morphological features that are seen in the build-up and how are they influenced by the large scale morphological shape?". The ship keel traces could be formed by ships running aground. It is seen in paragraph 2.3.2 that these features are strongly linked to a relative height. It is expected that the features are not linked to large scale morphological shape, only to relative height.

Two types of investigations are done to evaluate on the ship keel traces' forming mechanism. The exact methodology is given first. The results are given afterwards. These are discussed next. At last, the expectations are evaluated and a conclusion is given on the mechanism that forms the ship keel traces and its dependence on large scale morphological shape.

### 3.6.1. Methodology

Two types of investigations are done to determine the ship keel traces' forming mechanism and its dependence on large scale morphological shape. Their methodology is discussed in separate sections. It is explained in the first section how aerial photographs and bottom shear stress estimates are used to determine the ship keel traces' persistence. This gives insight in the forming mechanism. Secondly, it is determined on which tidal flats the ship keel traces are observed and what their distance to the shipping channels is.

#### Ship keel traces persistence

Aerial photographs and bottom shear stress estimates are used to investigate whether ships running aground can form the ship keel traces. The boats running aground compress the sediment with their large weight, and thereby strengthened the soil. Large indents can also be expected. Therefore, it would be logical if the features are seen at the same location in several subsequent aerial photographs. Aerial photographs of the tidal flats that are investigated in chapter 2 are analyzed to see if this is true. Bottom shear stresses are estimated with a 1D model. This model is elaborated on in paragraph 3.2.1. The model output is used to see whether the persistence of the features could be explained by small erasing forces, instead of large compression forces.

#### Occurrence ship keel traces and proximity shipping channels

It is listed on which tidal flats the ship keel traces are seen. The location of these flats is linked to the shipping channels. The ship keel traces' link with large scale morphological shape and the forming mechanism are investigated in this way. The tidal flats that are investigated in chapter 2 are looked into. The features should be seen more on a certain shape, if they depend on large scale morphological shape. The occurrence on a certain shape is only counted once, because the features are expected to be seen several years on the same spot. The location of the shipping channels and tidal flats with ship keel traces indicate whether the features are indeed formed by ships running aground. These flats should be located near channels, if this is indeed the forming mechanism.

### 3.6.2. Results

The results of two investigations are given in this section. The first part discusses the persistence of the ship keel traces. The second investigation shows the influence of large scale morphological shape and proximity of the shipping channels.

#### Ship keel traces persistence

Aerial photographs of ship keel traces at Waarde show that the features remain at the same location for multiple years. Aerial photographs of ship keel traces at Waarde's second transect in 2005, 2012 and 2013 are shown in figure 3.20. Several ship keel traces can be recognized from 2005 in the photograph from 2012. The features start to disappear in 2013. This is probably due to large accretion rates seen at this transect, see the elevation measurements in appendix A.

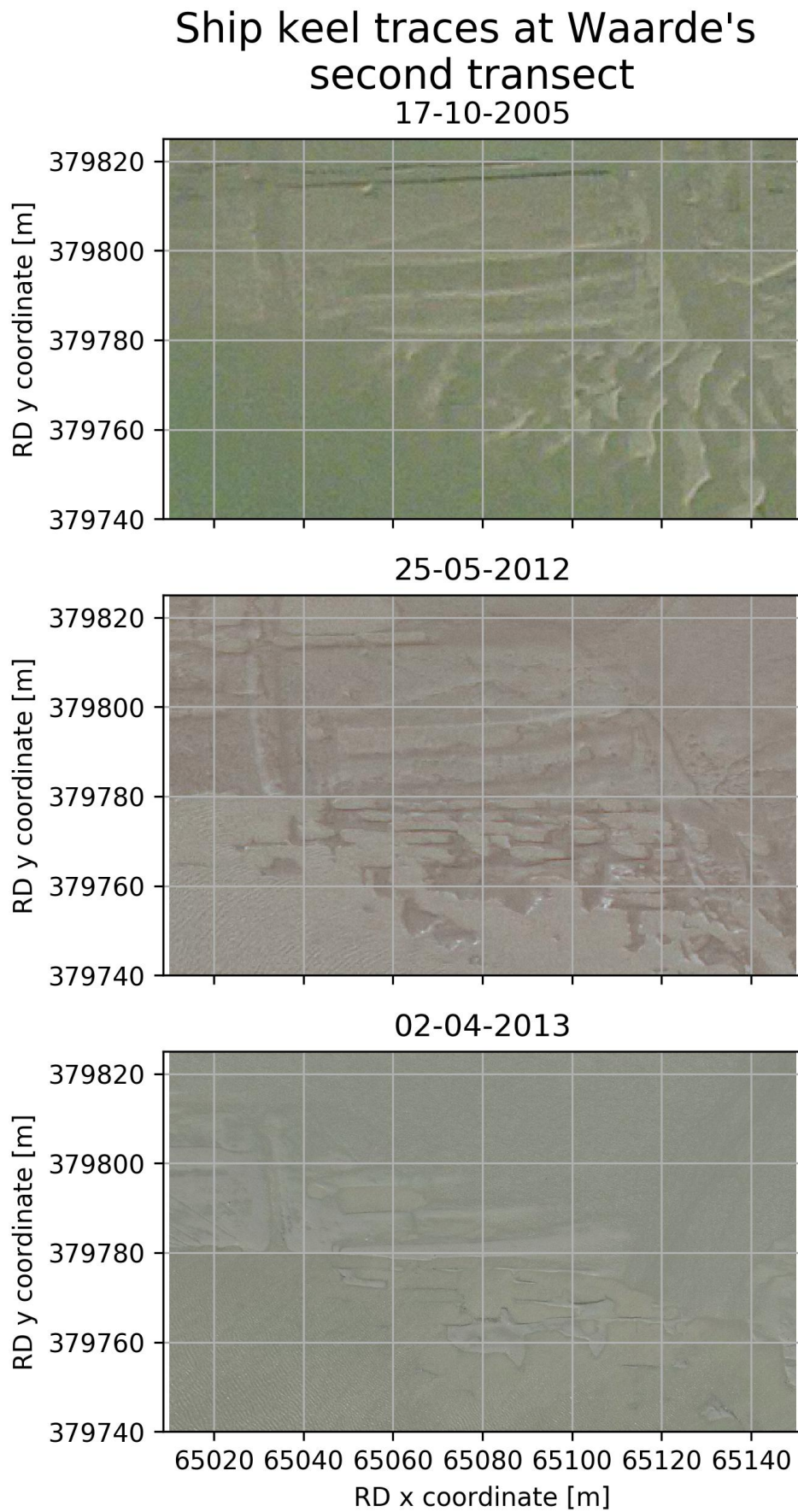


Figure 3.20: Aerial photographs of ship keel traces at Waarde's second transect. They are taken in 2005, 2012 and 2013.

The erasing forces are relatively large at the location of the ship keel traces. Bottom shear stress estimates are obtained by a 1D model that makes use of SWAN. The results are shown in paragraph 3.2.2. Large wave induced bottom shear stresses are found to be the mechanism that erases small scale features, see paragraph 3.2.4. These wave induced stresses are large at the channel side of convex profiles, compared to the land side. This makes them relatively large at the area where ship keel traces are observed in the build-up, see figure 2.7. Note that category (g) is the ship keel traces category, in order to read out the figure.

### Occurrence ship keel traces and proximity shipping channels

In this section is first shown that a weak link exists between ship keel trace occurrence and the large scale shape of the tidal flat. Secondly, it is argued that the occurrence of the ship keel traces is influenced by the tidal flat location with respect to the shipping channels. The first, weaker, link arises from the relation between ship keel trace occurrence and shipping channel proximity.

Table 3.2 shows at which tidal flats the ship keel traces are seen. The flats are sorted in columns, based on their large scale shape. These shapes are determined in paragraph 2.3.1. If two large scale morphological shapes are observed at one tidal flat, then the flat is mentioned in two columns. Whether the ship keel traces are seen in aerial photographs can be seen in appendix B. The ship keel traces are observed at five out of the eight convex profiles, one out of the four linear profiles and one out of the two concave profiles. Tidal flat shape seems important according to this finding.


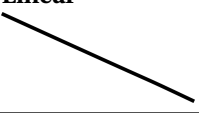
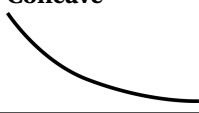
<b>Convex</b> 	<b>Linear</b> 	<b>Concave</b> 
<b>Baalhoek</b> Ship keel traces seen	<b>Kats</b> Ship keel traces <b>not</b> seen	<b>Annajacobapolder</b> Ship keel traces <b>not</b> seen
<b>Bath</b> Ship keel traces seen	<b>Waarde, 1<sup>st</sup> transect</b> Until approx. 2002. Ship keel traces seen	<b>Waarde, 2<sup>nd</sup> transect</b> Until approx. 2003. Ship keel traces seen
<b>Knuitershoek</b> Ship keel traces seen	<b>Zandkreek</b> Ship keel traces <b>not</b> seen	
<b>Land van Saeftinghe</b> Ship keel traces <b>not</b> seen	<b>Zuidgors</b> Until 2001. Ship keel traces <b>not</b> seen	
<b>Waarde, 1<sup>st</sup> transect</b> Starting approx. 2005. Ship keel traces <b>not</b> seen		
<b>Waarde, 2<sup>nd</sup> transect</b> Starting approx. 2009 Ship keel traces seen		
<b>Waarde, 3<sup>rd</sup> transect</b> Ship keel traces seen		
<b>Zuidgors</b> Starting approx. 2005. Ship keel traces <b>not</b> seen		

Table 3.2: This table shows whether ship keel traces are seen for all tidal flats that are analyzed in chapter 2. The flats are categorized based on their large scale shape. This results in the three columns.

Whether ship keel traces are seen can be explained to a large extent by the proximity of a shipping route, instead of the weak link with large scale shape. Shipping channel locations are indicated in figure 3.21, they are obtained from OpenSeaMap. Also the tidal flat locations are given in this figure. The three tidal flats in the Eastern Scheldt don't show the ship keel traces and no major shipping routes are seen in that estuary. These flats are Anna Jacobapolder, Kats and Zandkreek. Baalhoek, Bath and Knuitershoek are located in the Western Scheldt near a shipping route and do show the ship keel traces. Land van Saeftinghe and Zuidgors

are the tidal flats in the Western Scheldt that don't show the ship keel traces. These flats are located further from the shipping channels. Waarde is the only exception. This tidal flat is also located far from the channels, but ship keel traces are seen. From the previous mentioned explanation can be concluded that the location dependency overrules the weak observed link with large scale morphological shape. This weak link is probably formed by the coupling between location and profile shape. E.g. that more convex profiles are seen in the Western Scheldt, where more shipping activity is seen.

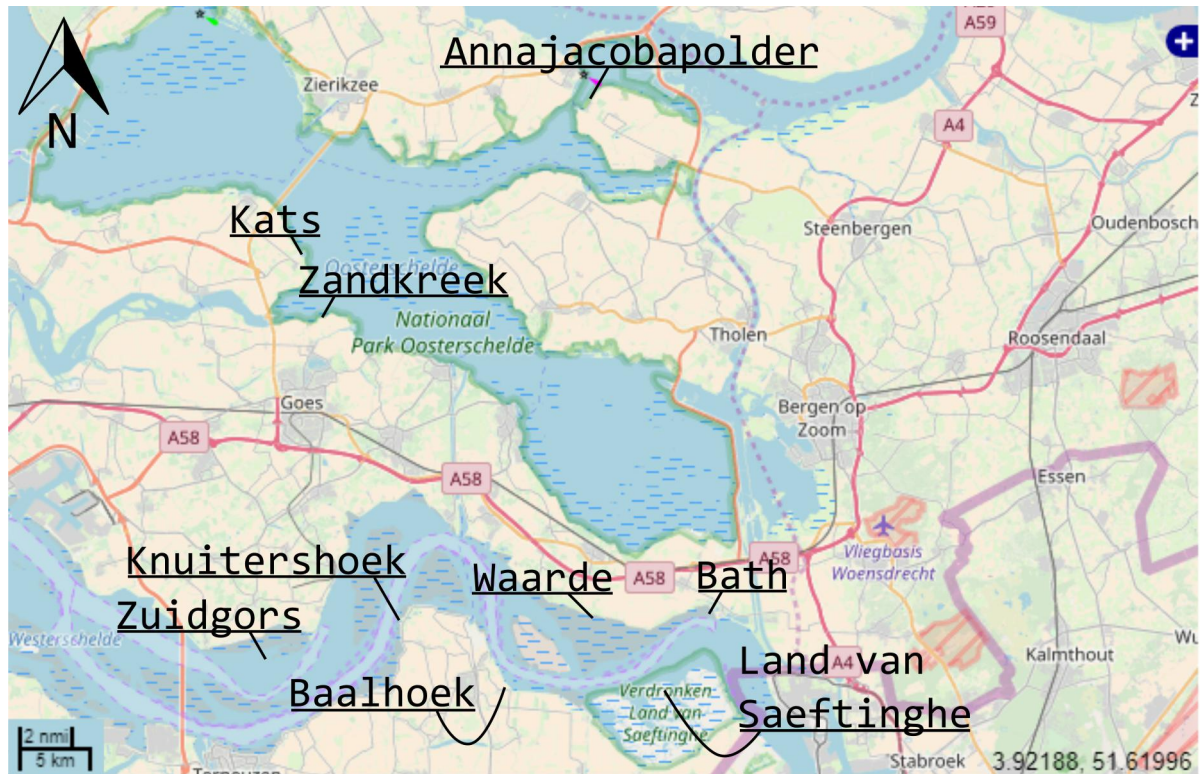


Figure 3.21: The locations of the investigated tidal flats and the shipping channels are indicated in this figure. The figure is obtained from OpenSeaMap.

### 3.6.3. Discussion

Ship keel traces are seen at Waarde, despite the fact that it is not located near a shipping channel, see paragraph 3.6.2. Another potential forming mechanism is indicated by this. The ship keel traces could be remnants of plowed fields on former reclaimed areas. The presence of the ship keel traces at Waarde can not be explained by the fact that headlands are constructed on this tidal flat between 2000 and 2003. The rocks for the headland construction are probably brought in with barges. The ship keel traces could be formed by these barges running aground. However, in the aerial photograph of 2000 an extensive amount of these traces is already seen. The traces could be the remnants of plowed fields on former reclaimed areas [Herman, 2017]. These reclaimed areas are persistent as well; They do not erode easily, just as the ship keel traces. Furthermore, they are seen at Waarde in older photographs. If the traces are remnants of former reclaimed areas, then they are still depending on location in the estuary and not on large scale morphological shape, as seen in paragraph 3.6.2. Large eroding forces close to the shipping channels could explain the coupling between location and the proximity of shipping activity. If the eroding forces are larger, then it is more likely that the traces are shown; The traces can be seen as a harder layer that is revealed when all the above is eroded. The reason for headland construction at Waarde is probably that the tidal flat was eroding too much. This explains the exception of ship keel traces occurring at Waarde.

The persistence of the ship keel traces could explain why they are seen at a specific relative height. The traces are not eroded easily. Therefore, if they are seen it will be seen at the height they were seen before.



### 3.6.4. Conclusion

In this section the following question is answered with respect to the ship keel traces: "Which mechanisms are responsible for forming the small scale morphological features that are seen in the build-up and how are they influenced by the large scale morphological shape?". The ship keel traces could be formed by ships running aground. It is seen in paragraph 2.3.2 that these features are strongly linked to a relative height. It is expected that the features are not linked to large scale morphological shape, only to relative height.

The ship keel traces can be formed by ships running aground or by the presence of a persistent layer of former reclaimed areas. The traces remain at the same location for multiple years, despite the presence of relatively large bottom shear stresses, see paragraph 3.6.2. This supports the hypothesized ship keel traces' forming mechanism, ships running aground. The sediment is compressed to a large extent by a ship that runs aground, because of the large weight. The features should therefore be very persistent and thus present for a long time. However, it could also indicate that the ship keel traces are actually remnants of plowed fields on former reclaimed areas, see paragraph 3.6.3. The remnants of plowed fields on former reclaimed areas are strong embedded as well. The persistence is indeed found in paragraph 3.6.2. It is also found that erasing forces are relatively large at the location where ship keel traces occur in the build-up. Therefore, small erasing forces can not explain why the traces are seen at the same location for multiple years. The persistence of the features could explain the small band width in the relative height confidence interval, found in paragraph 2.3.2.

The occurrence of the ship keel traces is influenced by the tidal flat location with respect to the shipping activity and not by the large scale morphological shape of the tidal flat, see paragraph 3.6.2. This outcome supports the second part of the hypothesis; The small scale features are only linked to a certain relative height and not to large scale morphological shape. It is shown that the traces are seen on tidal flats near shipping channels, except for Waarde. The exception of Waarde indicates that the traces could also be remnants of plowed fields on former reclaimed areas, see paragraph 3.6.3. Larger eroding forces near the shipping channel can explain the relation with shipping activity when the remnants form the traces.

It can be argued that the ship keel traces do not belong in the build-up definition, which serves as indicator for convex profiles. The ship keel traces are linked to proximity to shipping activity and possibly to the history of the tidal flat. They are not linked to large scale morphological shape, only to a certain relative height. Therefore, these features do not help to distinguish convex, linear and concave profiles. Consequently, it can be argued that they don't belong in the definition of a general indicator for convex profiles, the build-up.

### 3.7. Megaripple forming mechanism

In this section the following question is answered with respect to the small scale morphological feature type megaripples: "Which mechanisms are responsible for forming the small scale morphological features that are seen in the build-up and how are they influenced by the large scale morphological shape?". The megaripples are formed by strong along shore currents, hypothetically. These features are found as indicator for (future) convex profiles. Therefore, it is known that they are coupled to convex large scale morphological shape. Why this link exists is investigated in this chapter.

The methodology of the research is given first. The results are given afterwards. These are discussed next, in the discussion. Finally, a conclusion is given on the megaripples' forming mechanism and its dependence on large scale morphological shape. This explains the indicator role of the megaripples.

#### 3.7.1. Methodology

Literature research is used to investigate whether strong along shore currents form the megaripples and why (future) convex profiles are indicated by megaripples. How the current velocities develop in cross shore direction is looked into with model results, obtained for the erasing mechanism. The model set-up is discussed in paragraph 3.2.1 and the results are shown in paragraph 3.2.2.

#### 3.7.2. Results

Literature research shows that megaripples are formed under strong flow velocities [Kennedy, 1969][Singh and Kumar, 1974]. These ripples are mostly more than 60 centimeters in length, ranging up to 30 meters, and their height ranges from 6 centimeters to 1.5 meters [Singh and Kumar, 1974]. Also smaller ripples can occur. These are called ripples instead of megaripples. They are formed by weaker currents and or waves, see paragraph 1.1.

The along shore currents form the megaripples. Along shore flow velocities are dominating the cross shore flow velocities. This is observed by the author during creation of the model that is used to estimate bottom shear stresses due to waves and currents. See paragraph 3.2.1 for more details on the model. The ripples' orientation corresponds to the expected along shore current direction, see definition of megaripples in paragraph 2.3.2. This also indicates that the along shore currents form the ripples. Figure 3.8 shows estimated bottom shear stresses on convex, linear and concave large scale morphological shape. The figure shows that further offshore the current induced bottom shear stresses are getting larger, for all three large morphological shapes. The increase of current induced bottom shear stresses indicates that higher flow velocities are found. Therefore, it is likely that the along shore currents at the channelward end of the tidal flats are capable, at some point in the cross shore, to create megaripples. Note that this is observed for all three large scale morphological shapes that are considered in this research.

The convex large scale morphological shape is coupled to strong along shore currents. This explains why the megaripples are linked to convex shape, see paragraph 2.5.3. Friedrichs and Aubrey [1996] state that convex tidal shapes are formed in systems dominated by tidal flow. The mentioned tidal flow is in cross shore direction. However, strong along shore currents are found in a long and narrow estuary with a substantial tidal range, like the Western Scheldt. A large tidal prism is seen, due to the tidal range and length of the estuary. This causes strong along shore currents, because the estuary is narrow. Hence, strong along shore currents are coupled to convex tidal flats, if the estuary shape is long and narrow. The link between convex shapes and strong along shore currents can explain why convex tidal flats are not observed in the Eastern Scheldt, see paragraph 2.5.1. This estuary is shorter than the Western Scheldt. Therefore, the tidal prism is smaller. Thus, the along shore currents are expected to be smaller.

Convex profile shapes are coupled to strong along shore currents on the long term and megaripples on the short term to strong currents. The large scale morphological shape should react slower to an increase in along shore currents than megaripples are formed, since much more sediment needs to be displaced. Therefore, this increase will be seen first by the presence of megaripples and afterwards a convex profile can be observed.

### 3.7.3. Discussion

Strong along shore currents are expected in the Western Scheldt and this is coupled to the convex large scale morphological shapes, see paragraph 3.7.2. However, also linear and concave profiles are observed in the Western Scheldt, see paragraph 2.5.1. This could be explained by three arguments. First of all, the occurrence of linear and concave profiles could be explained by the tidal flats not being in equilibrium with the hydrodynamic conditions. Secondly, the importance of tidal flow in cross shore direction is determined by tidal flat shape as well and not only by tidal range, which is linked to along shore current velocity in paragraph 3.7.2. The third argument is that waves are possibly more important on some tidal flats than on others. This makes the relative importance of tidal flow less. Therefore, some flats could be non-convex.

Only non-convex tidal flats developing to convex tidal flats are seen in this research. Hence, it is not observed whether megaripples are absent before a convex tidal flat changes to a non-convex flat. This would be interesting to investigate.

### 3.7.4. Conclusion

In this section the following question is answered with respect to the small scale morphological feature type megaripples: "Which mechanisms are responsible for forming the small scale morphological features that are seen in the build-up and how are they influenced by the large scale morphological shape?". Strong along shore currents form the megaripples, hypothetically. These features are found as indicator for (future) convex profiles. Therefore, it is known that they are coupled to convex large scale morphological shape. Why this link exists is investigated in this chapter.

Strong along shore currents form the megaripples, see paragraph 3.7.2. Megaripples are found to be formed by strong currents. The orientation of these ripples is in a direction that matches to the along shore currents. Furthermore, the along shore current is found to dominate the cross shore current. Additionally, the along shore currents increase in strength towards the channel, for convex, linear and concave profiles. Therefore, the required strength is obtained at some point. Considering all the above, it is concluded that strong along shore currents form the megaripples.

Megaripples are coupled to (future) convex profile shapes. This can be explained by combining two facts. Both are given in paragraph 3.7.2. First of all, convex profile shapes are coupled to strong alongshore currents on the long term. Secondly, strong along shore currents form megaripples on the short term. Therefore, megaripples can indicate current convex profiles and profiles that develop to a convex profile.

Megaripples are always seen at the seaward end in the build-up. This can be explained by the increase in current velocities in channelward direction, seen in paragraph 3.7.2. The energy of the flow increases in the direction of the channel. This makes that the megaripples dominate the other categories.

### 3.8. Conclusion: Answer to sub-question

"Why is the build-up in small scale morphological feature categories coupled to the convex large scale morphological shape?" is the sub-question answered in this chapter. This question covers indirectly the other indicators. All the feature categories in the build-up are indicators on their own, see paragraph 2.5. The megaripples indicate (future) convex profiles. Additionally, all the features indicate a certain relative height and slope when they are seen within the build-up. Together they form the build-up and indicate a convex profile.

First of all, a brief summary of the feature forming mechanisms is given below to explain the individual indicator roles. Why megaripples indicate (future) convex profiles is addressed in the summary as well. In addition to the feature forming mechanisms, the erasing mechanism is also discussed. The summary of the mechanisms is later on combined to explain why the build-up indicates convex profiles. The height and slope where the feature forming mechanisms are important is crucial to explain why build-up indicates convex profiles.

#### 3.8.1. Summary

The feature forming and erasing mechanisms are summarized in this section.

1. **Pool shaped features**

The pool shaped features are formed by the described mechanism with positive feedback, see paragraph 3.3.4. The mechanism requires a relative height that allows for submergence and emergence. Furthermore, a mild slope that allow water to remain at the tidal flat is necessary.

2. **Gullies**

Drainage causes the formation of gullies that are seen in the build-up, see paragraph 3.4.4. This requires mild slopes. However, a minimum slope and/or drainage volume has to be present as well. The gully forming mechanism get weaker in channelward direction on convex profiles, after the minimum requirements are met. It is approximately equal in the cross shore for linear profiles.

3. **(Nearly) smooth areas**

The erasing mechanism is stronger than the forming mechanisms at the (nearly) smooth areas in the build-up, see paragraph 3.5.4. The (nearly) smooth areas are seen on steeper slopes and lower relative heights than required for the gullies. The mechanism forming (nearly) smooth areas in the build-up gets stronger in channelward direction on convex profiles and stays approximately equal on linear profiles, when only the gully forming mechanism is considered.

4. **Ship keel traces**

The ship keel traces could be formed by ships running aground or by erosion and the presence of former reclaimed areas, see paragraph 3.6.4. The occurrence of the ship keel traces is influenced by the tidal flat location and not by the large scale morphological shape of the tidal flat. The features are seen on a specific relative height. It could be argued that these features do not belong in the build-up definition, because they do not help to distinguish convex, linear and concave profiles.

5. **Megaripples**

Megaripples indicate (future) convex profile shapes. This can be explained by combining two facts, see paragraph 3.7.4. First of all, convex profile shapes are on the long term coupled to strong alongshore currents. Secondly, megaripples are linked to strong along shore currents on the short term. Therefore, megaripples can indicate current convex profiles and profiles that develop to a convex profile. They are always seen at the seaward end of the build-up. Thus, the other categories dominated by the megaripples at the seaward end. The reason is that current velocities increase in channelward direction.

6. **Erasing mechanism**

Large wave induced bottom shear stresses erase the small scale morphological features, see paragraph 3.2.4. They are smaller on the upper part of convex profiles than seen on top of linear and concave profiles. Furthermore, bottom shear stresses due to the combination of waves and currents decrease in landward direction for convex profiles, remain approximately constant for linear profiles and increase for concave profiles.

### **3.8.2. Explain build-up as indicator**

Build-up is not seen on concave profiles. This can be explained by the dependence of pool shaped feature formation on large scale morphological shape. The pool shaped features are seen on mild slopes and relative heights that allow for submergence and emergence, see paragraph 3.8.1. This situation is not observed on concave profiles and is on linear and convex profiles. Hence, the pools are not formed on concave profiles.

Convex profiles show the build-up more than linear profiles, because the transition from pools to gullies and from (vague) gullies to (nearly) smooth areas is forced stronger. The forming mechanism for pools and gullies depend both on mild slopes, see paragraph 3.8.1. However, milder slopes are required for the pool shaped feature forming mechanism than for gully formation. Pool formation relies on water retaining on the tidal flat, where the gully forming mechanism relies on water draining from the tidal flat. Water retaining on the tidal flat is more likely for milder slopes. Convex profiles are mildly sloped on top and the slope gets steeper in direction of the channel. This forces a transition from pool shaped features to gullies. On linear profiles the slope is approximately equal, per definition. Hence, the transition is not forced and more subject to temporal variability in the forces, e.g. eroding mechanism. The forming mechanism for (nearly) smooth areas increases in channelward direction on convex profiles and stays approximately equal on linear profiles, see paragraph 3.8.1. For gully formation the strength decreases in channelward direction on convex profiles and stays approximately equal on linear profiles. Both developments together force a transition from (vague) gullies to (nearly) smooth areas on convex profiles and not on linear profiles.



# 4

## Discussion

The research' most important points of discussion are given in this chapter. The applicability of the found indicators in other systems is the bottom line. The discussion points are:

1. The investigated convex profiles are only located in the Western Scheldt, see paragraph 2.5.1. All the found indicators are related to convex profile shape. Therefore, the applicability in other estuaries has to be proven.
2. The temporal behavior of the indicators is not explained this research. The build-up is not observed in every aerial photograph of the convex profiles with regularly observed build-up, see paragraph 2.4.2. The megaripples are not always seen on convex profiles as well. This has been blamed on temporal variability of important mechanisms and some unfortunately timed photographs. The temporal variation of the mechanisms is not looked into in this research. Hence, it is not clear why indicators are sometimes not observed. The temporal variation could be different in other systems, possibly changing the occurrence ratio of the indicators. Furthermore, the unknown temporal variation makes it more difficult to determine when aerial footage of tidal flats should be acquired. This makes using the indicator more challenging.
3. The build-up is not regularly seen on all convex tidal flats, see paragraph 2.4.2. When build-up is observed in more than half of the processed aerial photographs it is considered to occur regularly. Four explanations are given for the irregular observations: dominating large scale channels, crooked profile shapes, tidal flats that are located just channelwards of the investigated flats and the presence of headlands. However, the exact reason for the deviating behaviors is not determined. Knowing it is important for the extension this research's outcome to other systems.
4. The influence of sediment composition is not known. Other estuaries or tidal flats could have different sediment compositions. This could change the appearance or occurrence of the indicators.
5. The conclusion on the pool shaped forming mechanism is mainly based on observations and rough comparisons, instead of (reproducible) measurements, see paragraph 3.3.3. Hence, it is important better substantiate the found pool shaped features' forming mechanism. Three reasons can be given for the relevance: the pools are crucial in the build-up definition, they explain why build-up is not observed on concave profiles and why build-up is observed a few times on linear profiles. The build-up can be applied with more certainty in other systems when the found pool forming mechanism is better substantiated.
6. The estimated bottom shear stresses play a major role in the explanation of most small scale feature forming mechanisms. This holds for the pool shaped features, the (nearly) smooth areas, river dunes and also the ship keel traces. A 1D model is used to estimate the bottom shear stresses. It is set up in cross shore direction. Therefore, only cross shore variations are considered. The analyzed transects are located mostly in the middle of the tidal flats as well. The bottom shear stress developments might be different in situations where the along shore variation is larger. This could change the occurrence and/or appearance of the indicators.

7. The influence of photograph resolution and contrast on the identification of small scale feature categories is not known. It is explained in paragraph 2.4.2 that two photographs of the same area at the same moment could be judged differently if the resolution and/or contrast differ(s). E.g., an area could be classified as (nearly) smooth with a low resolution, while texture is seen in a high resolution photograph. It is not investigated whether resolution and contrast indeed influence the identification of small scale feature categories. The minimum requirements for identification is not given as well. However, this knowledge is of importance to apply the found indicators.



# 5

## Conclusion

Knowledge about the development of intertidal flats and salt marshes is crucial for a good coastal zone management, since they fulfill a broad range of functions. The management could benefit from current technological progress if small scale morphological features can be used as indicators for large scale morphological shape and development. The potential is the incentive for this research, see chapter 1. Hence, the research aim is to find small scale morphological features that are indicators for large scale morphological shape and development and gather sufficient knowledge to make them applicable. The aim can be split in two aspects. The first aspect is whether the small scale morphological features are indicators for large scale morphological shape and development. The second aspect is about gathering knowledge to make sure the indicator can be used properly. The aspects are treated in chapters 2 and 3, respectively. The outcome will be summarized below. Hereafter, the main question is answered. Finally, the contribution of this research to the available literature is reflected on.

### 5.1. Indicator detection and explanation

Several indicators are found in chapter 2. This fulfills the first aspect that is important to make sure small scale features can be used as indicators. A build-up in small scale morphological feature categories is an indicator for convex large scale morphological shape and indirectly for accreting behavior. The definition of the build-up is:

1. It starts at the landward side of the tidal flat with pool shaped features or pools with gully formation.
2. At least two of the following categories are seen channelwards of this start: pools with gully formation, pools and gullies, gullies, vague gullies, (nearly) smooth, ship keel traces and megaripples.
3. The consecutive categories are in the order mentioned. Some exceptions are made:
  - (a) The following categories may once be reversed: vague gullies with (nearly) smooth areas and ship keel traces with megaripples
  - (b) Sometimes one or two arbitrary categories are seen between the build-up and salt marsh/dyke. This is neglected in the required order, as long as their coverage is small. These categories are mostly (vague) gullies or (nearly) smooth areas.
  - (c) Areas with texture (contrast is seen but no distinguishable features) or tidal flat sized channels sometimes disturb the build-up, this is neglected.

Furthermore, all the feature categories in the build-up are indicators on their own. The megaripples indicate (future) convex profiles. Additionally, all of them indicate a certain relative height and slope when they are seen within the build-up. Together they form the build-up and indicate a convex profile.

The found indicator roles are explained in chapter 3. This satisfies the second aspect that is important to make sure small scale features can be used as indicators. The forming mechanisms of all the features in the build-up are given, just as their erasing mechanism. Hence, their individual indicator role of relative height and slope is explained by giving the important hydrodynamic conditions. Additionally, the indicator role of megaripples is clarified. Furthermore, it explained why build-up indicates convex profiles. The forming mechanisms of pool

shaped features, gullies and (nearly) smooth areas are combined for this purpose. The pool shaped feature forming mechanism explains why build-up is not seen on concave profiles. Convex profile shape forces a transition between pools and gullies and between (vague) gullies and (nearly) smooth areas. This transition is not forced on linear profiles. The forcing explains why build-up is much more often seen on convex profiles than on linear profiles. Also an improvement of the build-up definition is given; The ship keel traces can be left out, since they do not help to distinguish convex, linear and concave profiles.

All the features in the build-up indicate ecological activity of an area. They are all linked to specific characteristics. For instance, the pool shaped features show a diverse area, which could enhance biodiversity. Wet and dry areas are seen with diverging bottom strengths, this indicates that the sediment properties also differ. It is also seen that the erasing force is small at the location of the pool shaped features. The morphology will be less dynamic than lower on the convex profile. Hence, ecology can be well established without being often removed.

## 5.2. Answer to the main question

The main question is: "Can small scale morphological features on estuarine tidal flats be used as indicators for large scale morphological shape and development?"

Small scale morphological features on estuarine tidal flats can be used as indicators in the Western Scheldt. This research detects and explains features that indicate large scale morphological shape, development, certain hydrodynamic conditions and ecological activity of an area, see paragraph 5.1. The applicability of the indicators in other systems should be proven by extending this research to other situations, see chapter 4. The author has confidence in the applicability in other systems. The reason is that ridge and runnel structures, gullies and megaripples are observed in other systems as well, see paragraphs 1.1, 3.4 and 3.7. The pool shaped features show resemblance with the ridge and runnel structures, see paragraph 3.3.4. Therefore, the found indicator roles of the small scale morphological features probably exist in other systems.

## 5.3. Contribution to literature

This research contributes on five fronts to the available knowledge in the literature. It was known at the start of this research that large scale morphological shape and development are coupled and that bedforms are present on tidal flats. The hydrodynamic conditions that form the small scale features were also familiar. The first contribution is the identification of other small scale morphological features, in addition to these known bedforms. Secondly, these and already known features are classified. Third, the observed features are linked to certain large scale shape and development, i.e. small scale morphological indicators are detected. Fourth, the hydrodynamic conditions that form and erase the features are elaborated on and combined to explain the found indicator roles. Finally, it is noted that the characteristics that belong the small scale features can be linked to ecological activity of an area.

# 6

## Recommendations

Recommendations are given in this chapter that concern the extension of this research to other systems. This research detects and explains small scale morphological features that indicate large scale morphological shape, development, certain hydrodynamic conditions and ecological activity of an area, see chapter 5. However, the applicability of the indicators in other systems should be proven by extending this research to other situations. Doing more research is therefore recommended. The recommendations are:

1. It is recommended to investigate aerial footage and elevation data from tidal flats in other estuaries. Only convex tidal flats located in the Western Scheldt are incorporated in this research, see chapter 4. All the found indicators are related to convex shape. Therefore, it would reveal general applicability when the indicators, build-up and megaripples, are found in other estuaries as well.

Looking at convex tidal flats in the Eastern Scheldt would be a logical start. The elevation measurements and aerial photographs that are used in this research cover more tidal flats than the investigated ones. These measurements could be used to look at convex tidal flats in the Eastern Scheldt.

It would be interesting to investigate an estuary with minimal human interventions, in addition to the Eastern Scheldt. This could reveal the importance of the interventions for the indicator. Build-up is not regularly found on all convex tidal flats in this research. This has been blamed on, among other things, crooked convex profile shapes, see paragraph 2.4.2. These crooked profile shapes might not occur without human interventions. Understanding the build-up without human interventions will aid appropriate use of the indicator when interventions are present.

2. The temporal behavior of the important forming and erasing mechanisms should be investigated and compared to the temporal behavior of the indicators. Both temporal behaviors are not looked at in this research, see chapter 4. Gathering this knowledge will help with planning a moment to collect valuable footage and determine whether the found indicators apply in other systems as well.

Investigating the seasonality of the wind climate will give insight in the temporal behavior of the erasing mechanism and the pool forming mechanism; Wind waves are important for both. Comparing wind speeds and directions with transect orientations and occurrences of build-up can be done to get insight in the seasonality.

How long it takes to develop the build-up after a complete wipe out is also valuable knowledge. This could be investigated by frequently gather aerial footage of a tidal flat after a big storm has occurred or by collecting images in the field on a regular interval.

3. It is recommended to find out why build-up is not regularly seen on all convex tidal flats. Five out of the eight convex profiles show build-up in more than half of the processed aerial photographs, see paragraph 2.4.2. This is considered as regular occurrence of the build-up. It is not investigated why three of the convex profiles do not show the build-up regularly. Knowing the reason behind the deviating behavior is important to determine whether this research is representative for other systems.

A first step could be to look at how all the important forming/erasing mechanisms differ between tidal flats where build-up is regularly and not regularly seen. The 1D model that makes use of SWAN could for instance be used to investigate the differences for the erasing mechanism. Note that this is not representative when alongshore variations are important, e.g. due to the presence of headlands.

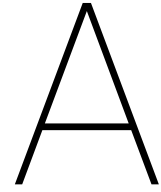
It would be valuable to know the influence of human interventions on the found indicators. The interventions possibly cause the irregular occurrence of the build-up on some convex tidal flats. This could be investigated by clearly indicate which interventions are done in the Western Scheldt and determine what morphological changes they have caused. Looking at another estuary with no/minimal human interventions would be another method. Human interventions are not important if irregular occurrence of build-up on convex tidal flats is seen with this last method as well.

4. Linking sediment composition and occurrence of the indicators is recommended to do. This will show if sediment composition has influence on them. In this research no attention has been given to the influence of sediment composition, see chapter 4. Sediment composition can be determined for the tidal flats investigated in this research. It would be even better if this determination is done at the same moment aerial footage is acquired; This allows using the exact composition.
5. It is recommended to do more research on the mechanism that forms pools. The conclusion on the pool shaped forming mechanism is mainly based on observations and rough comparisons, instead of (reproducible) measurements, see paragraph 3.3.3. However, the pool shaped features' forming mechanism is important to understand completely for three reasons: the pools are crucial in the build-up definition, they explain why build-up is not observed on concave profiles and why build-up is observed a few times on linear profiles. Therefore, gaining more knowledge about the pool forming mechanism would add great value to this research and assure that the indicators can be used in other situations.

The pool forming mechanism could be investigated by visually follow pool evolution and do bottom elevation measurements at the same time. Pointing a camera on one or more pool shaped features can capture the pool evolution. The bottom elevation in- and outside the pool(s) should be measured at the same time. This gives the evolution of the pool(s) on a high temporal resolution. The results will provide more knowledge on the forming mechanism with positive feedback. The change after a period of submergence indicates whether the erosion takes place during this period and if it is indeed stronger inside the pools than outside. The pools should evolve in the period of emergence when there is a lot of wind and/or strong drainage. The influence of a negative feedback mechanism can be determined from the bottom elevation measurements as well.

Measuring the height of wind waves in the pools during emergence and modeling the induced bottom shear stresses will provide more information about their potential to cause uneven critical bed shear stresses. Adding sediment measurements in and around the pools will give even more insight in the unequal soil strengths and erosion. A high spread in the wet density measurements in and around pool shaped features is seen in this research. This made the measurements unreliable. However, the observations could represent the reality. Therefore, the sediment measurements should be done by a proven method or the possible high spread should be taken into account in another way.

6. The influence of resolution and contrast in the aerial photographs on the category determination should be investigated. No attention has been paid to this, see chapter 4. It could be investigated by changing resolution and contrast of one photograph to create multiple photographs. Hereafter, different people should determine which categories are seen in the photographs.



## Elevation measurements

Bottom elevation measurements are given in this appendix for all the investigated transects, see figure A.1 up to and including A.11. These elevations are measured with GPS by Rijkswaterstaat [2017a] since 1991, 1993 or 1994, depending on the transect of interest. The measurements up to 2016 are shown. On all tidal flats one transect is investigated, except for Waarde. Three transects are looked into for Waarde. The limits of both axis are kept the same in each figure to allow for a quick comparison.

### A.1. Anna Jacobapolder

An eroding concave profile is found at Anna Jacobapolder's analyzed transect, see figure A.1. This profile is retreating until 2005, the whole profile moves landward, and remains approximately stable after that. The upper part of the profile keeps eroding/retreating.

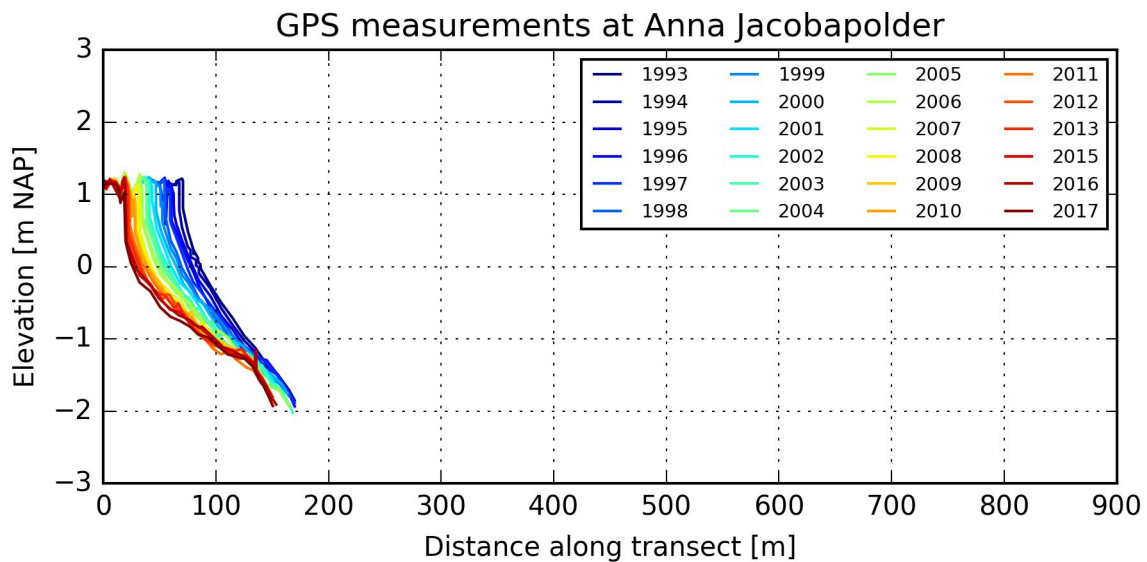


Figure A.1: This figure shows the bottom elevation of the investigated transect on the tidal flat Anna Jacobapolder for several years. These elevations are measured with GPS by Rijkswaterstaat [2017a].

## A.2. Baalhoek

A convex profile is seen at Baalhoek, see figure A.2. This profile is retreating and stable at the upper part until 2005. In 2005 it starts accreting at the upper part and eroding lower in the profile. A crooked profile develops, due to this split behavior. In 2010 it starts to expand at the most channelward tip.

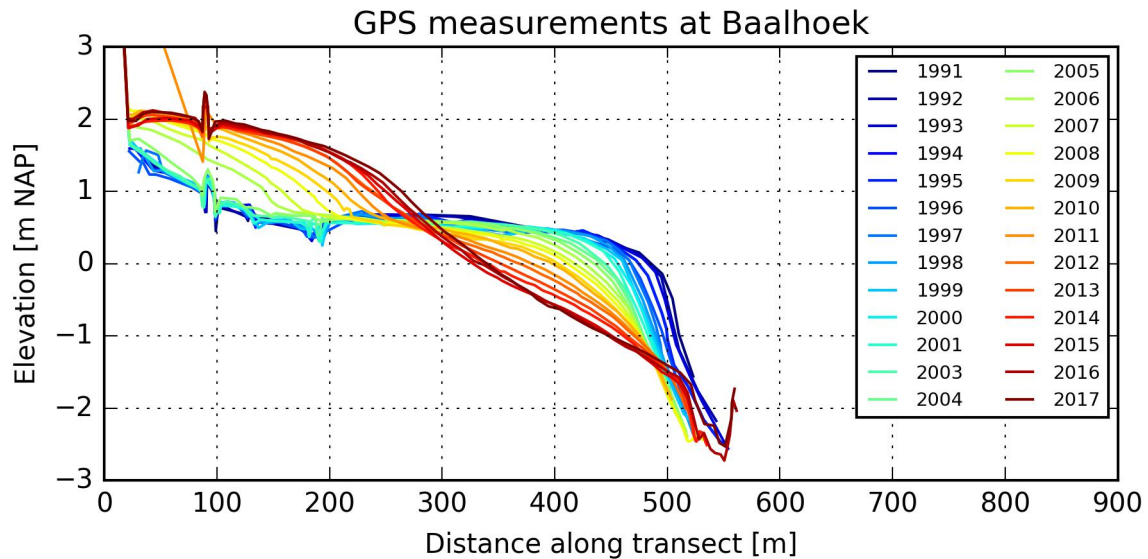


Figure A.2: This figure shows the bottom elevation of the investigated transect on the tidal flat Baalhoek for several years. These elevations are measured with GPS by Rijkswaterstaat [2017a].

## A.3. Bath

At Bath a convex profile is found that is slightly accreting and retreating, see figure A.3.

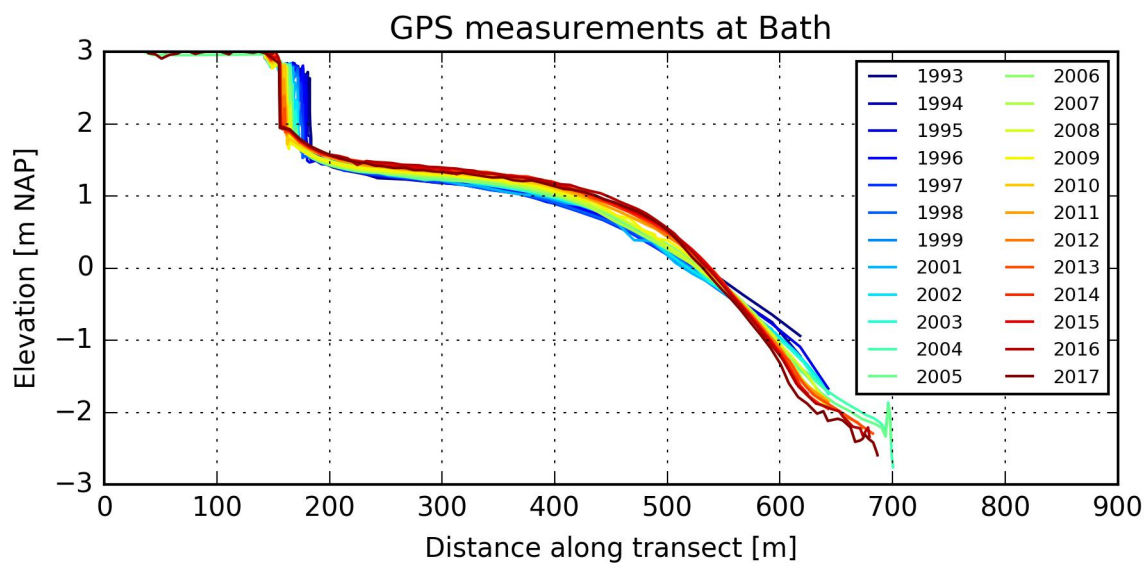


Figure A.3: This figure shows the bottom elevation of the investigated transect on the tidal flat Bath for several years. These elevations are measured with GPS by Rijkswaterstaat [2017a].

## A.4. Kats

A linear profile is found at Kats, see figure A.4. This profile shows erosion except for one spot, around 180 meter distance. It seems approximately stable in cross shore direction.

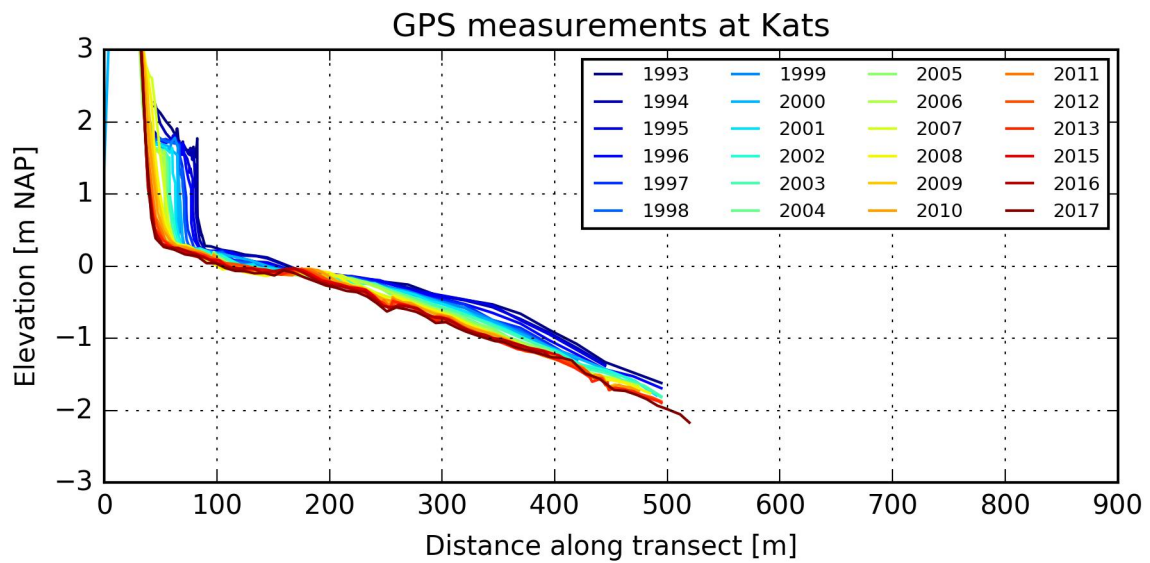


Figure A.4: This figure shows the bottom elevation of the investigated transect on the tidal flat Kats for several years. These elevations are measured with GPS by Rijkswaterstaat [2017a].

## A.5. Knuitershoek

At Knuitershoek an accreting and eroding convex profile is found, see figure A.5. It is accreting at the landward side of the upper part. At the channelward side of the upper part it is eroding. Therefore, the profile deforms over the years. In the figure can be seen that the profile is a bit crooked; It is not a convex profile with smooth transitions. The profile at Knuitershoek is retreating. The years 2015 and 2016 form an exception on this retreating behavior. In these years expansion is seen on a part of the seafront. The other part is approximately stable.

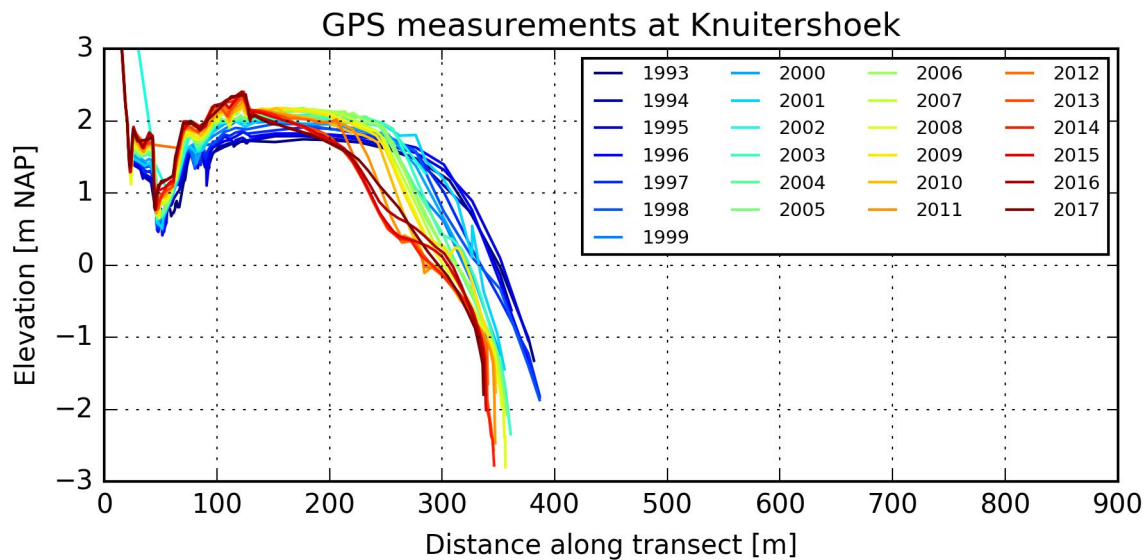


Figure A.5: This figure shows the bottom elevation of the investigated transect on the tidal flat Knuitershoek for several years. These elevations are measured with GPS by Rijkswaterstaat [2017a].

## A.6. Land van Saeftinghe

An accreting, retreating convex profile is found at Land van Saeftinghe, see figure A.6.

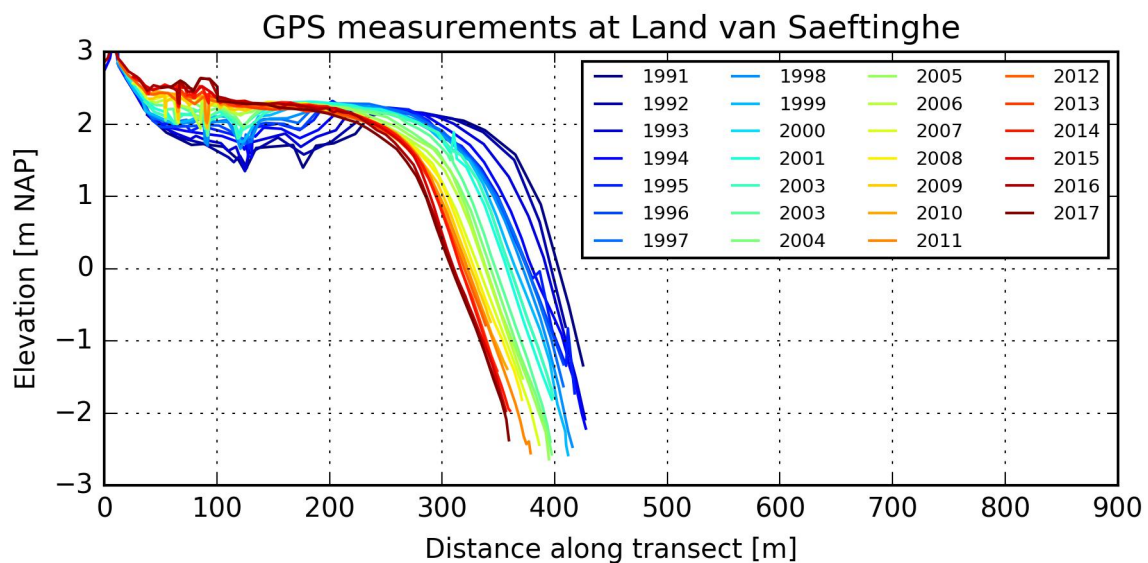


Figure A.6: This figure shows the bottom elevation of the investigated transect on the tidal flat Land van Saeftinghe for several years. These elevations are measured with GPS by Rijkswaterstaat [2017a].



## A.7. Waarde's 1<sup>st</sup> transect

Waarde's 1<sup>st</sup> transect shows two large scale morphological profile shapes in the measured period, see figure A.7. Until approximately 2002 this profile is linear and from 2005 onwards it is convex. The split in shape is probably due to two headlands that are constructed at the tidal flat Waarde.

When the profile is linear it shows erosion at the upper part and is approximately stable in cross shore direction, until 2000. Starting in 2000 the upper part is approximately stable and the profile is expanding. The convex shape of Waarde's 1<sup>st</sup> transect is mainly accreting and expanding. In 2013 the accreting behavior stabilizes at the channelward side of the mildly sloped part. Accreting is still seen at the upper most landward part of the transect after 2013. In 2012 the expanding behavior becomes retreating.

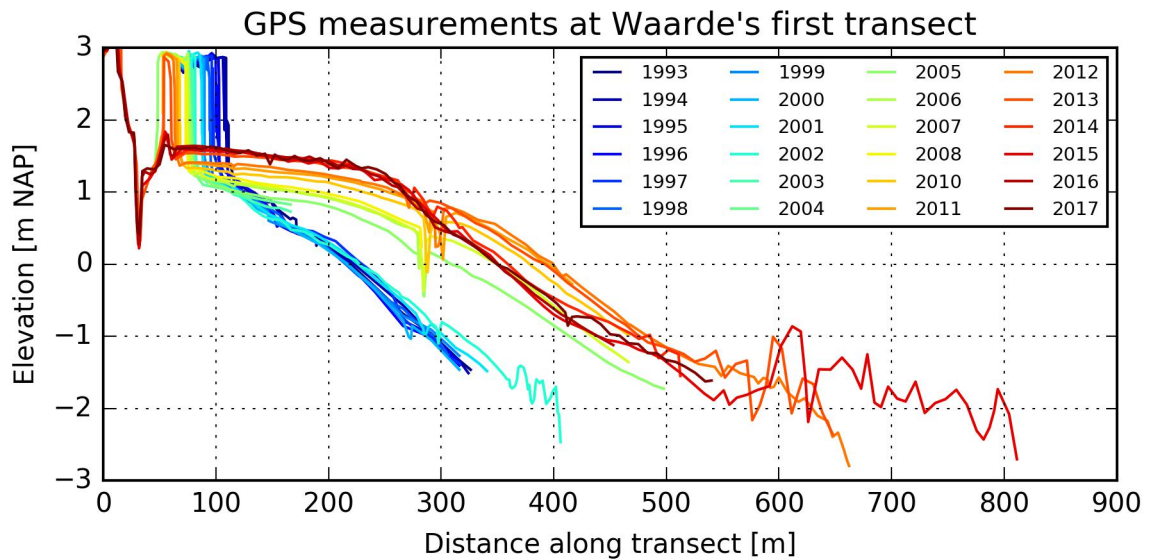


Figure A.7: This figure shows the bottom elevation of the 1<sup>st</sup> transect on the tidal flat Waarde for several years. These elevations are measured with GPS by Rijkswaterstaat [2017a].

### A.8. Waarde's 2<sup>nd</sup> transect

Also at Waarde's 2<sup>nd</sup> transect two different shapes are found in the measured period, see figure A.8. Until approximately 2003 it is concave and starting in 2009 it can be called convex.

The concave profile is eroding and approximately stable in the cross shore direction. The convex profile is accreting and expanding.

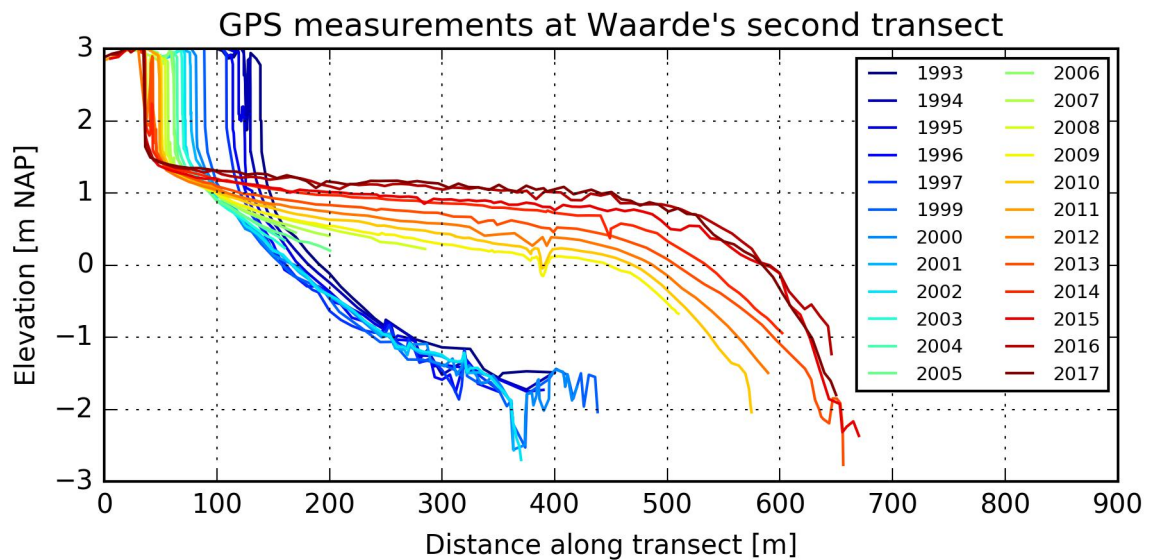


Figure A.8: This figure shows the bottom elevation of the 2<sup>nd</sup> transect on the tidal flat Waarde for several years. These elevations are measured with GPS by Rijkswaterstaat [2017a].

## A.9. Waarde's 3<sup>rd</sup> transect

An eroding and retreating convex profile is found at Waarde's 3<sup>rd</sup> transect, see figure A.9. This profile is connected to an offshore sand bank up to 2006. After 2006 this connection is mostly gone.

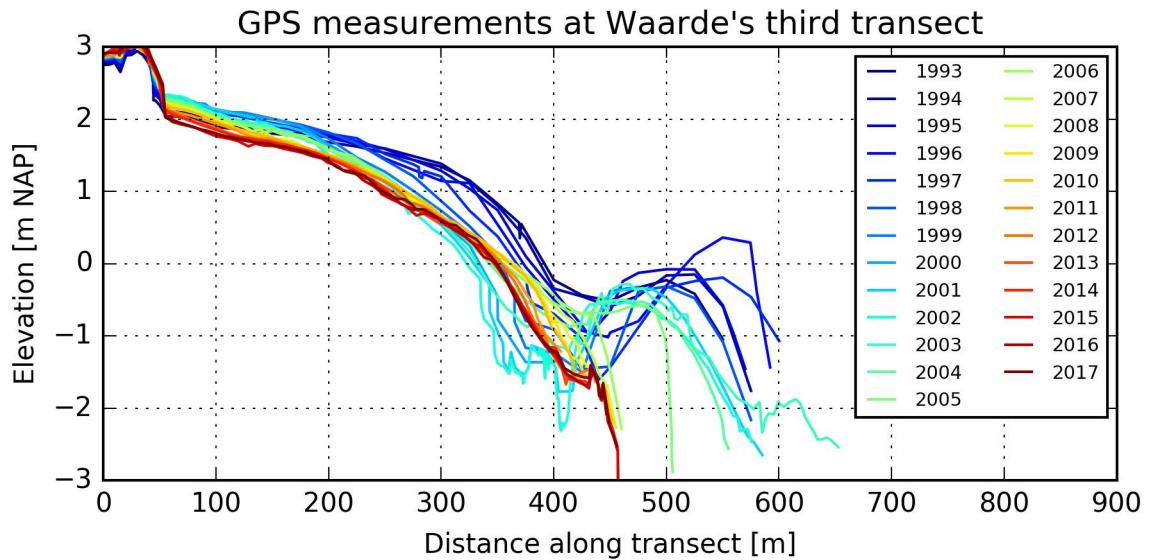


Figure A.9: This figure shows the bottom elevation of the 3<sup>rd</sup> transect on the tidal flat Waarde for several years. These elevations are measured with GPS by Rijkswaterstaat [2017a].

## A.10. Zandkreek

Zandkreek's transect is found to be linear, see figure A.10. This profile is slightly eroding and stable in cross shore direction.

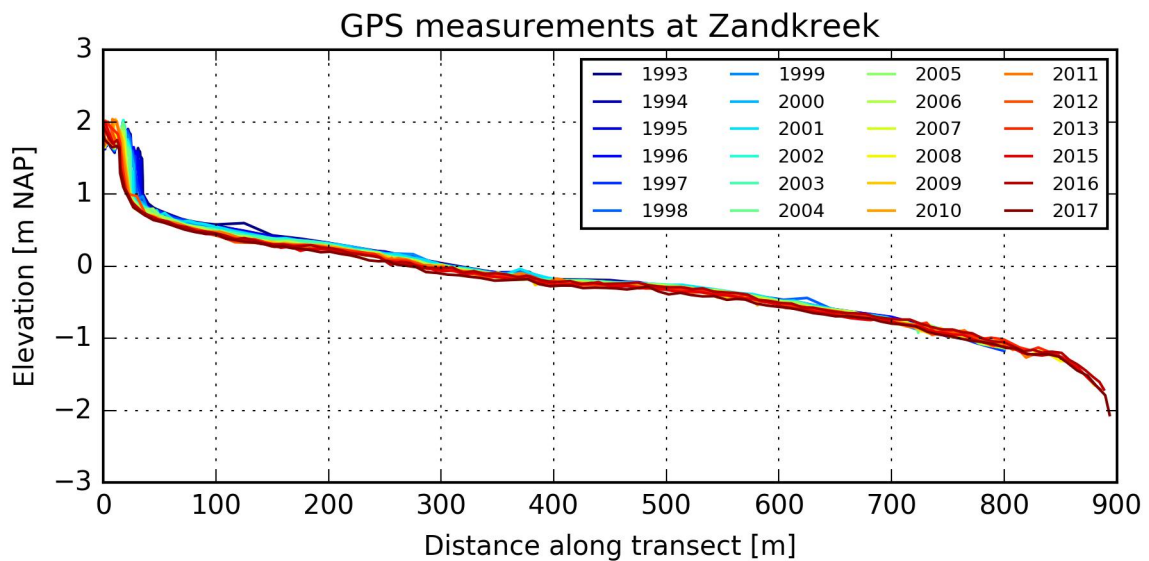


Figure A.10: This figure shows the bottom elevation of the investigated transect on the tidal flat Zandkreek for several years. These elevations are measured with GPS by Rijkswaterstaat [2017a].

### A.11. Zuidgors

At Zuidgors two different shapes are seen, see figure A.11. Until 2001 this profile is linear and starting in 2005 this is classified as convex. The linear profile is eroding and approximately stable in the cross shore direction. The convex profile is accreting and expanding. After 2011 retreat is observed in some years and expansion in other years.

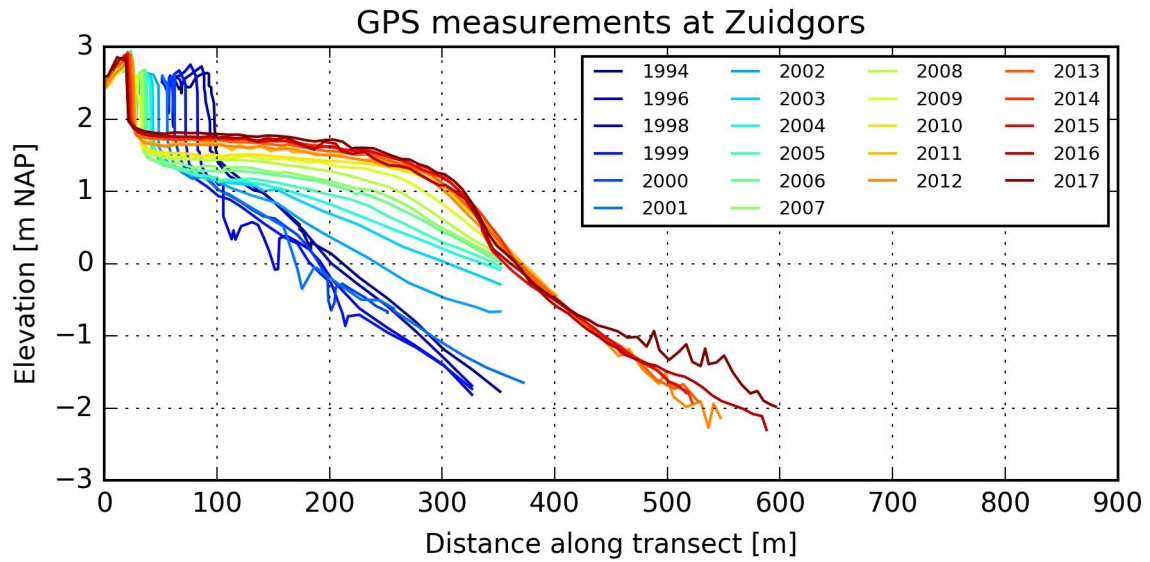


Figure A.11: This figure shows the bottom elevation of the investigated transect on the tidal flat Zuidgors for several years. These elevations are measured with GPS by Rijkswaterstaat [2017a].

# B

## Categorized aerial photographs

The categorizing aerial photographs of all analyzed transects are given in this appendix, on alphabetical order. Photographs of a rectangle around the transect of interest are used to identify which small scale feature category in seen where and in which year. The categories are elaborated on in paragraph 2.3.2. The rectangle covers 25 meters on both sides of the transect and is oriented parallel to it. The bed elevation measurements, temporally least far apart from the moment the photograph is taken, are visualized in every image.

### B.1. Anna Jacobapolder

At Anna Jacobapolder mostly the category algae mats is observed, see figure B.1. This figure displays the categorization of the aerial footage of Anna Jacobapolder's transect. In the figure also (nearly) smooth areas, vague gullies and texture are observed.

#### Anna Jacobapolder

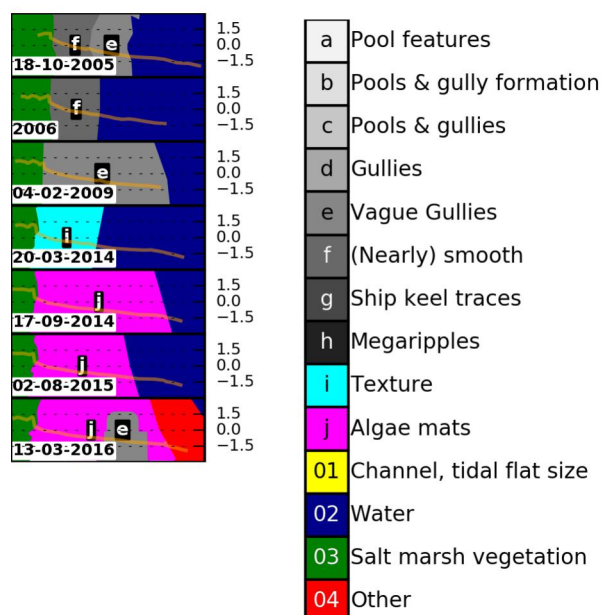


Figure B.1: This figure displays the categorized aerial photographs of several years for an area around the transect at Anna Jacobapolder. The categories mentioned in paragraph 2.3.2 are used for this. The area is a rectangle around the transect that covers 25 meters on both sides of it and is oriented parallel to it. The temporally closest elevation measurement series is displayed in each photograph. On the right side of each photograph is the measured height displayed in m NAP. The date the photos are taken is displayed on at the lower left of each categorized photograph.

## B.2. Baalhoek

Three times is the build-up in categories seen from salt marsh to waterfront at Baalhoek, see figure B.2. See paragraph 2.3.2 for the build-up definition. In 2000 pool shaped features (a) are followed by nearly smooth (f) and vague gully areas (e). Between the pools and salt marsh a nearly smooth area is observed. The build-up starts in 2003 with pools and gully formation (b). Then it goes to pools and gullies (c), vague gullies (e) and nearly smooth (f). Between the build-up and salt marsh an area categorized as (nearly) smooth (f) is seen. Also in 2006 build-up is seen. The area between dyke and build-up is categorized as (nearly) smooth (f) and fairly large. The size of this area is tolerated, since a large part of this area was considered to be salt marsh vegetation in 2003 and the elevation measurements also still show a change in slope. In the aerial photograph still some patches of vegetation are seen, but not enough to classify the area as salt marsh vegetation. The build-up itself starts with pools and gully formation (b), then continues in vague gullies (e) and ends in ship keel traces (g).

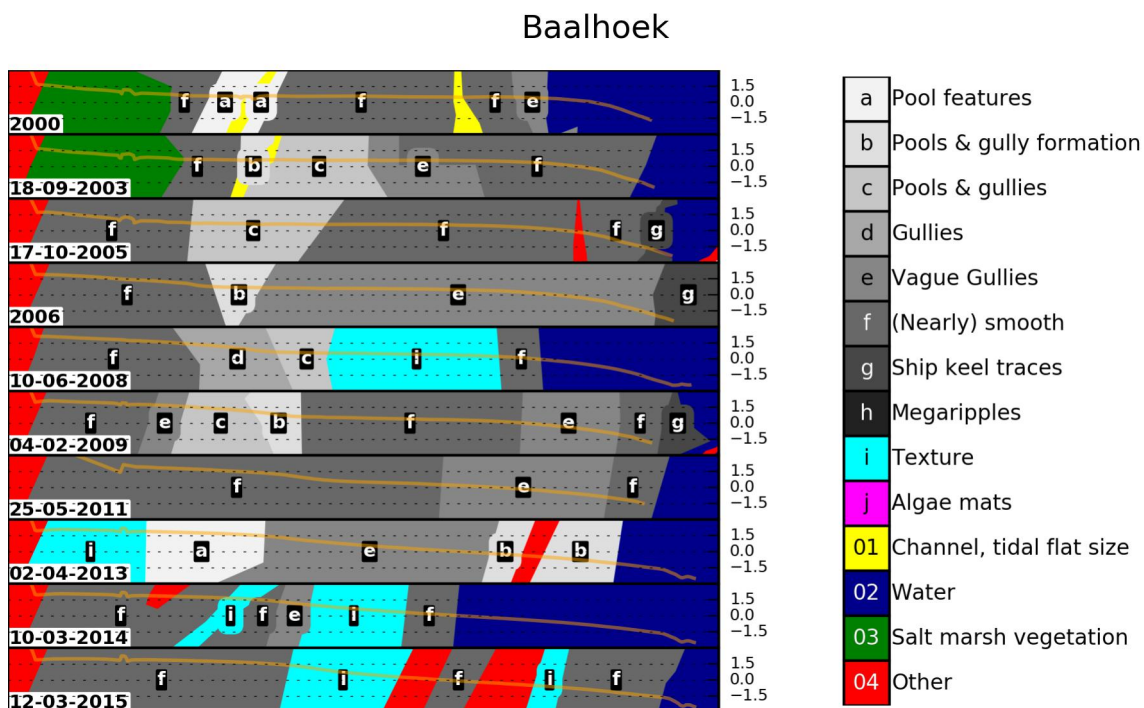


Figure B.2: This figure displays the categorized aerial photographs of several years for an area around the transect at Baalhoek. The categories mentioned in paragraph 2.3.2 are used for this. The area is a rectangle around the transect that covers 25 meters on both sides of it and is oriented parallel to it. The temporally closest elevation measurement series is displayed in each photograph. On the right side of each photograph is the measured height displayed in m NAP. The date the photos are taken is displayed on the lower left of each categorized photograph.

### B.3. Bath

At Bath's analyzed transect is mainly the build-up in categories seen, see figure B.3. See paragraph 2.3.2 for the build-up definition. Ten out of thirteen images shows this build-up. 2005, 2013 and 2014 show no build-up. In 2014 the build-up is interrupted once by category (a) at the wrong place. Mostly an area categorized as (nearly) smooth or vague gullies is seen between the build-up and salt marsh. Once two small strips of arbitrary categories are seen in between build-up and salt marsh.

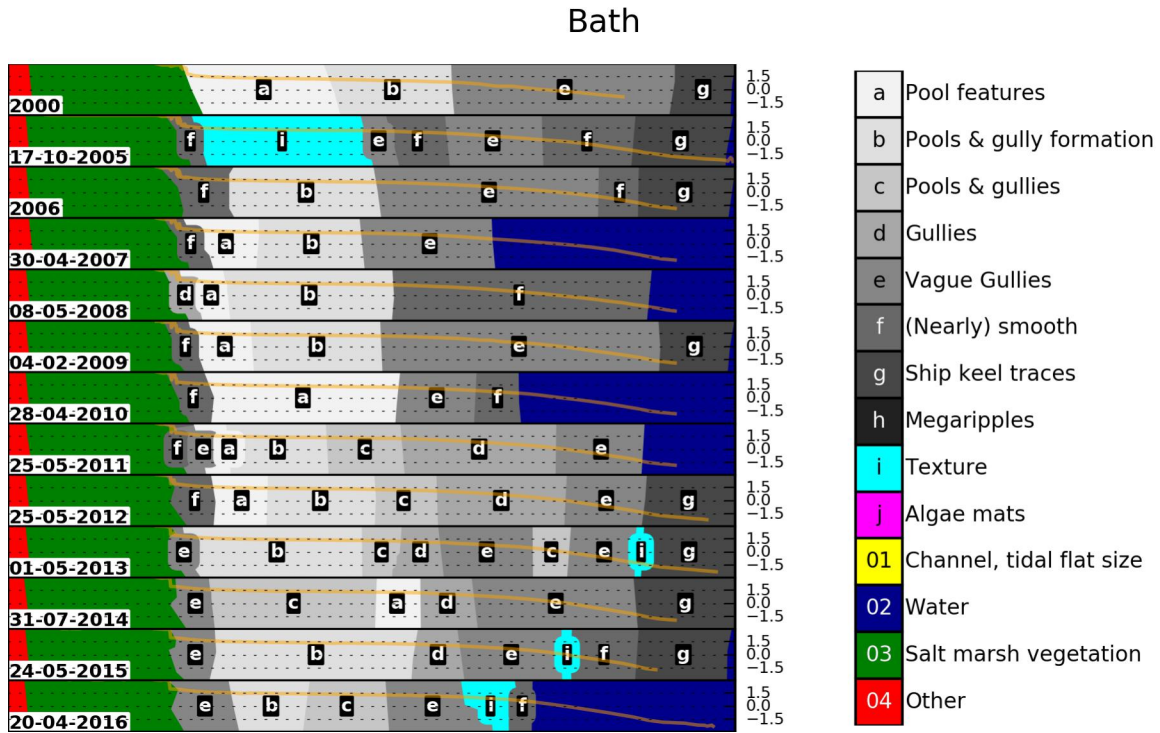


Figure B.3: This figure displays the categorized aerial photographs of several years for an area around the transect at Bath. The categories mentioned in paragraph 2.3.2 are used for this. The area is a rectangle around the transect that covers 25 meters on both sides of it and is oriented parallel to it. The temporally closest elevation measurement series is displayed in each photograph. On the right side of each photograph is the measured height displayed in m NAP. The date the photos are taken is displayed on at the lower left of each categorized photograph.

## B.4. Kats

At the tidal flat Kats is build-up only observed twice, in 2009 and 2010, see figure B.4. See paragraph 2.3.2 for the build-up definition. Between these build-ups and the salt marsh a small area categorized as (nearly) smooth is seen. Note that in 2009 deviant behavior is seen channelwards of the tidal flat sized channel. This deviant behavior is neglected in determining whether build-up is observed.

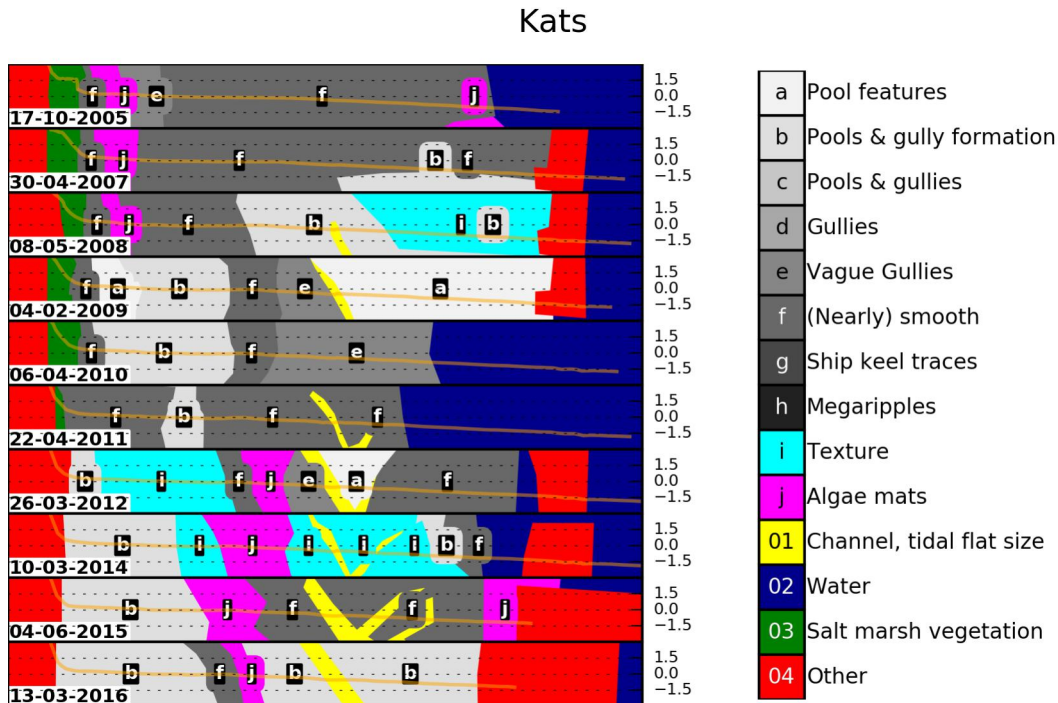


Figure B.4: This figure displays the categorized aerial photographs of several years for an area around the transect at Kats. The categories mentioned in paragraph 2.3.2 are used for this. The area is a rectangle around the transect that covers 25 meters on both sides of it and is oriented parallel to it. The temporally closest elevation measurement series is displayed in each photograph. On the right side of each photograph is the measured height displayed in m NAP. The date the photos are taken is displayed on at the lower left of each categorized photograph.



### B.5. Knuitershoek

Knuitershoek shows the build-up in categories four times, 2006, 2008, 2009 and 2013, see figure B.5. See paragraph 2.3.2 for the build-up definition. No arbitrary category between the salt marsh and build-up is seen. In 2005 also a build-up in mentioned categories is seen. This is not seen as a build-up in categories, because category (b) is tiny and located far away from the transect. Note the difference in large scale morphological shape between 2013 and the surrounding years. In 2012 and 2014 a sharper transition in slopes is seen than in 2013. The transition between higher elevated part and lower part is smoother in 2013. The transition between higher elevated part and lower part is smoother in 2013.

#### Knuitershoek

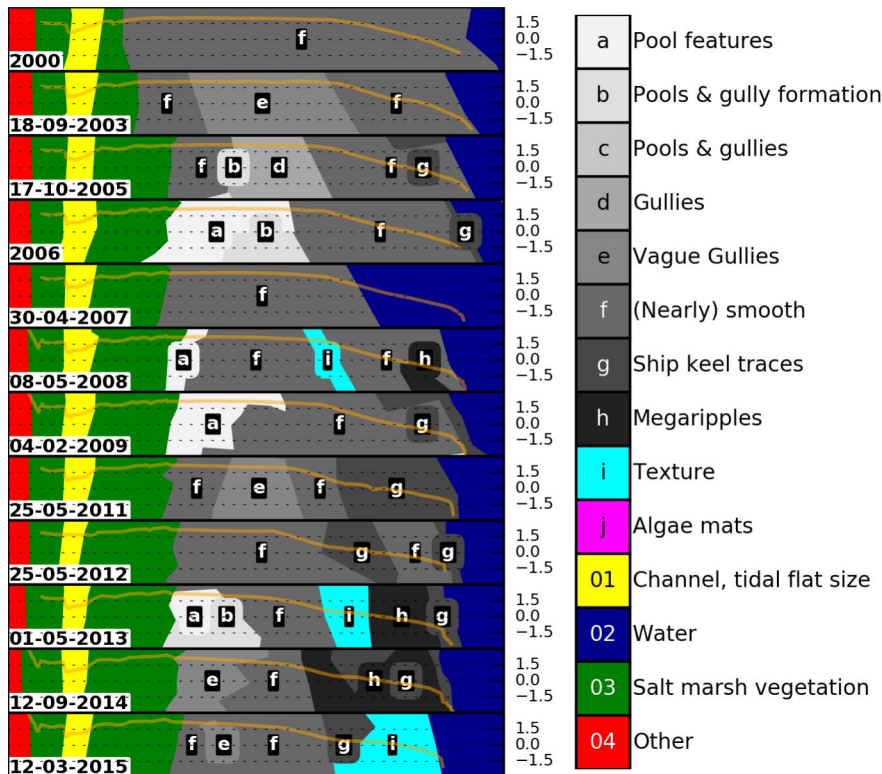


Figure B.5: This figure displays the categorized aerial photographs of several years for an area around the transect at Knuitershoek. The categories mentioned in paragraph 2.3.2 are used for this. The area is a rectangle around the transect that covers 25 meters on both sides of it and is oriented parallel to it. The temporally closest elevation measurement series is displayed in each photograph. On the right side of each photograph is the measured height displayed in m NAP. The date the photos are taken is displayed on at the lower left of each categorized photograph.

### B.6. Land van Saeftinghe

Land van Saeftinghe shows eight times a build-up in categories and five times it is not observed, see figure B.6. See paragraph 2.3.2 for the build-up definition. It is not observed in 2000, 2005, 2011, 2013 and 2016. Only once an arbitrary category is seen between the build-up and salt marsh. It is never interrupted by areas with texture.

Land van Saeftinghe

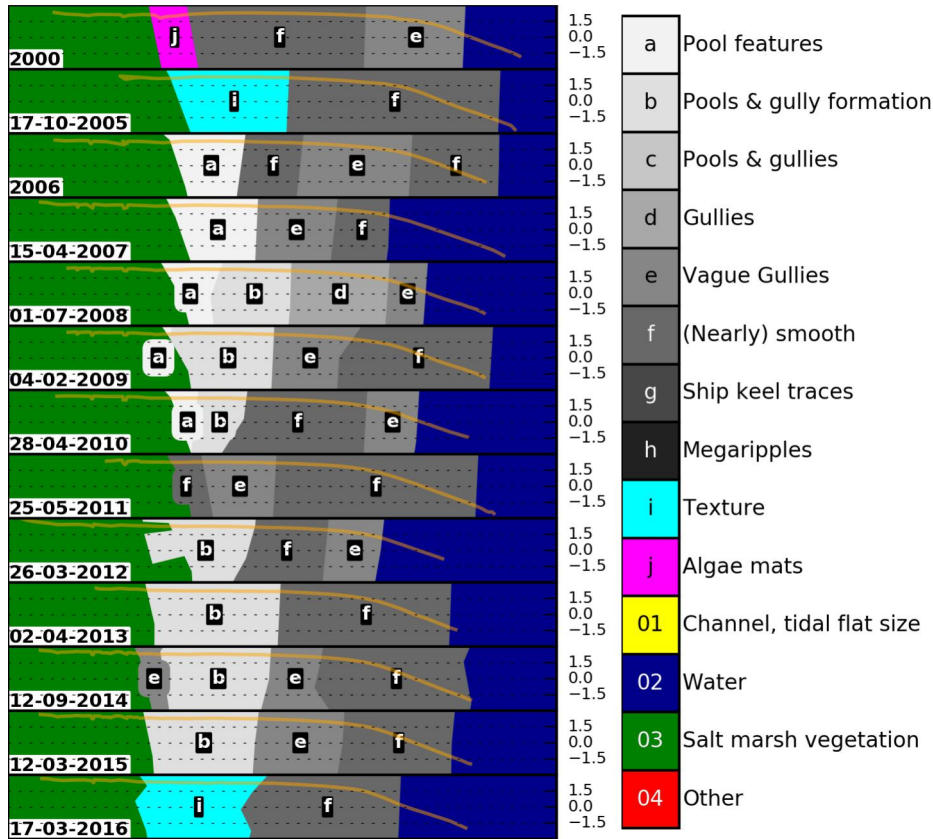


Figure B.6: This figure displays the categorized aerial photographs of several years for an area around the transect at LandvanSaeftinghe. The categories mentioned in paragraph 2.3.2 are used for this. The area is a rectangle around the transect that covers 25 meters on both sides of it and is oriented parallel to it. The temporally closest elevation measurement series is displayed in each photograph. On the right side of each photograph is the measured height displayed in m NAP. The date the photos are taken is displayed on at the lower left of each categorized photograph.

### B.7. Waarde's 1<sup>st</sup> transect

At Waarde's 1<sup>st</sup> transect only 3 times the build-up in categories is observed, in 2000, 2008 and 2011, see figure B.7. See paragraph 2.3.2 for the build-up definition. All times the tidal flat sized channel is seen within the build-up. In 2008 deviant behavior around the tidal flat sized channel is ignored.

Waarde's first transect

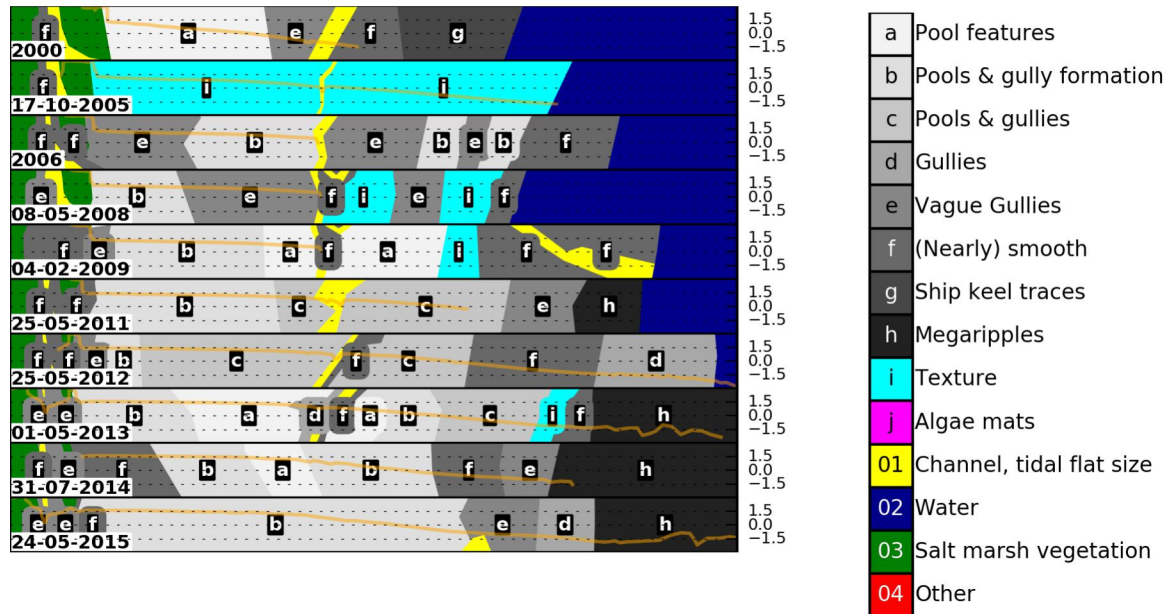


Figure B.7: This figure displays the categorized aerial photographs of several years for an area around the 1<sup>st</sup> transect at Waarde. The categories mentioned in paragraph 2.3.2 are used for this. The area is a rectangle around the transect that covers 25 meters on both sides of it and is oriented parallel to it. The temporally closest elevation measurement series is displayed in each photograph. On the right side of each photograph is the measured height displayed in m NAP. The date the photos are taken is displayed on at the lower left of each categorized photograph.

## B.8. Waarde's 2<sup>nd</sup> transect

The build-up in categories is observed once at Waarde's 2<sup>nd</sup> transect, in 2009, and it is seen thrice until the tidal flat sized channel enters the analyzed rectangle, in 2013, 2015 and 2016, see figure B.8. See paragraph 2.3.2 for the build-up definition. In 2009 two arbitrary categories are seen between the salt marsh and build-up and the build-up is interrupted once by an area with texture. In 2013, 2015 and 2016 no arbitrary categories between build-up and salt marsh or interruptions are seen.

Waarde's second transect

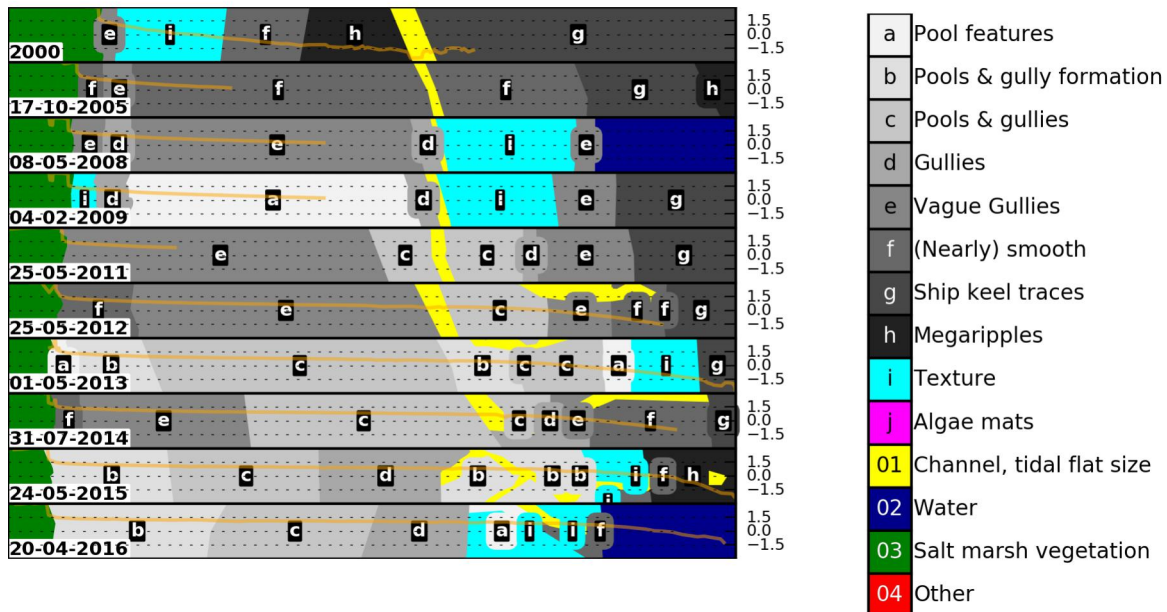


Figure B.8: This figure displays the categorized aerial photographs of several years for an area around the 2<sup>nd</sup> transect at Waarde. The categories mentioned in paragraph 2.3.2 are used for this. The area is a rectangle around the transect that covers 25 meters on both sides of it and is oriented parallel to it. The temporally closest elevation measurement series is displayed in each photograph. On the right side of each photograph is the measured height displayed in m NAP. The date the photos are taken is displayed on the lower left of each categorized photograph.

### B.9. Waarde's 3<sup>rd</sup> transect

The 3<sup>rd</sup> transect at Waarde shows the build-up in categories seven times, but only if deviant behavior around the tidal flat sized channels is neglected. It is not seen in 2005, 2008 and 2012, see figure B.9. See paragraph 2.3.2 for the build-up definition. Approximately half of the times areas with vague gullies (e) or (nearly) smooth (f) areas are seen between salt marsh and build-up.

Waarde's third transect

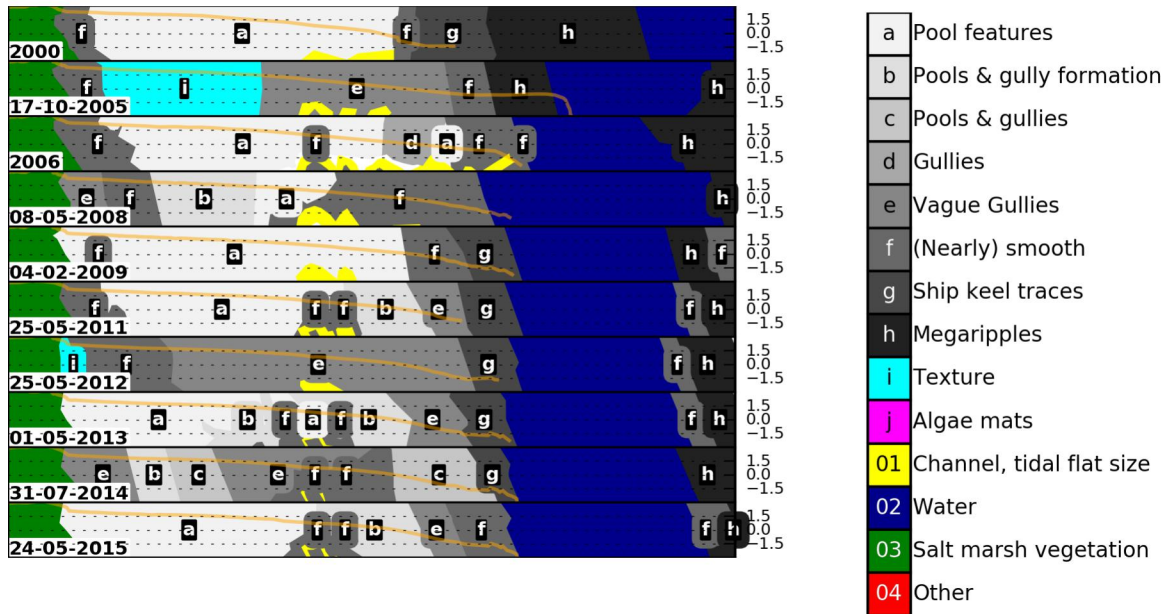


Figure B.9: This figure displays the categorized aerial photographs of several years for an area around the 3<sup>rd</sup> transect at Waarde. The categories mentioned in paragraph 2.3.2 are used for this. The area is a rectangle around the transect that covers 25 meters on both sides of it and is oriented parallel to it. The temporally closest elevation measurement series is displayed in each photograph. On the right side of each photograph is the measured height displayed in m NAP. The date the photos are taken is displayed on at the lower left of each categorized photograph.

### B.10. Zandkreek

At Zandkreek no build-up is seen, see figure B.10 and paragraph 2.3.2 for the build-up definition.

#### Zandkreek

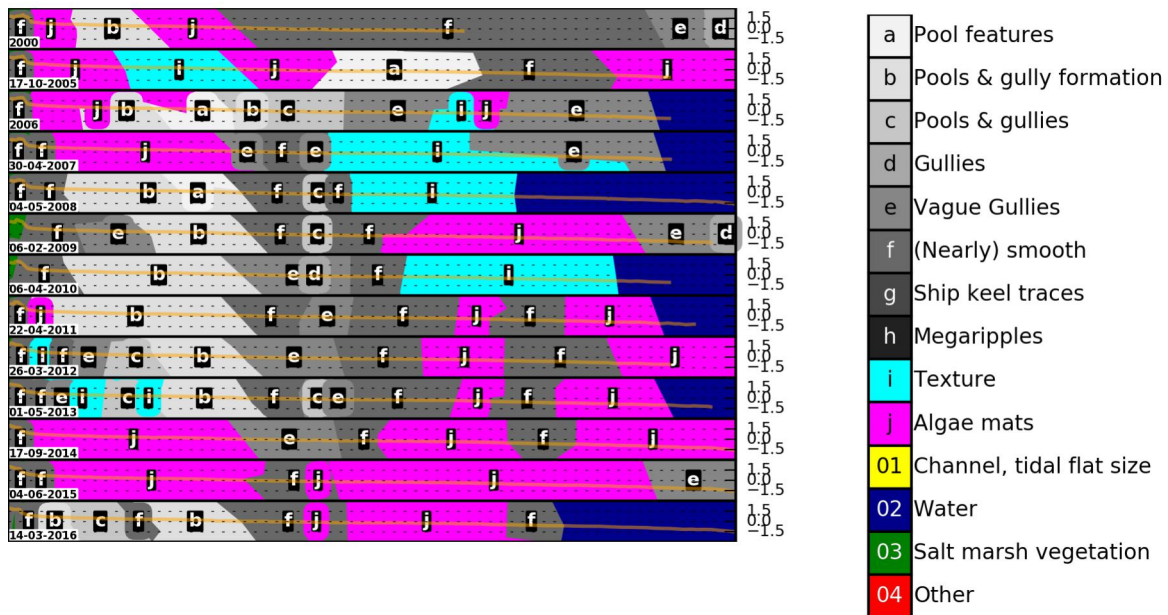


Figure B.10: This figure displays the categorized aerial photographs of several years for an area around the transect at Zandkreek. The categories mentioned in paragraph 2.3.2 are used for this. The area is a rectangle around the transect that covers 25 meters on both sides of it and is oriented parallel to it. The temporally closest elevation measurement series is displayed in each photograph. On the right side of each photograph is the measured height displayed in m NAP. The date the photos are taken is displayed on at the lower left of each categorized photograph.

## B.11. Zuidgors

Zuidgors shows a build-up in categories nine times, if two times the influence of a tidal flat sized channel is neglected, see figure B.11. See paragraph 2.3.2 for the build-up definition. The build-up is thrice interrupted by areas with texture and mostly a (nearly) smooth area is sandwiched between the salt marsh and build-up. The build-up is not observed in 2000, 2003, 2008 and 2009.

Zuidgors

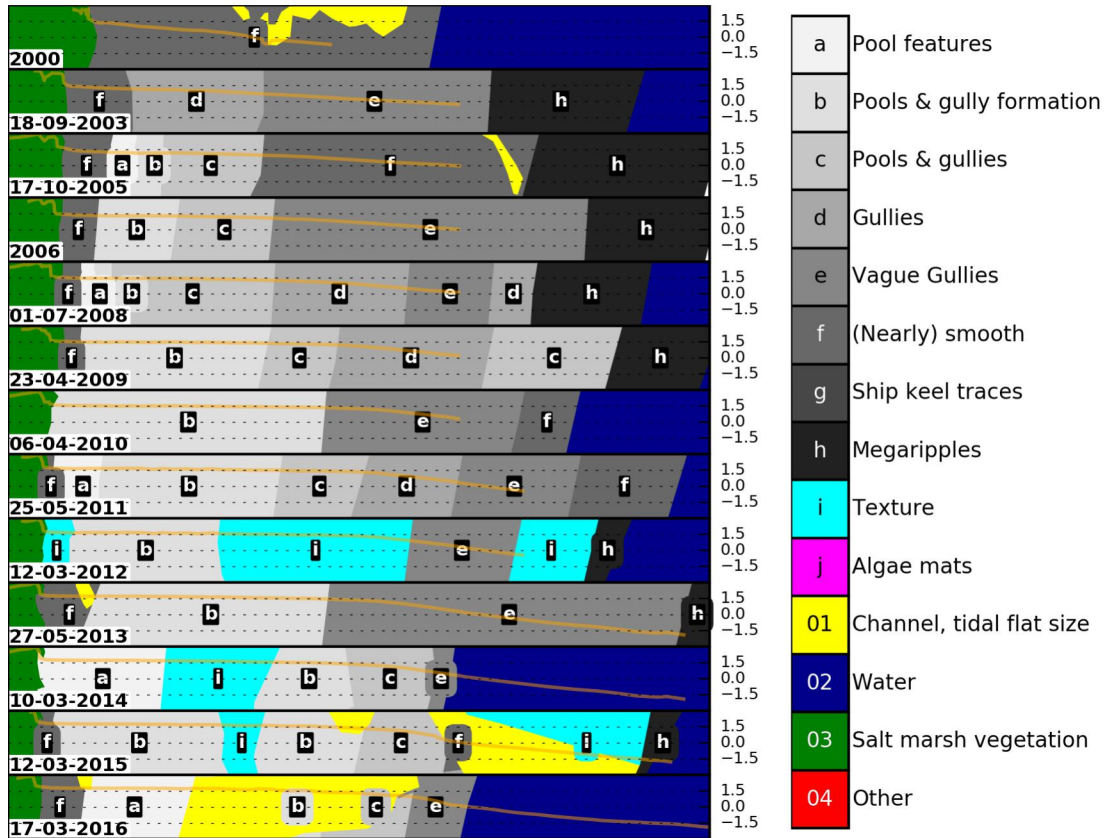
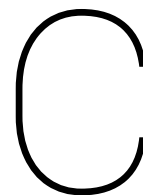


Figure B.11: This figure displays the categorized aerial photographs of several years for an area around the transect at Zuidgors. The categories mentioned in paragraph 2.3.2 are used for this. The area is a rectangle around the transect that covers 25 meters on both sides of it and is oriented parallel to it. The temporally closest elevation measurement series is displayed in each photograph. On the right side of each photograph is the measured height displayed in m NAP. The date the photos are taken is displayed on at the lower left of each categorized photograph.







## 1D SWAN model

In this appendix is explained what the input is for the 1D model that makes use of SWAN, how this input is determined and how the model output is used to estimate bottom shear stresses. What the input is and how this is determined is treated first. After that the model output is discussed. In the remaining part of the appendix this model is also referred to as SWAN model, because another 1D model is used in this research as well. "SWAN is a third-generation wave model, developed at Delft University of Technology, that computes random, short-crested wind-generated waves in coastal regions and inland waters", according to The SWAN Team [2017]. It is used to calculate wave propagation under influence of currents. Bottom shear stresses are estimated with help of this propagation.

### C.1. Model input

The model takes several input parameters: a bottom profile, a JONSWAP spectrum (constructed from wind speed, wind direction and fetch length) and water levels. They are treated one by one in this section.

#### C.1.1. Bottom levels

An equally spaced computational grid, containing bottom levels, is required for the model. Bottom levels measured with GPS at the transect of interest are used to get the bottom elevation. These measurements are interpolated linearly on a one meter spaced grid. The measurements are extrapolated to depths significantly below low water, if necessary. This extrapolation could result in unrealistic water depths. However, a sufficient water depth makes sure that instabilities due to boundary conditions have damped before they reach the area of interest. The part of the tidal flat that emerges during low water is of interest. The stress behavior at the area with unrealistic water depths is less important than at the area of interest. Therefore, the used approach is justified.

#### C.1.2. Wind speed, wind direction and fetch length

The waves are estimated by a JONSWAP spectrum at the offshore boundary of the computational grid. This is induced by local wind velocities with a certain fetch. The fetch length is the distance to upwind coastlines [Holthuijsen, 2009], i.e. the distance over which wind can generate waves. The approach means that only locally generated wind waves are considered. The JONSWAP spectrum can be calculated with formula C.1 and its directional spreading can be calculated with formula C.2 [Holthuijsen, 2009]. This spectrum represents a fetch or duration limited sea state. Le Hir et al. [2000] states that waves reach their fully developed state after 30 to 40 minutes for a fetch length of 5 km, depending on wind speed. This makes fetch length mostly the limiting factor for tidal flats in estuaries, not time of constant wind. Therefore fetch is based on maximum available fetch length in the estuary, not on time to develop the spectrum. The fetch length is determined with Qgis and Python, when it is required to be realistic. A polygon is drawn in Qgis that represents the hard boundaries of the Western Scheldt, based on satellite images. The distance between transect and boundary

is determined for all angles of interest in Python. This is visualized in figure C.1 for Zuidgors. Wind speed and direction can be extracted from hourly measurements from the KNMI [2017]. They have several measurement stations around the Western and Eastern Scheldt.

$$E_{JONSWAP}(f) = \alpha g^2 (2\pi)^{-4} f^{-5} \exp\left[-\frac{5}{4}\left(\frac{f}{f_{peak}}\right)^{-4}\right] \gamma \exp\left[-\frac{1}{2} * \left(\frac{f/f_{peak}-1}{\sigma}\right)^2\right] \quad (C.1)$$

$$\sigma_{\theta} = \begin{cases} 26.9 \frac{f}{f_{peak}}^{-1.05}, & [^{\circ}], \text{ for } f < f_{peak} \\ 26.9 \frac{f}{f_{peak}}^{0.68}, & [^{\circ}], \text{ for } f \geq f_{peak} \end{cases} \quad (C.2)$$

with:

$\alpha$  = energy scale parameter

$g$  = gravitational acceleration  $\left[\frac{m}{s^2}\right]$

$f$  = wave frequency [Hz]

$\gamma$  = shape parameter (3.3)

$$\sigma = \begin{cases} \sigma_a = 0.07 \text{ if } f \leq f_{peak} \\ \sigma_b = 0.09 \text{ if } f > f_{peak} \end{cases}$$

$$f_{peak} = \frac{g}{U_{10}} 2.18 \left(\frac{gF}{U_{10}}\right)^{0.27} = \text{peak frequency [Hz]}$$

$U_{10}$  = wind speed at 10 m above water level  $\left[\frac{m}{s}\right]$

$F$  = fetch length [m]

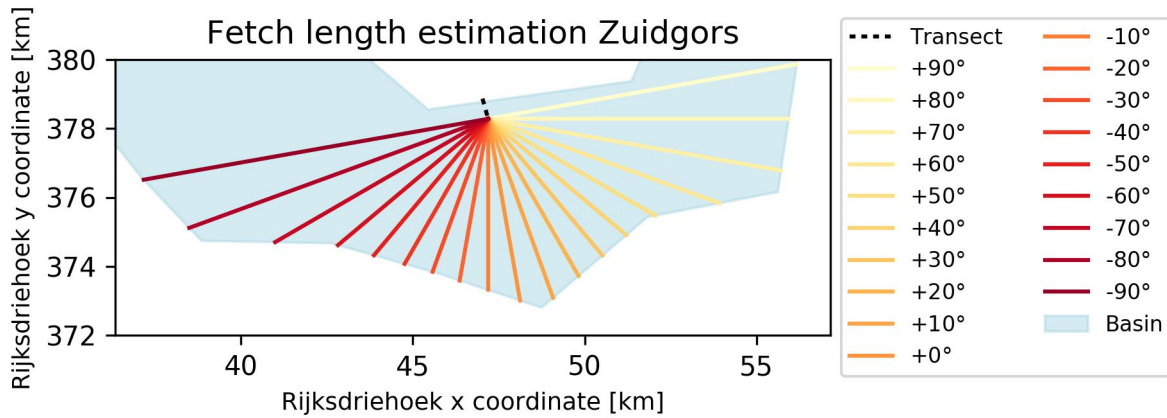


Figure C.1: Visualization of fetch length determination at Zuidgors. Fetch length is the distance to upwind coastlines and is determined for all angles that deviate less than 90 degrees from the transect.

### C.1.3. Water level measurements

Water levels measured by Rijkswaterstaat [2017c] are used, they have a temporal resolution of ten minutes. Every time a new water level is measured the water level is changed in a new run of the SWAN model. The influence of the tide is represented in this way. Thus, every ten minutes a new SWAN run is done to calculate the wave propagation. The minimum water depth is set at five centimeters. Every positive water depth small than this is set to five centimeters. Wind and wave induced setup is neglected in this model.

Cross and along shore currents are calculated individually, both addressed below. The measured water levels from Rijkswaterstaat [2017c] are used for both determinations.

### Cross-shore tidal currents

Cross shore tidal currents are determined by using volume conservation in cross shore direction with a tide quasi static propagation. This means that the surface level is assumed to be horizontal and the current speed through a certain plane is determined by volume balance. In other words, the currents through a plane are determined by tidal range and height of hinter lying mudflat. This can be calculated with formula C.3. The water levels are determined by measurements as close as possible to the tidal flat, done by Rijkswaterstaat [2017c].

$$u_{cross}(x, t) = \frac{\Delta V(x, t)}{\Delta t * h(x, t) * B} \quad (C.3)$$

with:

$$u_c(x, t) = \text{Cross shore current at location } x \text{ at time } t \left[ \frac{m}{s} \right]$$

$$\Delta V(x, t) = \text{Volume of water that must pass through a vertical plane at location } x \text{ at time } t [m^3].$$

$$\Delta t = \text{Time in which volume of water passes through plane [s].}$$

$$h = \text{Water depth at location } x [m].$$

$$B = \text{Alongshore width of the flat} = 1 [m].$$

### Along shore tidal currents

The along-shore currents on the tidal flat are approximated with a volume balance in along shore direction and the Chézy formula. The net discharge that has to go through the plane in tidal flat's transect direction is determined first, with formula C.4. Water level measurements upstream of the tidal flat of interest are used to calculate the net volume change upstream of the tidal flat. This is equal to the net discharge that has to go through the plane in tidal flat's transect direction when it is divided by the time interval. The wet area around each measuring station is estimated in Qgis, based on satellite images. The net volume change acquired by summing up the products of water level change and area for all considered measurement stations. The average current velocity through the plane is determined on basis of the average water depth and net volume change, see formula C.5. The average water depth and plane width are estimated based on Delft3D model input used in van der Werf et al. [2015]. The average along-shore current is scaled with the square root of the water depth, according to Chézy, see formula C.5. This is done to obtain along-shore currents over the whole tidal flat.

$$Q(t) = \frac{\Delta V}{\Delta t} = \sum (A_i * \frac{\Delta h_i}{\Delta t}) \quad (C.4)$$

with:

$$A_i = \text{area belonging to water level measurement station } i [m^2]$$

$$\Delta h_i = \text{change in water level between two measurements in station } i [m]$$

$$\Delta t = \text{measurement interval} = 10 \text{ minutes}$$

$$U_{along}(x, t) = U_{avg\ along}(t) * \sqrt{\frac{h(x, t)}{h_{avg}(t)}} \quad (C.5)$$

with:

$$U_{avg\ along}(t) = \frac{Q(t)}{\text{cross section width} * h_{avg}(t)}$$

$$h(x, t) = \text{water depth at } x \text{ on tidal flat } [m]$$

$$h_{avg}(t) = \text{average water depth cross section (depends on water level)} [m]$$

## C.2. Model output

In this section is explained how the wave induced, current induced and combined bed shear stresses are calculated from the SWAN output, in that order. The resolution of the water level measurements is ten minutes. For every new water level the wave propagation is determined with SWAN. Following on that are the bottom shear stresses determined from the SWAN output, how is explained below. Thus, every ten minutes a SWAN run is done. This results in a bottom shear stress distribution over the cross shore. The 90<sup>th</sup> percentile during each tidal cycle is determined for these stresses. The higher bed shear stresses are more important for sediment entrainment. Therefore, the 90<sup>th</sup> percentile during a tidal cycle is calculated and compared. Stretches of the tidal flat that are not covered with water are neglected in this determination.

### C.2.1. Wave induced bottom shear stress

Bottom shear stress due to waves can be estimated based on the SWAN output with formula C.6, according to Jonsson [1966]. Swart [1974]'s definition of the friction coefficient is used. The maximum orbital motion near the bed and particle excursion amplitude close to the bed are SWAN outputs. These parameters are determined for the waves under influence of currents.

$$\tau_{wave} = 0.5 * \rho * f_w * u_{wave}^2 \left[ \frac{N}{m^2} \right] \quad (C.6)$$

with:

$$\rho = \text{water density} = 1000 \frac{kg}{m^3}$$

$$u_{wave} = \text{maximum orbital motion near the bed} \left[ \frac{m}{s} \right]$$

$$f_w = \text{friction} [-] = \begin{cases} 0.00251 * e^{(5.21 * \frac{A}{k_s} - 0.19)} & \text{for } \frac{A}{k_s} > 1.57 \\ 0.3 & \text{for } \frac{A}{k_s} \leq 1.57 \end{cases}$$

$$k_s = \text{Nikuradse roughness length} [m] = 2.5 * d_{50}$$

$$d_{50} = 75 \mu m$$

$$\zeta = \text{particle excursion amplitude close to the bed}$$

### C.2.2. Current induced bottom shear stress

The bed shear stresses due to along and cross shore currents are calculated with formula C.7, according to Soulsby et al. [1993]. Pythagoras is used to sum up cross-shore and along-shore currents, both are obtained from the SWAN output.

$$\tau_{cur} = \rho * C_d * u_c^2 \left[ \frac{N}{m^2} \right] \quad (C.7)$$

with:

$$u_c = \sqrt{u_{cross}^2 + u_{along}^2} \left[ \frac{m}{s} \right]$$

$$\rho = \text{water density} = 1000 \left[ \frac{kg}{m^3} \right]$$

$$C_d = \left( \frac{0.40}{\ln\left(\frac{h}{z_0}\right) - 1} \right)^2$$

$$h = \text{water depth} [m]$$

$$z_0 = \frac{2.5 * d_{50}}{30}$$

$$d_{50} = 75 \mu m$$

### C.2.3. Combined bed shear stresses

The maximum bed shear stress under combined waves and currents during a wave cycle is calculated with equation C.8 [Soulsby and Davies, 1995]. This results in a maximum total bed shear stress development over the tidal flat for 10 minutes.

$$\tau_{max} = \sqrt{(\tau_m + \tau_{wave}|\cos\theta|)^2 + (\tau_{wave}|\sin\theta|)^2} \quad (C.8)$$

with:

$\theta$  = angle between current and wave direction [°]

$$\tau_m = \tau_{cur} * \left(1 + 1.2 * \left(\frac{\tau_{wave}}{\tau_{cur} + \tau_{wave}}\right)^{3.2}\right)$$





## Influence tidal range SWAN run

In paragraph 3.2.1 is explained that different tidal ranges are applied in the investigation of large scale morphological shape's influence on bottom shear stresses. The bottom shear stresses are given in this appendix for three different tidal ranges. These tidal ranges are acquired by multiplying the measured water levels by 0.8, 1.0 or 1.2. Figures D.1, D.2 and D.3 don't show significant differences. The current velocities are slightly higher for a bigger tidal range. Where shear stresses are observed is also influenced by the tidal range.

Water levels multiplied by 0.8

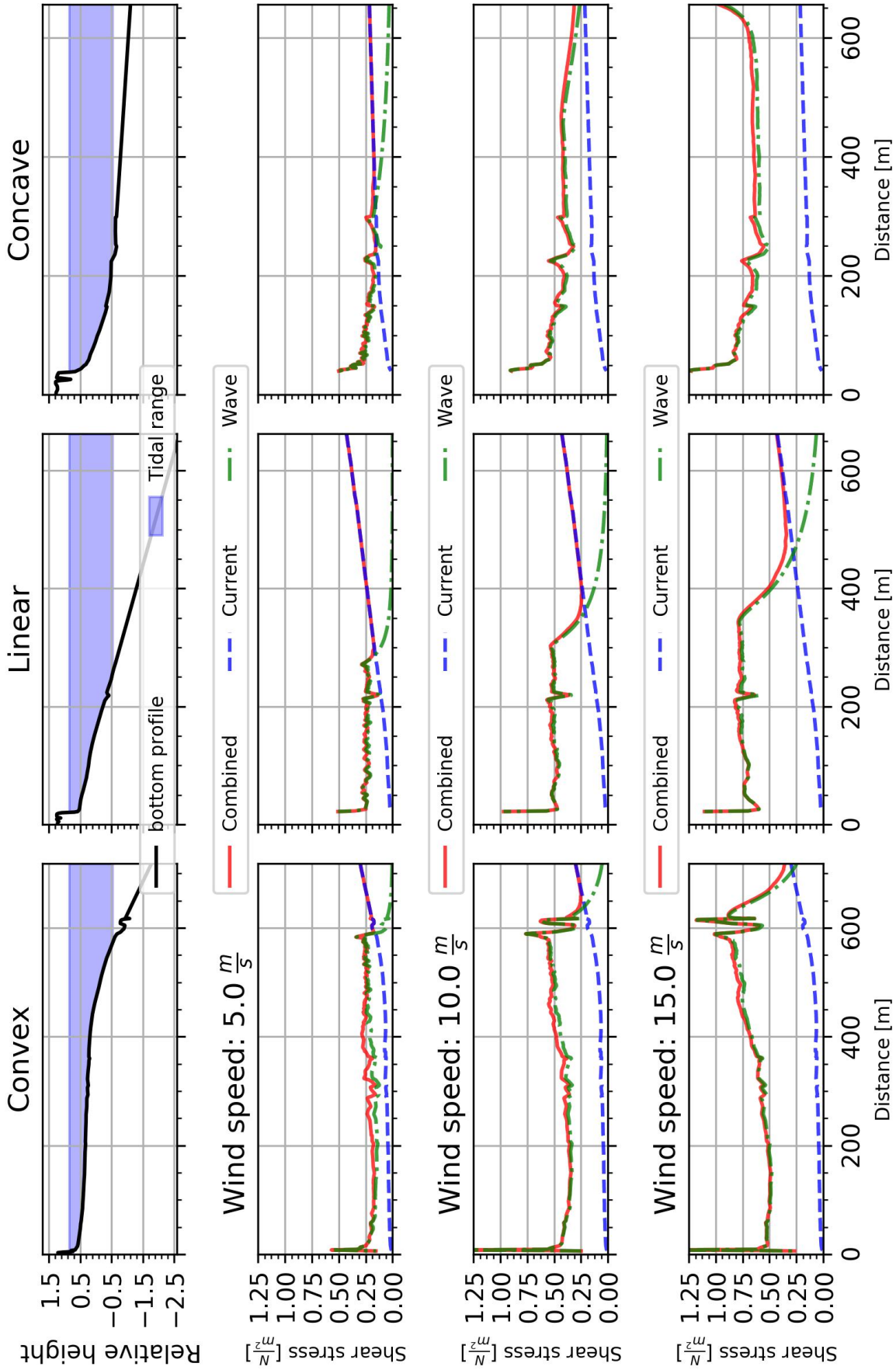


Figure D.1: This figure shows the estimated 90<sup>th</sup> percentile bottom shear stresses due to waves, currents and a combination of both for one tidal cycle under different forcing conditions and for different large scale morphological shapes. These estimates are done with a 1D SWAN model, the set-up is explained in paragraph 3.2.1 and details are given in appendix C. Every large scale morphological shape has its own column. The left column displays the estimates for three different wind speeds for a convex profile. In the middle and right column this is done for respectively linear and concave profiles. The estimated bottom shear stresses belonging to one wind speed are displayed in the same row. This holds for the bottom three rows. The upper row shows the highest and lowest water level in the analyzed tidal cycle and the bottom profile that is used as model input. The water levels are multiplied by a factor 0.8 to create a smaller tidal range.



## Water levels multiplied by 1.0

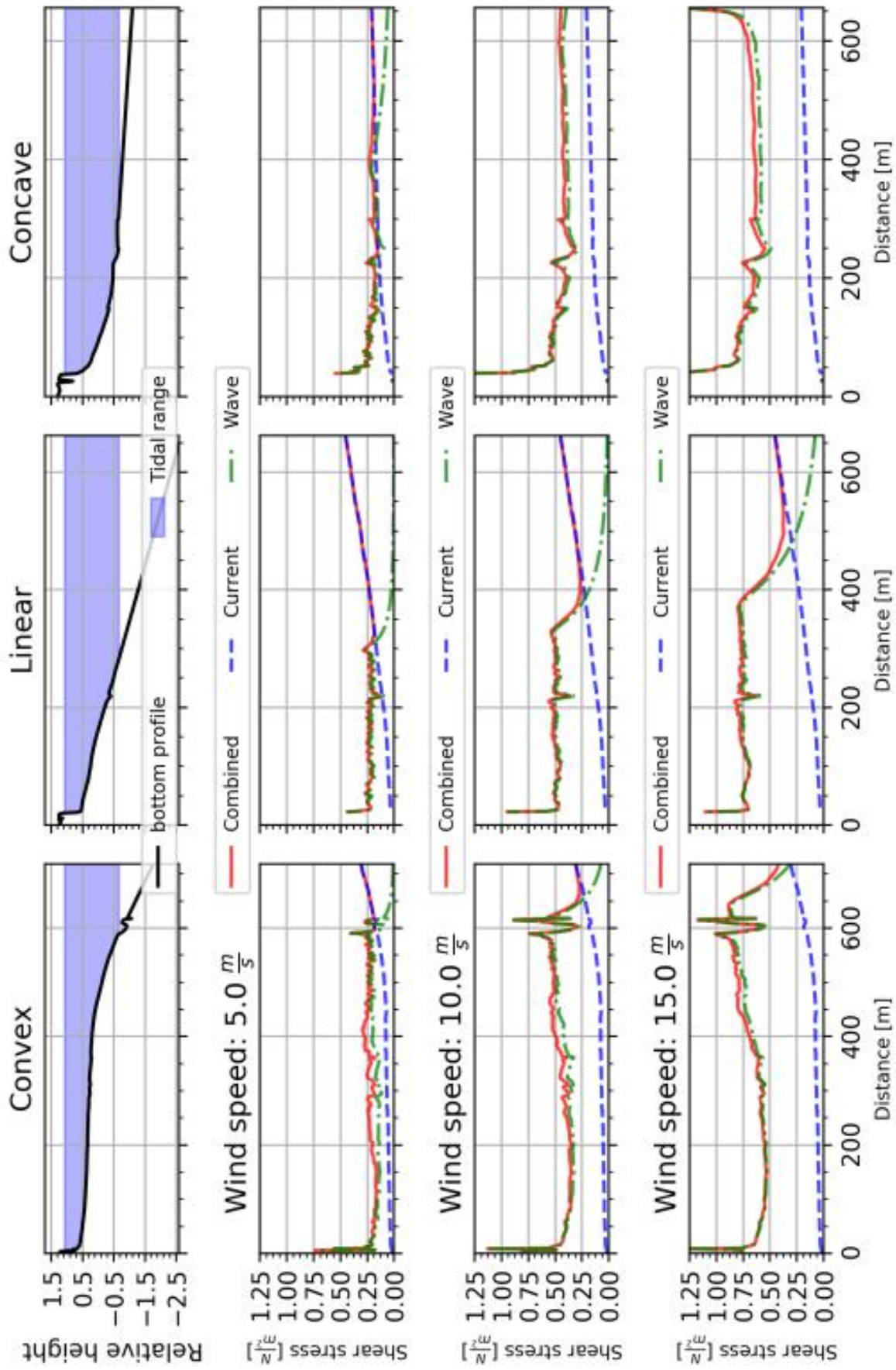


Figure D.2: This figure shows the estimated 90<sup>th</sup> percentile bottom shear stresses due to waves, currents and a combination of both for one tidal cycle under different forcing conditions and for different large scale morphological shapes. These estimates are done with a 1D SWAN model, the set-up is explained in paragraph 3.2.1 and details are given in appendix C. Every large scale morphological shape has its own column. The left column displays the estimates for three different wind speeds for a convex profile. In the middle and right column this is done for respectively linear and concave profiles. The estimated bottom shear stresses belonging to one wind speed are displayed in the same row. This holds for the bottom three rows. The upper row shows the highest and lowest water level in the analyzed tidal cycle and the bottom profile that is used as model input. The water levels are multiplied by a factor 1.0.

Water levels multiplied by 1.2

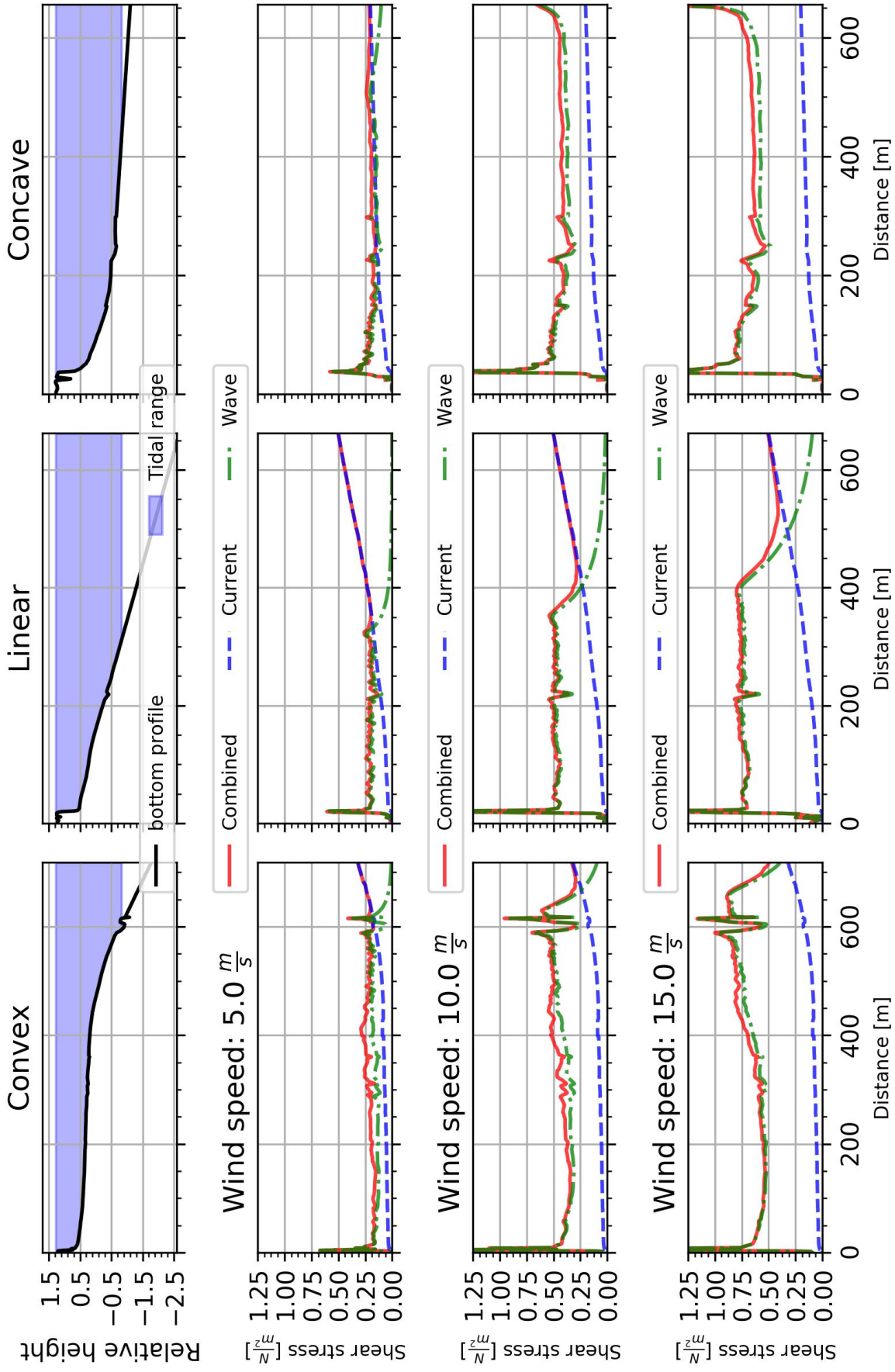


Figure D.3: This figure shows the estimated 90<sup>th</sup> percentile bottom shear stresses due to waves, currents and a combination of both for one tidal cycle under different forcing conditions and for different large scale morphological shapes. These estimates are done with a 1D SWAN model, the set-up is explained in paragraph 3.2.1 and details are given in appendix C. Every large scale morphological shape has its own column. The left column displays the estimates for three different wind speeds for a convex profile. In the middle and right column this is done for respectively linear and concave profiles. The estimated bottom shear stresses belonging to one wind speed are displayed in the same row. This holds for the bottom three rows. The upper row shows the highest and lowest water level in the analyzed tidal cycle and the bottom profile that is used as model input. The water levels are multiplied by a factor 1.2 to create a larger tidal range.

## Wet density measurements pool shaped features

This appendix gives the measured wet densities in and around two pool shaped features at Zuidgors on 25 October 2017, see figure E.1 and E.2. The methodology is explained in paragraph 3.3.1. The location and height of the samples is given in the figures. The height of several points at the contour of the pools is also given. The measured wet densities differ a lot between the measurements, for in- and outside both pools. The height difference between in- and outside is approximately four and two centimeters for respectively pool A and B. Photographs of both pools in the field are given in figure E.3 and E.4

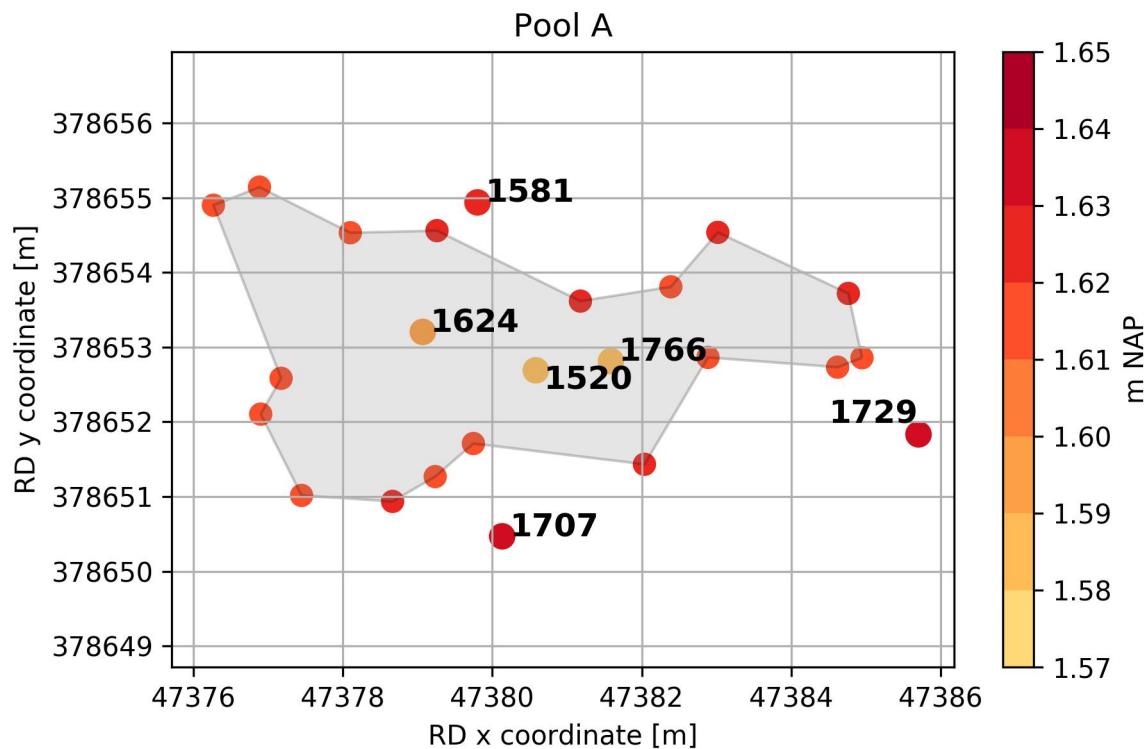


Figure E.1: Measured wet densities in and around pool A. The given values are in  $\frac{kg}{m^3}$ . The height and location of the samples is measured with GPS and indicated in the figure. Also the height of the pool's contour is given.

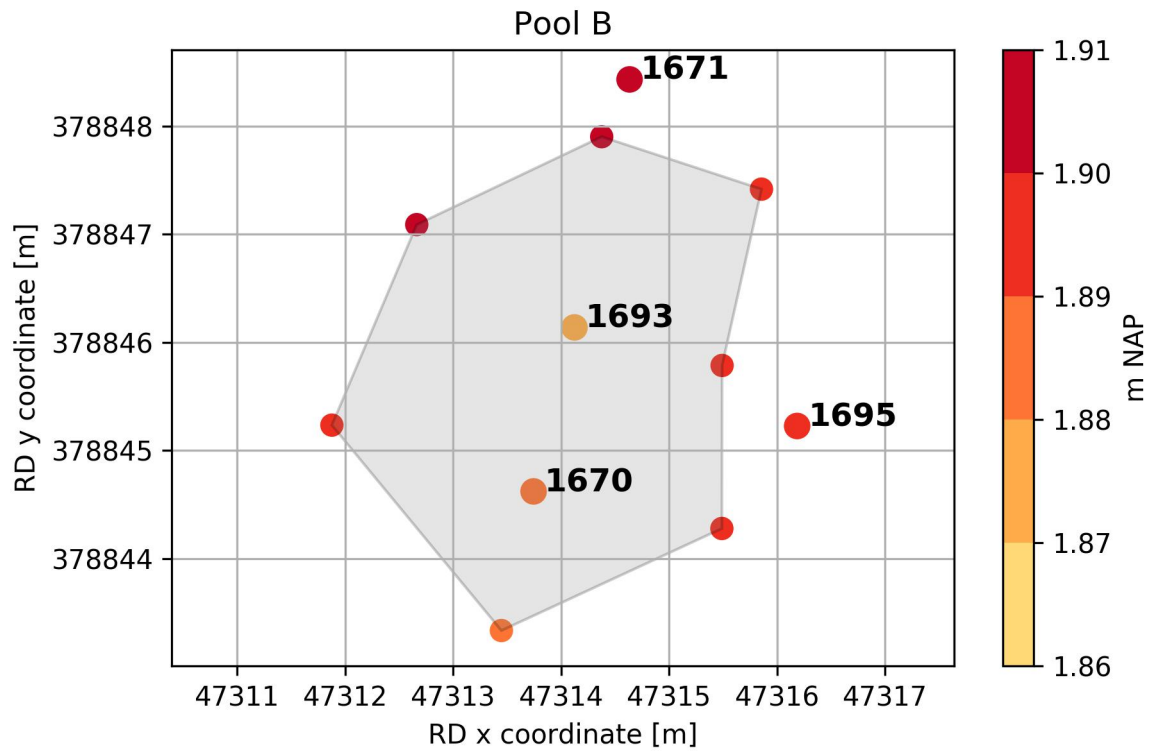


Figure E.2: Measured wet density in and around pool B. The given values are in  $\frac{kg}{m^3}$ . The height and location of the samples is measured with GPS and indicated in the figure. Also the height of the pool's contour is given.



Figure E.3: Photograph of pool A in the field.



Figure E.4: Photograph of pool B in the field.



# Bibliography

- J.A. Bearman, C.T. Friedrichs, B.E. Jaffe, and A.C. Foxgrover. Spatial Trends in Tidal Flat Shape and Associated Environmental Parameters in South San Francisco Bay. *Journal of Coastal Research*, 262:342–349, 2010. ISSN 0749-0208. doi: 10.2112/08-1094.1.
- T.J. Bouma, J. van Belzen, T. Balke, J. van Dalen, P. Klaassen, A.M. Hartog, D.P. Callaghan, Z. Hu, M.J.F. Stive, S. Temmerman, and P.M.J. Herman. Short-term mudflat dynamics drive long-term cyclic salt marsh dynamics. *Limnology and Oceanography*, 61(6):2261–2275, 2016. ISSN 19395590. doi: 10.1002/lno.10374.
- N.J. Cooper. Wave dissipation across intertidal surfaces in the Wash Tidal Inlet, Eastern England. *Journal of Coastal Research*, 21(1):28–40, 2005. ISSN 0749-0208. doi: 10.2112/01002.1.
- K.R. Dyer, M.C. Christie, and E.W. Wright. The classification of intertidal mudflats. *Continental Shelf Research*, 20(10-11):1039–1060, 2000. ISSN 02784343. doi: 10.1016/S0278-4343(00)00011-X.
- S. Fagherazzi and P.L. Wiberg. Importance of wind conditions, fetch, and water levels on wave-generated shear stresses in shallow intertidal basins. *Journal of Geophysical Research: Solid Earth*, 114(3):1–12, 2009. ISSN 21699356. doi: 10.1029/2008JF001139.
- C.T. Friedrichs and D.G. Aubrey. Uniform Bottom Shear Stress and Equilibrium Hypsometry of Intertidal flats. In: *Coastal and Estuarine Studies*. 50:405–429, 1996.
- Geomart.com. CIR (Color Infrared) Aerial Photography - Explained. URL: <https://www.geomart.com/products/aerial/cir.htm>. Date accessed: 2017-11-27.
- K. Hasselmann. Measurements of wind wave growth and swell decay during the Joint North Sea Wave Project (JONSWAP). *Deutsch.Hydrogr.Z.*, A8:95, 1973.
- P.M.J. Herman. Personal conversation, 2017.
- P.M.J. Herman, J.J. Middelburg, and C.H.R. Heip. Benthic community structure and sediment processes on an intertidal flat: Results from the ECOFLAT project. *Continental Shelf Research*, 21(18-19):2055–2071, 2001. ISSN 02784343. doi: 10.1016/S0278-4343(01)00042-5.
- L.H. Holthuijsen. *Waves in oceanic and coastal waters*. 2009.
- I. Jonsson. Wave boundary layers and friction factors. *Coastal Engineering Proceedings*, pages 127–148, 1966. ISSN 2156-1028. doi: 10.1111/joms.12088.
- J.E. Kennedy. The Formation of Sediment Ripples, Dunes, and Antidunes. *Annual Review of Fluid Mechanics*, 1(1):147–168, 1969. ISSN 0066-4189. doi: 10.1146/annurev.fl.01.010169.001051.
- J.R. Kirby and R. Kirby. Medium timescale stability of tidal mudflats in Bridgwater Bay, Bristol Channel, UK: Influence of tides, waves and climate. *Continental Shelf Research*, 28(19):2615–2629, 2008. ISSN 02784343. doi: 10.1016/j.csr.2008.08.006.
- M.A.F. Knaapen, H. Holzhauser, S.J.M.H. Hulscher, and W L Delft Hydraulics. On the modelling of biological effects on morphology in estuaries and seas. In: *Sánchez-Arcilla, A., Bateman, A. (Eds.), Proceedings of the Third IAHR Symposium on River, Coastal and Estuarine Morphodynamics Conference*, pages 773–783, 2003.
- KNMI. Uurgegevens van het weer in Nederland - Download, 2017. URL: <http://projects.knmi.nl/klimatologie/uurgegevens/selectie.cgi>. Date accessed: 2017-05-24.
- S. Lawson, P. Wiberg, K. McGlathery, and D. Fugate. Wind-driven sediment suspension controls light availability in a shallow coastal lagoon. *Estuaries and Coasts*, 30(1):102, 2007. ISSN 1559-2723. doi: 10.1007/bf02782971.

- P. Le Hir, W. Roberts, O. Cazaillet, M. Christie, P. Bassoullet, and C. Bacher. Characterization of intertidal flat hydrodynamics. *Continental Shelf Research*, 20(12-13):1433–1459, 2000. ISSN 02784343. doi: 10.1016/S0278-4343(00)00031-5.
- D.C. Maan, B.C. van Prooijen, Z.B. Wang, and H.J. de Vriend. Journal of Geophysical Research : Earth Surface Do intertidal flats ever reach equilibrium ? 2015. doi: 10.1002/2014JF003311.Received.
- R. Marciano, Z.B. Wang, A. Hibma, H.J. De Vriend, and A. Defina. Modeling of channel patterns in short tidal basins. *Journal of Geophysical Research: Earth Surface*, 110(1):1–13, 2005. ISSN 21699011. doi: 10.1029/2003JF000092.
- OpenSeaMap. die freie Seekarte. URL: <http://openseamap.org>. Date accessed: 2017-11-26.
- A.J. Paarlberg, M.A.F. Knaapen, M.B. De Vries, S.J.M.H. Hulscher, and Z.B. Wang. Biological influences on morphology and bed composition of an intertidal flat. *Estuarine, Coastal and Shelf Science*, 64(4):577–590, 2005. ISSN 02727714. doi: 10.1016/j.ecss.2005.04.008.
- J.S. Pethick. *Geomorphology of mudflats. In: Estuarine shores : evolution, environments, and human alterations*. Wiley, Chichester ;, 1996. ISBN 0471965960.
- I.C. Potter, B.M. Chuwen, S.D. Hoeksema, and M. Elliott. The concept of an estuary: A definition that incorporates systems which can become closed to the ocean and hypersaline. *Estuarine, Coastal and Shelf Science*, 87(3):497–500, 2010. ISSN 02727714. doi: 10.1016/j.ecss.2010.01.021.
- F. Ribas, A. Falqués, H.E. Deèswart, N. Dodd, R. Garnier, and D. Calvete. Understanding coastal morphodynamic patterns from depth-averaged sediment concentration. *Reviews of Geophysics*, 53(2):362–410, 2015. ISSN 19449208. doi: 10.1002/2014RG000457.
- Rijkswaterstaat. Elevation measurements on transects in Eastern and Western Scheldt by department Centrale Informatievoorziening, Inwinning en Gegevensanalyse, 2017a.
- Rijkswaterstaat. Landelijke luchtfoto's by department Centrale Informatievoorziening, 2017b.
- Rijkswaterstaat. Waterhoogte beschikbaar via waterinfo, 2017c. URL: <https://waterinfo.rws.nl/{#}!/kaart/waterhoogte-t-o-v-nap/>.
- G.J. Schiereck. *Introduction to Bed, Bank and Shore protection*. VSSD, second edi edition, 2012. ISBN 978-90-6562-306-5. URL: [www.vssd.nl/hlf/f007.htm](http://www.vssd.nl/hlf/f007.htm).
- C. Schwarz, Q.H. Ye, D. Wal, L.Q. Zhang, T. Bouma, T. Ysebaert, and P.M.J. Herman. Impacts of salt marsh plants on tidal channels initiation and inheritance. *Journal of Geophysical Research: Earth Surface*, pages 385–400, 2014. doi: 10.1002/2013JF002900. URL: <http://onlinelibrary.wiley.com/doi/10.1002/2013JF002900/full>.
- I.B. Singh and S. Kumar. Mega- and giant ripples in the Ganga, Yamuna, and Son rivers, Uttar Pradesh, India. *Sedimentary Geology*, 12:53–66, 1974.
- R.L. Soulsby. Dynamics of marine sands: a manual for practical applications. chapter Chapter 3, page 53. 1997.
- R.L. Soulsby and A.G. Davies. Bed shear-stresses due to combined waves and currents. *Advances in coastal morphodynamics*, 4:4–23, 1995.
- R.L. Soulsby, L. Hamm, G. Klopman, D. Myrhaug, R.R. Simons, and G.P. Thomas. Wave-current interaction within and outside the bottom boundary layer. 21:41–69, 1993.
- G.S. Stelling and S.P.A. Duinmeijer. A staggered conservative scheme for every Froude number in rapidly varied shallow water flows. *International Journal for Numerical Methods in Fluids*, 43(12):1329–1354, 2003. ISSN 02712091. doi: 10.1002/fld.537.
- D.H. Swart. Offshore sediment transport and equilibrium beach profiles. page 302, 1974.
- The SWAN Team. Scientifictechnical Documentation SWAN.



- The SWAN Team. SWAN webpage, 2017. URL: <http://swanmodel.sourceforge.net/>. Date accessed: 2017-02-06.
- J. van der Werf, T. van Oyen, B. de Maerschalck, A. Nnafie, A. van Rooijen, M. Taal, T. Verwaest, P.L.M. de Vet, J. Vroom, and M. van der Wegen. Modeling the morphodynamics of the mouth of the Scheldt estuary. pages 1–7, 2015.
- B. van Eck. *de Scheldeatlas : een beeld van een estuarium*. Schelde Informatiecentrum,, Middelburg :, 1999. ISBN 90-369-3434-6.
- B.C. van Prooijen, F. Grasso, P. le Hir, P.L.M. de Vet, Z.B. Wang, B. Walles, and T. Ysebaert. Equilibria and Evolution of Estuarine Fringing Intertidal Mudflats. 2017.
- L.C. Van Rijn. *Principles of sediment transport in rivers, estuaries and coastal seas*. 1993.
- R.J.S. Whitehouse, P. Bassoullet, K.R. Dyer, H.J. Mitchener, and W. Roberts. The influence of bedforms on flow and sediment transport over intertidal mudflats. *Continental Shelf Research*, 20(10-11):1099–1124, 2000. ISSN 02784343. doi: 10.1016/S0278-4343(00)00014-5.
- H. Winterwerp. Erosion, lecture Sediment Dynamics TU Delft on 26-04, 2015.
- W. Xie, Q. He, K. Zhang, L. Guo, X. Wang, J. Shen, and Z. Cui. Application of terrestrial laser scanner on tidal flat morphology at a typhoon event timescale. *Geomorphology*, 2017. ISSN 0169555X. doi: 10.1016/j.geomorph.2017.04.034.

